Robust Self-Cleaning Coatings

Yao Lu

Department of Chemistry, University College London 2017

About the cover

Water (dyed blue) is framed by a superhydrophobic painting

This image is reproduced with permission from Ref.

“Y. Lu et al., *Science* 2015, 347, 1132-1135”

Robust Self-Cleaning Coatings

Yao Lu

Supervised by Professor I. P. Parkin and C. J. Carmalt

Department of Chemistry

University College London

2017

I, Yao Lu, confirm the work presented in this thesis as my own. Where information has been derived from other sources, I confirm that this has been indicated in this thesis.

Abstract

Self-cleaning, refers to a surface that has the ability to repel contamination (e.g. mud water, spilt ink etc.) or get itself cleaned under a natural circumstance (e.g. rain etc.). This thesis presents the synthesis, characterization and application of two types of self-cleaning surfaces, which are Lotus leaf-inspired superhydrophobic surfaces that repel water, and *Nepenthes* pitcher plant-inspired omniphobic surfaces that repel both water and liquid hydrocarbons (e.g. cooking oil). The surface durability of these surfaces is also investigated to engage practical applications. The self-cleaning properties and surface durability are studied in three stages.

In the first stage, superhydrophobic mild steel surfaces were fabricated through chemical etching of $CuCl_2$ solution followed by low surface energy modification with fluorosilane or Sylgard. To reduce the pressure on the environment, some of the by-products from the chemical etching and fluorosilane processes were used to treat soft porous materials such as sponge, cotton and paper to make superhydrophobic surfaces. In one pot, this method was used to make superhydrophobic coatings on both hard (steel) and soft (cotton etc.) substrates. Due to the superhydrophocity and oleophilicity, mild steel mesh was made superhydrophobic using this method for oil-water separation. Mechanical robustness of the superhydrophobic mild steel plate was further tested *via* sandpaper abrasion; most areas on the surface lost superhydrophobicity after 6 cycles of abrasion.

To improve the mechanical durability of superhydrophobic surfaces and further reduce the pressure on the environment, the second-stage of the work introduces a paint-like suspension that can be treated on both hard (glass and steel) and soft substrates (cotton and paper) to make superhydrophobic coatings without by-products. The suspension, fabricated through mixing dual scaled TiO_2 nanoparticles and fluorosilane-ethanol solution, can be simply sprayed or dip coated onto various substrates. Mechanical robustness of painted superhydrophobic surfaces can be greatly improved through combining the substrates and the paint using commercial adhesives such as double sided tapes and spray adhesive. The superhydrophobic surfaces retained water repellence after knife cut, finger print and even 40 cycles of sandpaper abrasion, showing remarkable robustness.

Although the superhydrophobic paint treated surfaces retained water repellence after being contaminated by oil, they would eventually be stained by oil. To resist oil contamination, the third stage of this thesis presents an omniphobic coating, which is known as slippery liquid infused porous surfaces (SLIPS). The SLIPS were fabricated by adding a lubricating layer onto the superhydrophobic painted surface. The prepared SLIPS repelled water, coffee, red wine, cooking oil and even ketchup with a low contact angle hysteresis. Apart from the surface mechanical durability, thermal and chemical stability have to be considered because the lubricating layer can be subject to extreme temperatures or corrosive liquids. The SLIPS samples retained omniphobicity after thermal tests at 200 °C and -196 °C, mechanical tests of knife scratch and Newton meter press at ~850 kPa, and chemical tests using corrosive liquids with pH from 0 to 14. Hopefully in near further, there would be innovative products available in the market based on this technique.

Acknowledgement

Firstly, I would like to thank my supervisors Professor Ivan Parkin and Professor Claire Carmalt for the support and guidance of my PhD study. I greatly enjoy my research and life in the Parkin-Carmalt group.

I would like to thank Dr. Zhimei Du for the help with my PhD applications, so that I can come to the UK and work on this PhD project.

I thank Dr. Sanjay Sathasivam for the help with my research and life in London throughout my PhD study just like an elder brother.

I thank Professor Jinlong Song for the long term collaboration and the help with building up my academic career.

Thanks to the departmental staff and technicians, Ninik Smith, Judith James, Nicola Best, Dr. Jadranka Butorac, Dr. Steve Firth, Martin Vickers, Dr. Tom Gregory and Kevin Reeves, for the help with administrative affairs and equipment training.

Finally, I would like to thank my parents for their endless love and support. In addition, massive thanks to my wife Nina Lu for the company of living in the UK.

Contents

List of Figures

Chapter 1 Introduction

Chapter 2 Making superhydrophobic surfaces via chemical methods

Chapter 3 Making robust superhydrophobic paint that can be treated on various substrates

Chapter 4 Making slippery liquid infused porous surfaces (SLIPS)

Chapter 5 Conclusions

List of Tables

List of Abbreviations

AACVD	Aerosol-assisted chemical vapour deposition
ATR-FTIR	Attenuated total reflectance Fourier transform infrared spectroscopy
CA	Contact angle
CAH	Contact angle hysteresis
CVD	Chemical vapour deposition
CDG	Captive-drop goniometry
ESEM	Environmental scanning electron microscope
FAS	Fluorosilane
RA	Rolling angle
SA	Sliding angle
SH	Superhydrophobic
SLIPS	Slippery liquid infused porous surfaces
SEM	Scanning electron microscopy
TA	Tilting angle
TEM	Transmission electron microscopy
TPG	Tilting-plate goniometry
UR	Useful range
WCA	Water contact angle
XRD	X-ray diffractometer
XPS	X-ray photoelectron spectroscopy
θ_{adv}	Advancing contact angle
θ_{rec}	Receding contact angle

Chapter 1
Introduction

Yao Lu

UCL CHEM

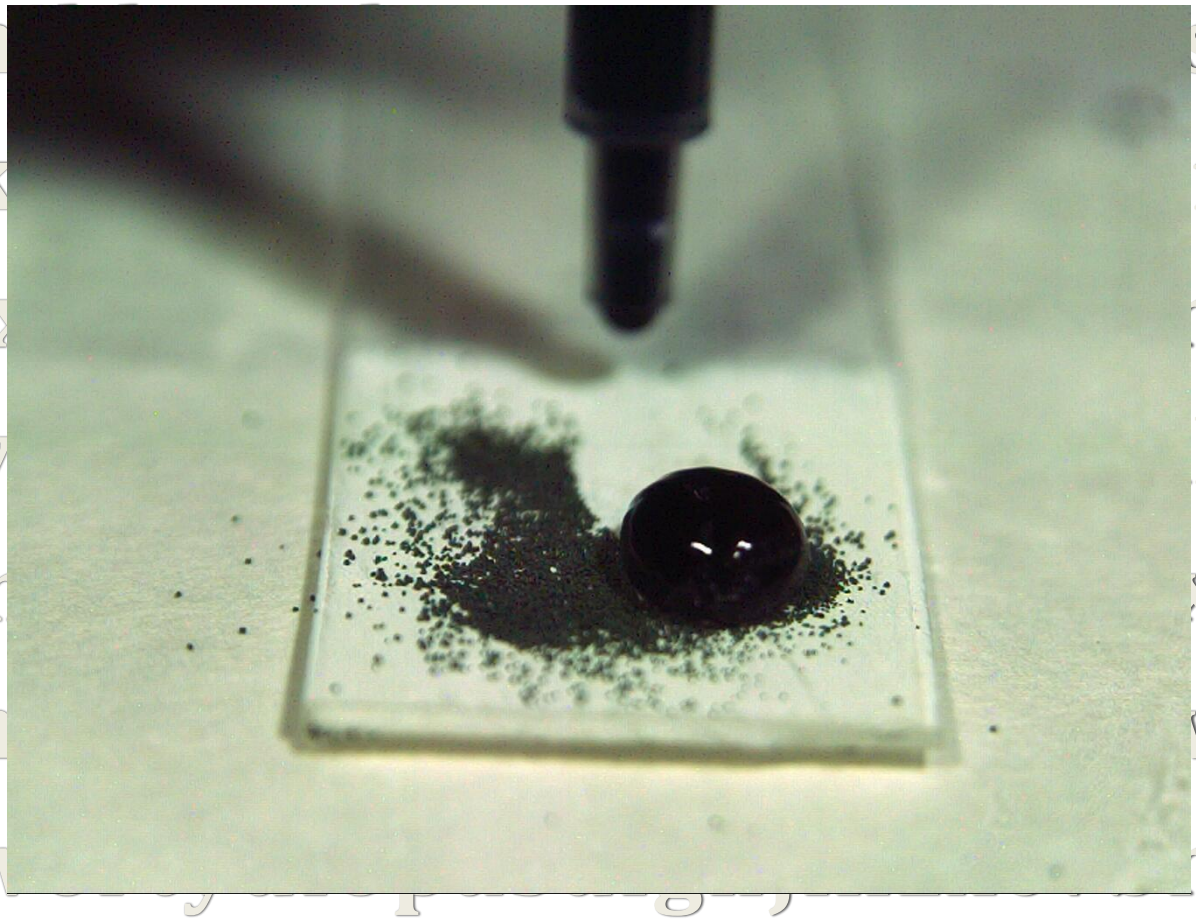

About the cover image of Chapter 1

A water droplet (dyed blue) removes dust on a self-cleaning surface without any traces of wetting or contamination.

Chapter 1
Introduction

1.1 Wetting

Wetting is one of the most common phenomena in people's daily life, from washing hands to printing, from rainfall to painting, and from drinking to irrigation and so on. An understanding of wetting and make use of the knowledge of wetting will greatly facilitate people's life in many aspects. This thesis introduces a super water repellent (superhydrophobic) material and its applications in self-cleaning, oil-water separation and so on. In addition, the surface could be transferred to repel not only water, but also some other liquids that may stain our clothes or carpet, such as coffee, red wine, and cooking oil – namely omniphobic surfaces. This thesis also reported a strategy to make these repellent coatings robust so that they can be used in practical conditions.

This chapter will give a brief introduction about how people are inspired by nature to make non-wettable materials and some fundamental knowledge about wetting characterizations. Classification of different types of repellent surfaces, their preparation and their applications are also introduced.

1.1.1 Wetting in nature

There are many examples of plants and animals in nature that have extreme wettability to aid their survival. For example, the Lotus plants, *Nepenthes* pitcher plants, cactuses and desert beetles and so on.

1. Lotus plant.

Lotus leaf is one of the best well-known examples in nature for water repellent surfaces. Water droplets bead up, roll off or bounce off Lotus leaves instead of wetting or staining the surfaces as shown in Fig. 1.1(a).[1, 2] The water proofing property is due to the micro and nano structures of the Lotus leaf surfaces [Fig. 1.1(b)] that reduce the contact ratio between liquid and solid phases; in addition, the Lotus leaf surfaces have a layer of epicuticular wax to reduce the water affinity (or surface energy).[3-5]

The function of water proofing leads to self-cleaning of Lotus leaves, here, self-cleaning refers to stain-repellence and dirt-removal. For example, when water is mixed with mud or artificial dye, it may stain our clothes, wall surfaces and so on. However, for Lotus plants that live in aqueous circumstances, the water mixed with mud cannot stain the Lotus leaf surfaces because of their water repellent properties, and this is the stain-repellence of self-cleaning. The function of dirt-removal is also an aspect of self-cleaning. Fig. 1.1(c) and (d) shows the

mechanism of dirt-removal properties. Fig. 1.1(c) shows that the dirt particles on a flat surface were not removed by a water droplet; Fig. 1.1(d) shows that on a water-repellent surface where the affinity between water and dirt particles is much greater than that between water and the water-repellent surface, dirt particles are easily picked up and removed by a rolling water droplet, and this is the dirt-removal aspect of self-cleaning.[1, 6, 7] The self-cleaning phenomenon of Lotus leaves is named the "Lotus Effect".

In nature, there are many other examples that also achieve the "Lotus Effect", such as Colocasia Esculenta surfaces,[8, 9] legs of water striders,[10, 11] wings of a butterfly[12, 13] and feathers of some birds.[14, 15]

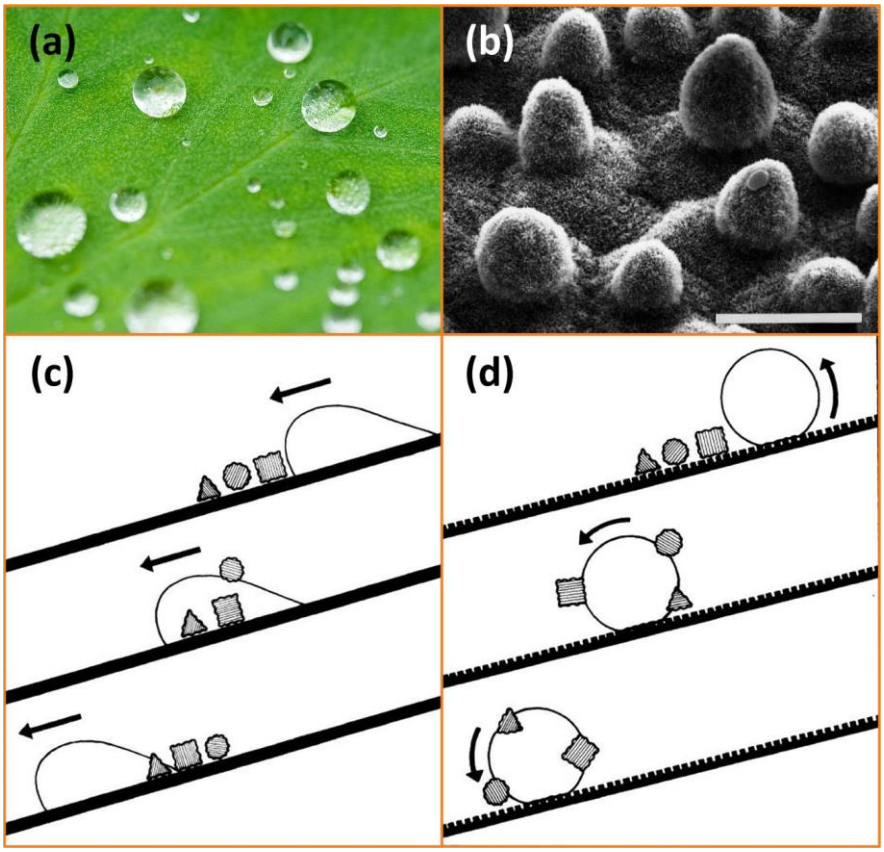

Fig. 1.1 (a) Water droplets bead on the Lotus leaf. (b) SEM images of a Lotus leaf shows the micro and nano structures that support the water droplets. Bar = 20 μm. (c) and (d) Schemes demonstrate the relationship between surface wettability and self-cleaning properties. (c) The dirt particles are redistributed by water on smooth surface. (d) The dirt particles were removed by water from the rough water-repellent surface.[1] (Figures reproduce with permission from Ref. 1 © Springer-Verlag 1997)

2. *Nepenthes* pitcher plants

Nepenthes pitcher plants have a peristome that becomes extremely slippery when it is wetted by rain; insects are then hunted through slipping into the pitcher of the *Nepenthes* pitcher plants (Fig. 1.2).[16, 17] Such surfaces clean themselves by locking a liquid layer as lubricants into the surface, to enable foreign bodies to slip off. There are many other examples of the liquid infused surfaces, such as human eyes,[18] lubricating surfaces in joints between bones,[19] and toe-pads of a frog.[20] These surfaces were designed by nature to gain their own functions for survival purposes through millions of years' evolution.

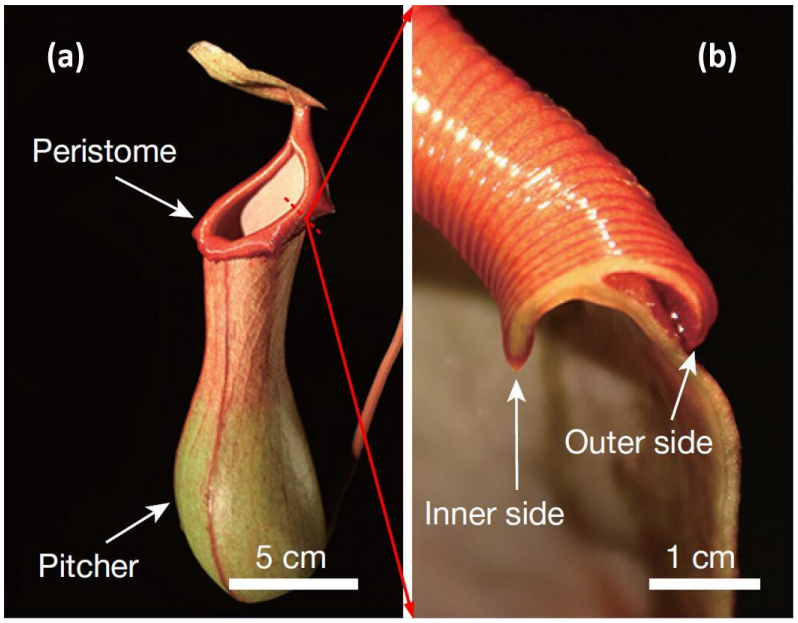

Fig. 1.2 (a) Optical images of a *Nepenthes* pitcher plant (N. *alata*). (b) The cross section of the peristome of the *Nepenthes* pitcher plant.[17] (Figures reproduce with permission from Ref. 17 © 2016 Macmillan Publishers Limited)

3. Desert beetles and cactus

Some species of beetles and cactus live in extreme drought areas, such as a desert. To survive with little water, these animals and plants have learnt a skill to collect fog in air through evolution.

The back of the desert beetle [Fig. 1.3(a)] contains both hydrophobic and hydrophilic regions, where the hydrophilic region is able to collect water from fog, and the collected water can then roll into the mouth of the desert beetle along the hydrophobic region when it is collected in a certain volume.[21, 22]

Cacti [Fig. 1.3(b)] use their conical spines to collect water from fog.[23] The fog in air is initially collected by the tips of the conical spines to form water droplets, and then the water droplets are transported by the stems of conical spines to the body of the cactus.[24-27]

Such animals and plants take advantages of wetting phenomena so that they are able to collect water and survive even in extremely dry places.

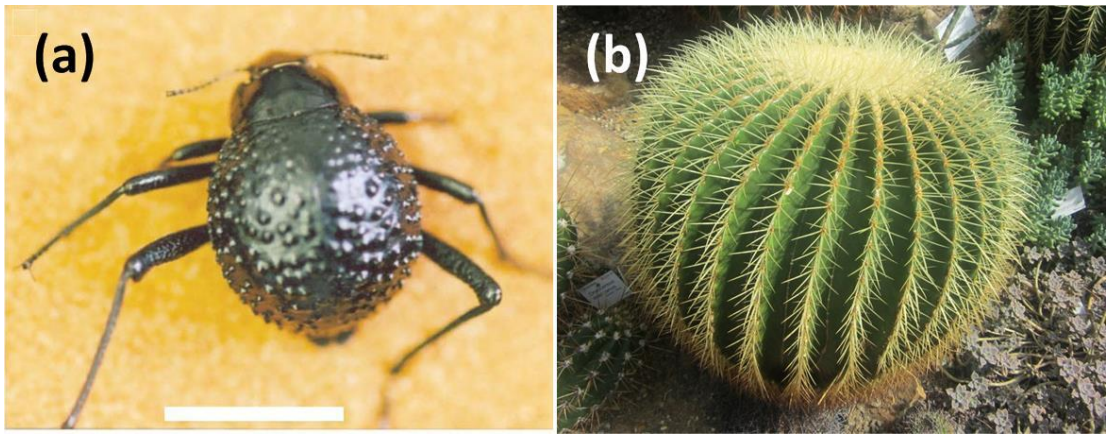

Fig. 1.3 (a) A desert beetle[21] (Figures reproduce with permission from Ref. 21 © 2001 Macmillan Magazines Ltd). (b) A cactus.

1.1.2 Contact angles

The wettability of a solid surface to a liquid is usually characterized using contact angles, whose abbreviation is CA in the literature.[28-30] The definition of contact angles depends on the contact line in the Young's model,[31] as shown in Fig. 1.4. The contact angle θ is determined by the interfacial tensions of liquid-vapor (γ_{lv}), solid-vapor (γ_{sv}) and solid-liquid (γ_{sl}):

$$\cos\theta = (\gamma_{sv} - \gamma_{sl})/\gamma_{lv} \qquad (1.1)$$

In Young's model, the surface is assumed to be perfectly smooth and flat as an ideal solid substrate and the contact angles are normally based on the surface chemistry compositions or properties; however, solid surfaces inevitably have some surface textures in the real world.

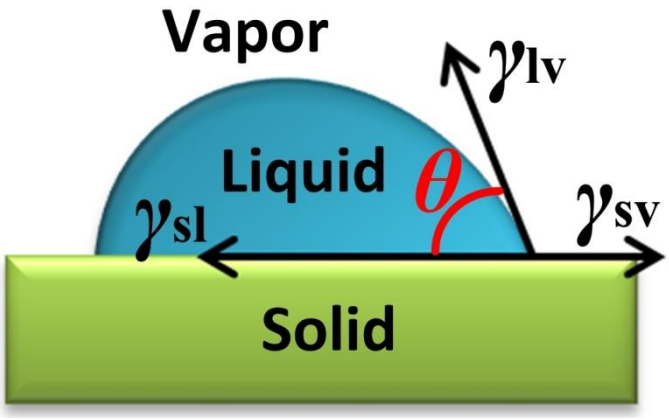

Fig. 1.4 Scheme of Young's model.[31]

To take the surface textures into consideration, Cassie-Baxter's model[32, 33] and Wenzel's model[34, 35] were developed to describe the surface wettability. In the model of Cassie-Baxter, surfaces are supposed to be completely "not wettable", where surface roughness with air pockets in between, supports liquid droplets and stops the contact between the liquid and the solid substrate, as shown in Fig. 1.5(a). The apparent contact angle θ^* in Cassie-Baxter state can be written as:

$$\cos \theta^* = f_s \cos \theta_s + f_v \cos \theta_v \qquad (1.2)$$

where f_s and f_v are respectively the fractions of the solid and vapor areas on the surface, so $f_s + f_v = 1$. The liquid contact angle on vapor θ_v is considered to be a constant of 180°, whereas the liquid contact angle on solid surface $\theta_s = \theta$ from the Young's model. Therefore, the Equation (1.2) can be simplified as:

$$\cos \theta^* = f_s (\cos \theta + 1) - 1 \qquad (1.3)$$

The Cassie-Baxter's model is usually used to describe water-repellent surfaces such as the aforementioned Lotus leaf surfaces.

In the Wenzel state, liquids are expected to completely fill in the surface structures as shown in Fig. 1.5(b); so that the actual contact area between liquid and solid interfaces is enlarged at a ratio of *r*. Here *r* equals the actual contact area divided by the apparent area, which characterizes the surface roughness and is normally greater than 1. The relationship among apparent contact angle θ^*, *r* and θ can be written as

$$\cos \theta^* = r\cos \theta \qquad (1.4)$$

Wenzel's model is usually used to describe hydrophilic surfaces which can be wetted by water.

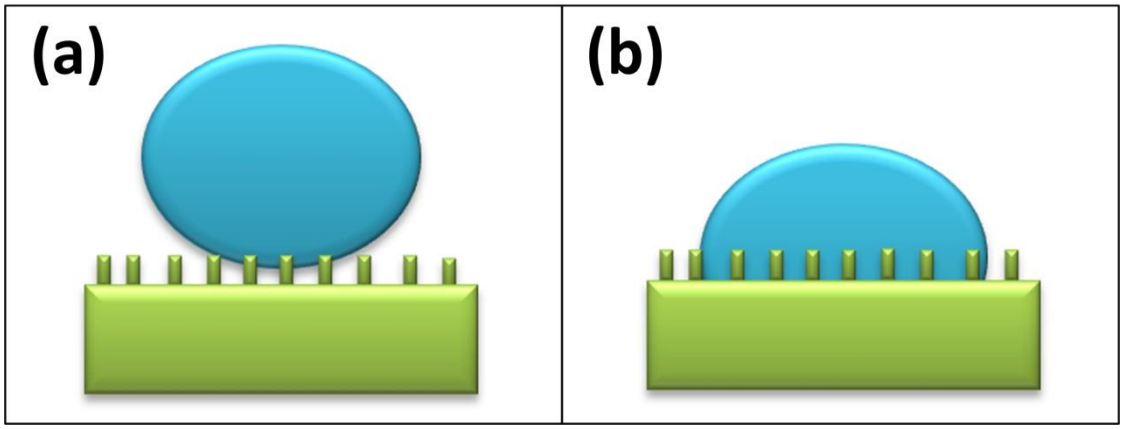

Fig. 1.5 Scheme of (a) Cassie-Baxter's model[32, 33] and (b) Wenzel's model.[34, 35]

The value of water contact angles (WCA) is used to define the surface wettability including hydrophilicity and hydrophobicity. There are two disciplines of the boundary between hydrophilicity and hydrophobicity; one is based on geometry, and the other is based on surface forces between water and solid surface.

In geometry, a hydrophilic surface refers to a surface with water contact angle below 90°, while surfaces with water contact angles greater than 90° are considered to be hydrophobic.[36-38]

According to the adhesion force between water and a solid substrate, the boundary between hydrophilicity and hydrophobicity is ~65°.[39-41] Fig. 1.6 shows the Berg Limit, where the attraction and repulsion of water is balanced.[42] The Berg Limit occurs when the water contact angle is ~65°. Therefore, based on the adhesion force, a hydrophilic surface refers to surfaces with water contact angles below 65° while the surfaces with water contact angles greater than 65° are hydrophobic surfaces.

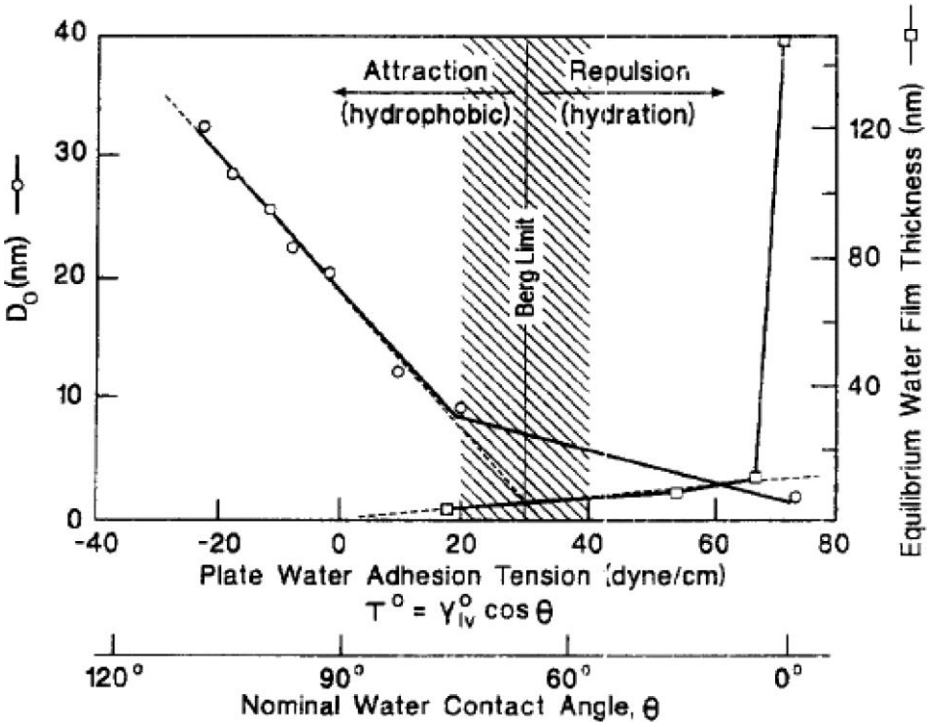

Fig. 1.6 Berg Limit based on water adhesion tension. The balance between attraction and repulsion is the Berg Limit where the water contact angle is ~65°.[42] (Figures reproduce with permission from Ref. 42 © 1998 Elsevier Science B.V.)

Fig. 1.7 shows some surfaces with different wettability. Fig. 1.7(a) shows a water droplet on a glass slide surface (VWR super premium microscope slides) with a water contact angle of 11.0°, the glass surface is hydrophilic based on the aforementioned identification of geometry or adhesion forces. Fig. 1.7(b) shows a water droplet on the surface of a plastic paraffin film (Bemis flexible packaging, Neenah, WI 54956); the water contact angle of this film was 106.2°, so that the surface is classified as hydrophobic.

There are also some examples of extreme wettability based on water contact angles, such as superhydrophilicity and superhydrophobicity. Fig. 1.7(c) shows that a water droplet readily spread throughout a filter paper surface (Whatman™, GE Healthcare UK Limited). In this case, the water contact angle is not even measurable because the water droplet was completely absorbed by the porous filter paper. Here, the water contact angle of the filter paper surface is considered to be ~0°, and a surface with water contact angle of ~0° is a superhydrophilic surface.[43-45] Superhydrophilic surfaces also have many examples in nature – for the purposes of drag reduction and self-cleaning in aquatic environment, such as shark skin,[46-48] anubias barteri leaves,[49] clam's shells[50] and so on.

In contrast, a surface with a water contact angle greater than 150° is a superhydrophobic surface, as shown in Fig. 1.7(d).[51-53] Among the aforementioned self-cleaning surfaces in nature, the water contact angles of the Lotus and Colocasia Esculenta leaves are 160.4 ± 0.7° and 159.7 ± 1.4°, respectively;[1] the water contact angle of water strider legs are 167.6 ± 4.4° etc.[11] These self-cleaning surfaces are also superhydrophobic surfaces.

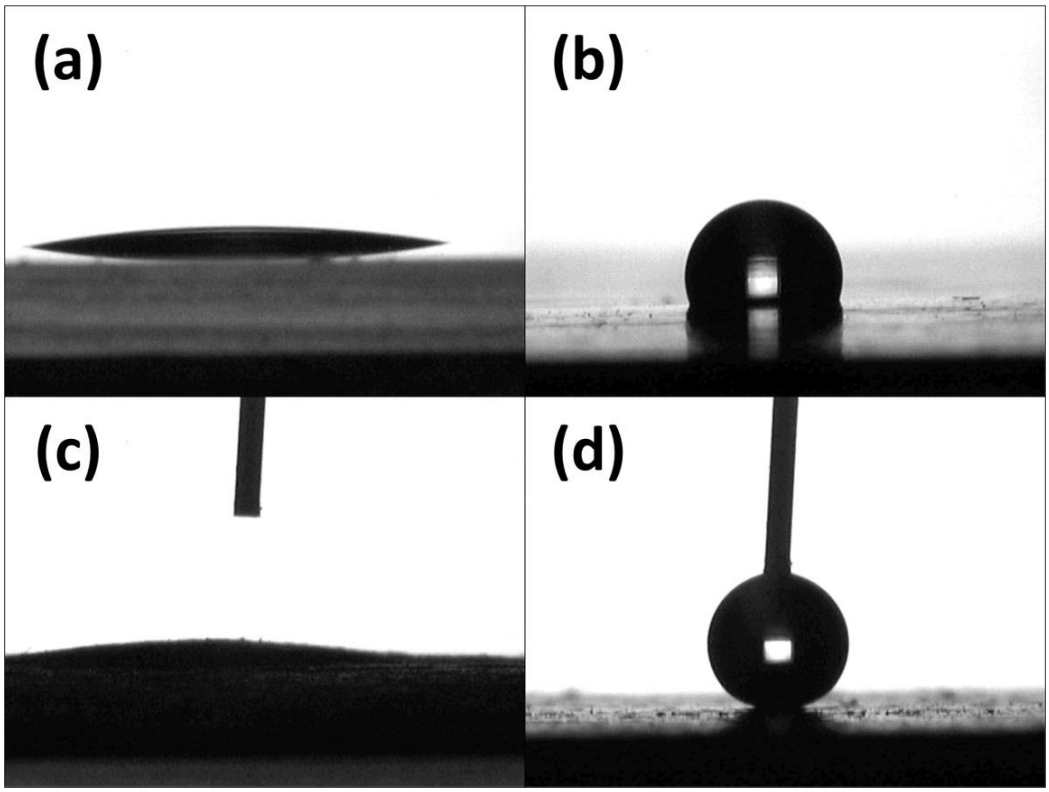

Fig. 1.7 Surfaces in different wettability. (a) A glass slide surface (water contact angle, 11.0°). (b) A plastic film surface (water contact angle, 106.2°). (c) A filter paper surface (water contact angle, ~0°). (d) A glass substrate painted with superhydrophobic coating (water contact angle, 165.6°).[54] The size of water droplets is ~5 μL.

1.1.3 Sliding angle

Contact angle usually refers to a static value that evaluates the wettability of a solid surface towards a liquid. However, this value does not reflect the mobility of liquid droplets, that is, how easily a liquid droplet rolls or slides off a surface.

Sliding angle, also known as SA, is used as one of the dynamic characterizations for the mobility of liquid droplets. However, it is not an angle between a liquid and solid, but the titled angle of the solid surface to a spirit level when the liquid just starts rolling or sliding as shown in Fig. 1.8.[55, 56] In some literature, sliding angle is also called rolling angle (RA)[57, 58] and tilting angle (TA).[59, 60]

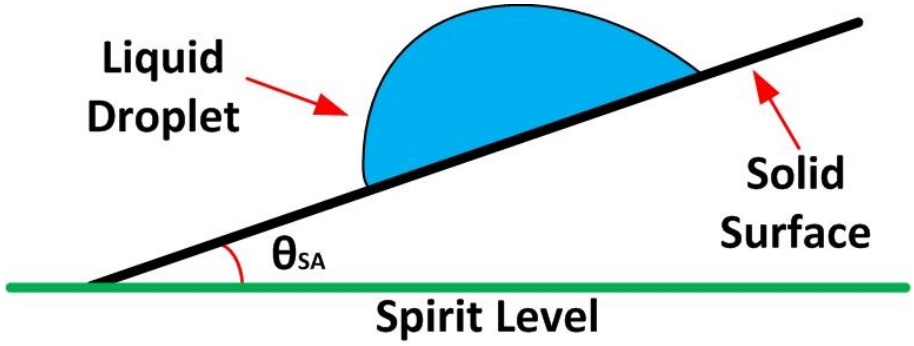

Fig. 1.8 When the liquid droplet starts sliding, the tilted angle between the solid surface and the spirit level is the sliding angle (θ_{SA}) of the solid surface.

Based on sliding angles, superhydrophobic surfaces can also be divided into low adhesion and high adhesion superhydrophobic surfaces. Low adhesion superhydrophobic surface refers to a surface with water contact angle greater than 150° and water sliding angle below 10°.[13, 51, 61] The Lotus leaf and Colocasia Esculenta are both low adhesion superhydrophobic surfaces, because water droplets bead up, roll off, and pick up dirt on these surfaces easily, so that such surfaces are able to clean themselves.

However, not all the superhydrophobic surfaces have self-cleaning properties. For high adhesion superhydrophobic surfaces, although they have water contact angles greater than 150°, water droplets are not able to roll off the surface even if the surface was turned upside down.[62, 63] Fig. 1.9 shows water droplets on the petal surface of Rosa, cv. Bairage with a water contact angle of 152°, and the droplet was suspended without leaving the petal surface even when the surface was turned upside down (180° tilted).[63] This phenomenon is called the "Petal Effect".[64-66] The "Petal Effect" is due to the petal surface which is in both a Cassie-

Baxter state and a Wenzel state, as shown in Fig. 1.10. On the nanoscale, water was supported by nano structures of the surface of a Cassie-Baxter state. However, in a microscale, the gaps between the microstructures are too large to stop water penetrating, resulting in a Wenzel state.[63] Another example of high adhesion superhydrophobic surfaces in nature is the foot of a gecko,[67-69] and this phenomenon can be used for no-loss liquid transportation.[62, 67]

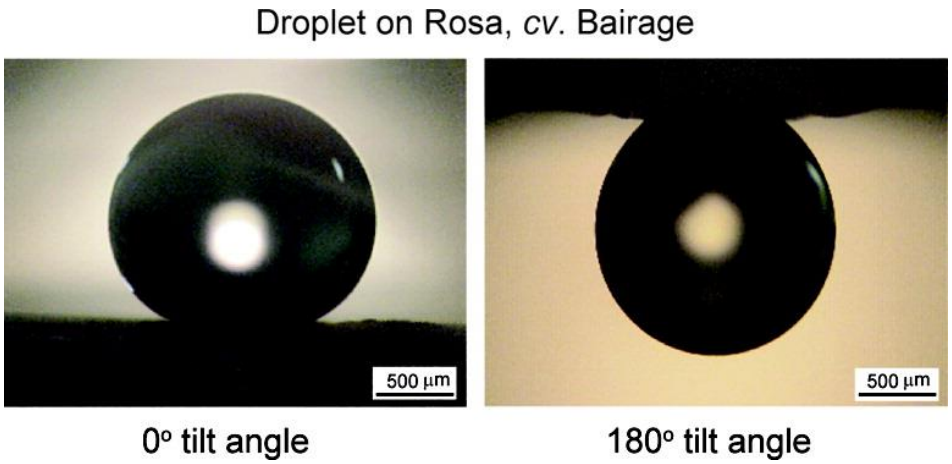

Fig. 1.9 High adhesion superhydrophobic surface. Water droplets on Rosa, cv. Bairage that was tilted at 0° and 180°. Droplet is suspended even when the surface is turned upside down.[63] (Figures reproduce with permission from Ref. 63 © 2010 American Chemical Society)

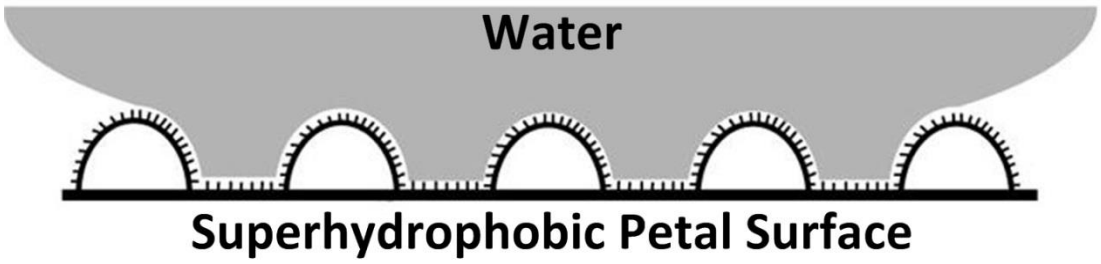

Fig. 1.10 Scheme showing the mechanism of high adhesion superhydrophobic surface.[63] (Figures reproduce with permission from Ref. 63 © 2010 American Chemical Society)

1.1.4 Contact angle hysteresis

Contact angle hysteresis, also known as CAH, is an alternative evaluation of liquid mobility on a surface apart from sliding angles. Different from sliding angles, contact angle hysteresis (θ_{CAH}) is an indirect value between liquid and solid surfaces, and it is defined as the difference between advancing contact angle (θ_{adv}) and receding contact angle (θ_{rec}):[70, 71]

$$\theta_{CAH} = \theta_{adv} - \theta_{rec} \qquad (1.5)$$

There are two methods that are widely used to measure the advancing and receding contact angles – the tilting-plate goniometry (TPG) and captive-drop goniometry (CDG).[72]

1. The tilting-plate goniometry

The tilting-plate goniometry captures the advancing and receding contact angles on both the left and right sides of a liquid droplet when the solid surface is tilted at the sliding angle (from 0 to 90°) of this droplet towards the surface, as shown in Fig. 1.11(a). In some cases, the liquid droplet does not leave the surface even when the surface is turned upside down (180°), here the advancing and receding contact angles are read when the surface is tilted at 90°.

2. Captive-drop goniometry

In the captive-drop goniometry, the advancing contact angle is read while adding volume into a droplet to the maximum before the increase of the contact line of solid-air-liquid phases, as shown in Fig. 1.11(b). The receding contact angle is measured when removing volume from a droplet just before the reduction of the contact line of solid-air-liquid phases, as shown in Fig. 1.11(c).

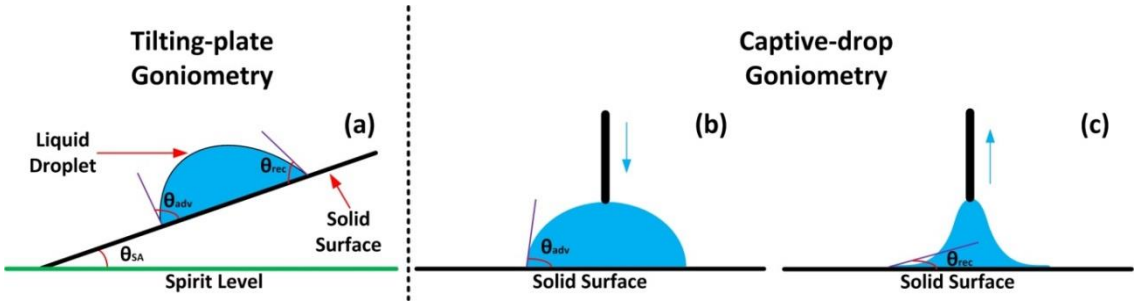

Fig. 1.11 Schemes of (a) the tilting-plate goniometry, and (b) and (c) the captive-drop goniometry.

1.2 Repellent surfaces

Repellent surfaces refer to a surface that repels one or multiple liquids, such as Lotus leaf inspired superhydrophobic surfaces,[22, 73, 74] superoleophobic surfaces,[75-77] and *Nepenthes* pitcher plant inspired slippery liquid infused porous surfaces (SLIPS).[78-80]

1.2.1 Superhydrophobic surfaces

Superhydrophobic surfaces refer to a surface with water contact angles greater than 150° as discussed previously; and the measurement of water contact angles is a way of identifying superhydrophobicity. The measurement of water contact angles depends on a contact line between water and the substrate; however, the contact line might not be obtainable in some cases resulting in the water contact angle being unable to be measured.

Fig. 1.12(a) shows a water contact angle measurement of a superhydrophobic Mg alloy surface, which was fabricated *via* electrochemical etching and low surface energy modification.[81] The contact line is clearly seen and the water contact angle can be simply obtained *via* aforementioned models. However, on some water repellent soft porous materials, water contact angles cannot be determined because the contact line is sometimes not obtainable, for example, a superhydrophobic scouring pad surface as shown in Fig 1.12(b).[82]

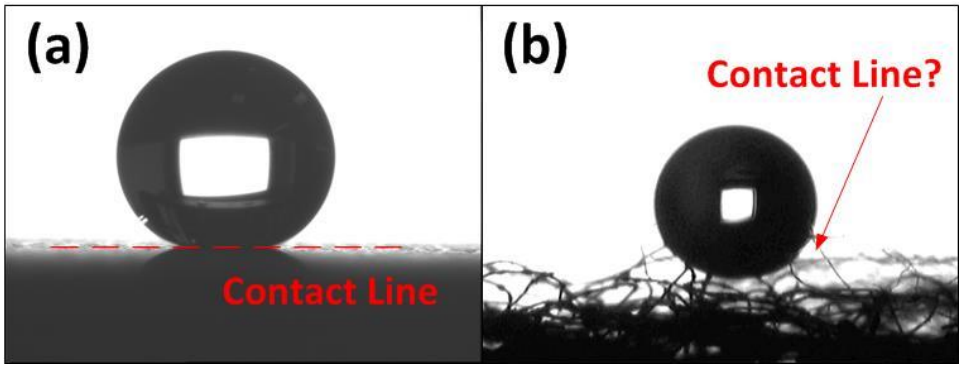

Fig. 1.12 (a) Superhydrophobic Mg[81] (Figures reproduce with permission from Ref. 81 © 2011 American Chemical Society) and (b) superhydrophobic scouring pad surfaces[82] (Figures reproduce with permission from Ref. 82 © The Royal Society of Chemistry 2014).

For these reasons, water droplet bouncing phenomena, for which contact lines are not necessary, are also used to demonstrate surface superhydrophobicity. Water contact time of a bouncing droplet was studied [Fig. 1.13(a)] to show that the contact time is independent of the impact velocity but depends on the drop radius.[83] It was then discovered that the non-axisymmetric water droplet recoil can shorten contact time, which is reduced by 37% to 7.8

ms, and such a system can be generalized to a wide range of materials, as shown in Fig. 1.13(b).[84] Liu et al.[85] developed the superhydrophobic surfaces patterned with a submillimetre-scale post matrix; water contact time was dramatically reduced because the drops spread on impact and then leave the surface in a flattened shape without retracting on these surfaces – forming a pancake bouncing as shown in Fig. 1.13(c).

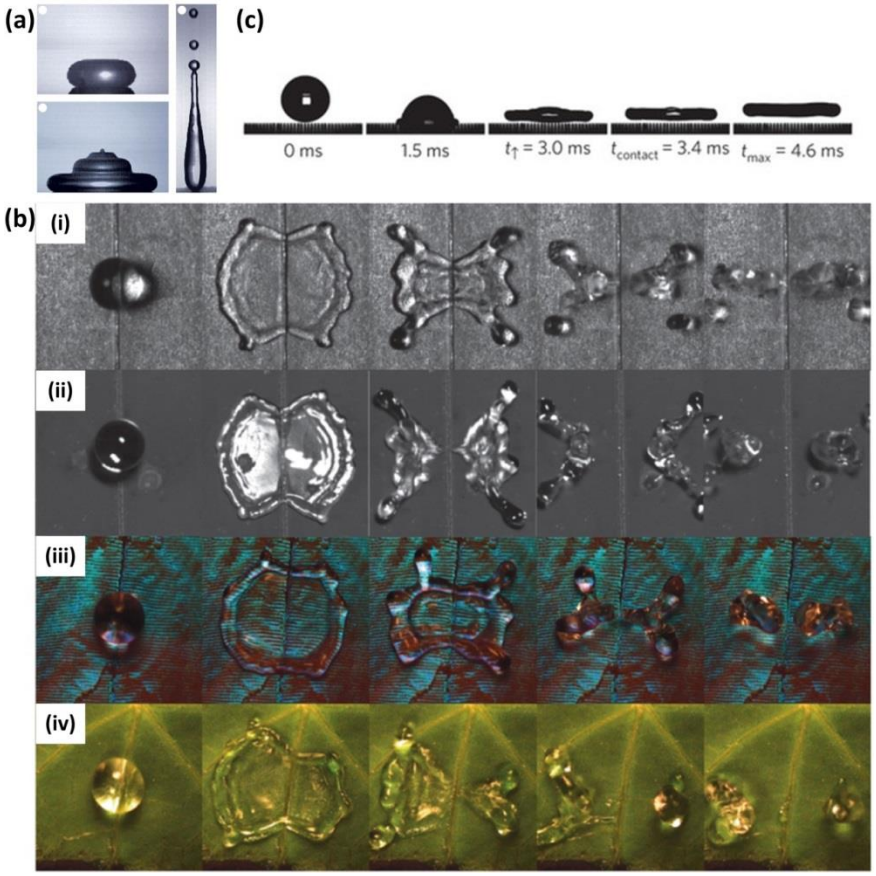

Fig. 1.13 (a) Water droplet bouncing on a superhydrophobic surface[83] (Figures reproduce with permission from Ref. 83 © 2002 Nature Publishing Group). (b) Water recoils on (i) a superhydrophobic anodized aluminium oxide surface, (ii) a superhydrophobic copper oxide surface, (iii) a vein on the wing of a Morpho butterfly and (iv) a vein on a nasturtium leaf[84] (Figures reproduce with permission from Ref. 84 © 2013 Macmillan Publishers Limited). (c) Pancake bouncing occurs on a submillimetre-posts-patterned superhydrophobic surface, the contact time is reduced to 3.4 ms[85] (Figures reproduce with permission from Ref. 85 © 2014 Macmillan Publishers Limited).

The preparation of superhydrophobic surfaces is usually based on two strategies – 1) roughen a surface that has a low water affinity; 2) lower the surface energy of a highly textured surface.[13, 86, 87] There are many methods of fabricating superhydrophobic surfaces, including a top-down or bottom-up method. Here top-down methods refer to removing materials from a substrate such as chemical etching[88-90] and electrochemical etching;[91-93] bottom-up methods depend on the growth of materials from a substrate, such as chemical vapour deposition (CVD)[94-96] and spray coating methods.[97-99]

1.2.2 Superoleophobic surfaces

Superhydrophobic properties are based on micro and nano hierarchical roughness [Fig. 1.14(a) and (b)] and low surface energy modifications.[100, 101] However, such surfaces lose their superhydrophobicity once being contaminated by oils, whose surface tensions are usually lower than that of water.[102] Tuteja et al. have designed re-entrant surface structures, as shown in Fig. 1.14(c), followed by lowering the surface energy, to make superoleophobic surfaces that repel water, oils and a range of organic liquids.[103] Here, superoleophobic surfaces refer to a surface that has an "oil" contact angle greater than 150°, however, different types of liquid hydrocarbons have different surface tensions – the higher surface tension a liquid has, the easier to repel the liquid – making it difficult to precisely define superoleophobicity.[104] In this thesis, hexadecane with a low surface tension (27.5 mN/m) was used as a threshold, that is, a surface with hexadecane contact angles greater than 150° is considered to be superoleophobic. In most cases, a superoleophobic surface also repels water, therefore, superoleophobic surfaces are sometimes also called superamphiphobic[105, 106] or superomniphobic[77, 107] surfaces based on a high contact angle of both water and oil. Fluoropolymer modified nanonails were then built up [Fig. 1.14(d)], which even repel ethanol [Fig. 1.14(e)].[108] Liu et al.[109] turned a surface superrepellent even to completely wetting liquids only by roughing the surface with doubly re-entrant structures [Fig. 1.14(f)] without any further low surface energy modifications. Even extremely wetting liquid – perfluorohexane (3M FC-72) can bounce on such surface roughness [Fig. 1.14(g)].

The techniques of fabricating superoleophobic surfaces are similar to those of superhydrophobic surfaces, such as chemical etching,[110, 111] electrochemical etching,[102] electrospinning,[103, 112] template[113] methods and so on.

These repellent surfaces retain self-cleaning properties through keeping themselves "dry" to repel contaminating liquids. Given the theories and experiments from superhydrophobic, superoleophobic to superrepellent materials to extremely wetting liquids, the low surface energy modification is not always necessary. However, the demands of surface micron morphology designs keeps increasing from micro-nano scaled hierarchical, re-entrant, nanonail to doubly re-entrant structures. These structures are all in micro or nano scales with a weak robustness, which greatly hinders the practical applications of these amazing surfaces.

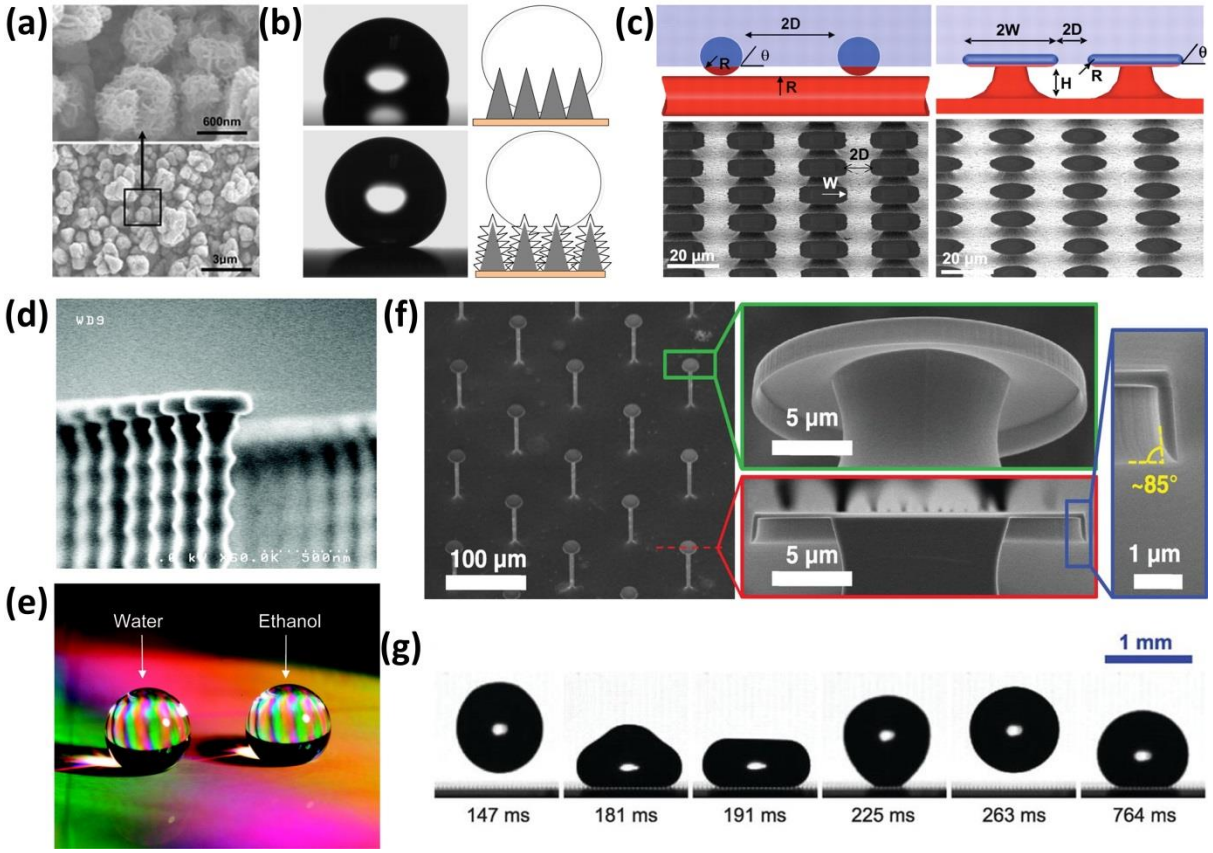

Fig. 1.14 (a) Scanning electron microscopy (SEM) images of the superhydrophobic metal surface in different magnifications; nano-scaled roughness can be seen on micro structures forming a micro-nano hierarchical morphology[100] (Figures reproduce with permission from Ref. 100 © The Royal Society of Chemistry 2005). (b) Water droplet on surfaces and the corresponding wetting models. It shows that single scaled roughness is not enough to support the water droplet, micro-nano dual structures can make water drops bead up[101] (Figures reproduce with permission from Ref. 101 © 2011 Elsevier B.V. All rights reserved). (c) Cartoons and the corresponding SEM images of re-entrant structures.[103] In the cartoons, the blue area is wetted while the red surface remains non-wetted when in contact with a liquid; two "micro-hoodoo" surfaces with square and circular flat caps are shown in the SEM images, respectively. The samples are viewed from an oblique angle of 30° (Figures reproduce with permission from Ref. 103 © 2007 AAAS). (d) SEM image of the nanonail covered surface, which repels (e) both water and ethanol[108] (Figures reproduce with permission from Ref. 108 © 2008 American Chemical Society). (f) SEM images of doubly re-entrant structures; such roughness, that is independent of low surface energy modification, enables (g) a FC-72 droplet bounce off[109] (Figures reproduce with permission from Ref. 109 © 2014 AAAS).

1.2.3 Slippery liquid infused porous surfaces (SLIPS)

In nature, the peristome of *Nepenthes* pitcher plants becomes slippery when it is wetted by rain, so that ants and other prey fall into it and are trapped by the stomach of *Nepenthes* pitcher plants.[16] Inspired by these plants, a slippery liquid-infused porous surface (SLIPS) was developed, which is omniphobic with self-cleaning properties. However, SLIPS functions to repel contaminating liquids only when it is wetted, and this is conceptually different from the "dry" superrepellent materials. The fabrication of SLIPS is to use micro-nano surface textures to lock in the lubricating fluids[114] and such slippery surfaces do not normally achieve high liquid contact angles, but an ultra-low contact angle hysteresis enables foreign liquids to readily slide off the slippery surfaces, resulting in self-cleaning/anti-fouling properties[115-117] as shown in Fig. 1.15(a). The design of SLIPS must follow three criteria:[114] (1) the substrate must be wetted and stably adhered by the lubricating liquid/lubricant; (2) the substrate must be preferentially wetted by the lubricant instead of the liquid that it is expected to repel; (3) the lubricant and the testing liquid that is expected to be repelled must be immiscible. In the concept of the "dry" superrepellent materials, droplets usually sit on the surface texture and are considered to have extremely high mobility with respect to the model of Cassie-Baxter;[32] while the Wenzel state usually refers to the droplets to be pinned.[34] While on SLIPS, droplets retain high mobility even in the Wenzel state and this challenged the conventional understanding of repellent materials – named the "slippery Wenzel state".[118] Gaining the "wet" self-cleaning, SLIPS can also be used for anti-icing as shown in Fig. 1.15(b),[119, 120] drag reduction,[121, 122] corrosion protection[123, 124] and other applications where most "dry" superrepellent materials are used, as shown in Fig. 1.15(c).[125-128] The advantage of using SLIPS instead of "dry" superrepellent surfaces is that the SLIPS repels water, oil and organic solvents without specially designing a re-entrant or double re-entrant roughness. In addition, SLIPS can be used in some conditions where "dry" superrepellent surfaces are not applicable, for example, lubricating components such as bearings and gears in a machine;[54] the SLIPS is self-healable after scratches because of the mobility of the lubricating layer while dry surfaces are usually not;[129] the air cushion of "dry" superrepellent materials is easy to break down when high pressure is applied, while the lubricating layer of SLIPS is somehow more stable than the air pockets between surface structures in terms of the pressure issues.[114, 130, 131] However, there are still some drawbacks of the SLIPS, for example, the SLIPS only functions when it is wetted, so that the durability is determined by how long the lubricant stays in the solid substrate instead of leaking or evaporating.[132, 133] The lubricant has to be immiscible with water, oil and organic solvents according to the third criterion of SLIPS

fabrication,[114] and this results in a limitation of the choice of lubricant.[132, 134] The surface structures (which are usually hydrophobic) of a substrate are expected to lock the lubricant to make a SLIPS, thus the robustness of the surface roughness on the substrate is another limitation that is similar to the robustness with respect to "dry" superrepellent surfaces. As a result, the durability and robustness of the SLIPS should be greatly enhanced before its practical applications can be realised.

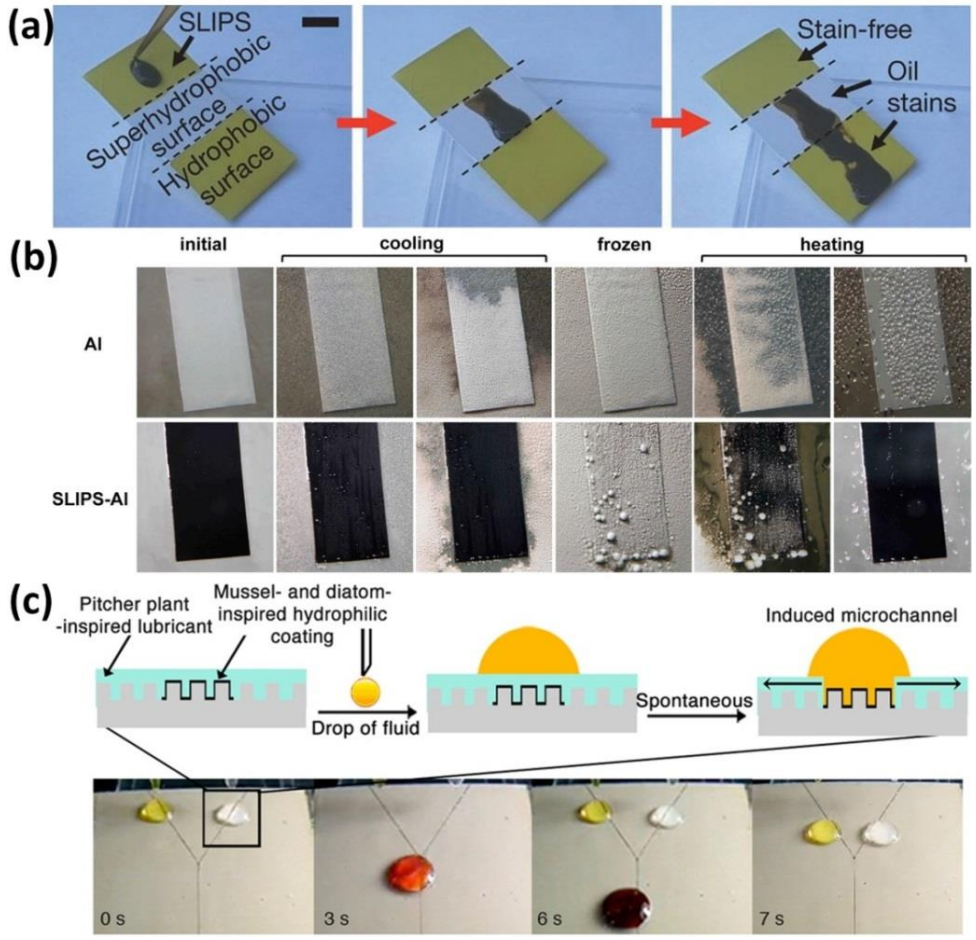

Fig. 1.15 Examples of SLIPS applications. (a) Light crude oil moved on SLIPS, superhydrophobic Teflon porous membrane and flat hydrophobic surface, respectively; SLIPS got stain-free while the other two surfaces were contaminated showing a superior self-cleaning property of the SLIPS[114] (Figures reproduce with permission from Ref. 114 © 2011 Macmillan Publishers Limited. All rights reserved). (b) Icing behaviour between the untreated and SLIPS Al surface were compared in high-humidity condition (60% RH). In the cooling cycle from room temperature to -10 °C at 5 °C/min, ice covered uniformly on the untreated Al surface while it seldom formed on the SLIPS Al substrate; in the heating cycle from -10 °C to 25 °C at 10 °C/min, SLIPS Al surface readily melted but the untreated Al surface got droplets pinned on. This test shows the anti-ice/frost properties of SLIPS[120] (Figures reproduce with permission from Ref. 120 © 2012 American Chemical Society). (c) Hydrophilic paths were created on hydrophobic patterned substrates, and then the resulting surface was lubricated by Fluorinert FC-70. Tetrahydrofuran (THF) solution of *o*-phenylenediamine and benzaldehyde (the left yellow droplet) and the THF solution of iodobenzene diacetate (the right colourless droplet) were then guided to travel along the path and join together to complete the organic reaction[126] (Figures reproduce with permission from Ref. 126 © 2014 American Chemical Society).

1.3 Applications of repellent surfaces

1.3.1 Applications of superhydrophobic surfaces

One of the most straightforward applications of superhydrophobic surfaces is to repel water. The water-repellent properties can be used to make waterproofing coats and electronic devices. Due to their water repellence, dyed water, mud water and even sometimes water-based acid and base are not able to stain superhydrophobic surfaces; the stain-resistance of superhydrophobic surfaces is one aspect of their self-cleaning functions or the "Lotus effect". The other aspect of self-cleaning is that running water easily picks up and removes dust and bacteria on the superhydrophobic surfaces; this property is called dirt-removal property as discussed above. Apart from water-repellence and self-cleaning properties, superhydrophobic surfaces have many other applications, such as anti-corrosion, drag reduction, anti-bacterial, anti-icing and oil-water separation.

1. Anti-corrosion

Metal corrosion is a significant problem for aircraft, automobiles, pipelines, and naval vessels, leading to huge economic losses.[135] One of the most well-known examples of metal corrosion is iron rusting, which is mainly due to the exposure of water and oxygen. Since oxygen is abundant in air, it is easier to prevent metal from water. There are many reports regarding the anti-corrosion properties using superhydrophobic surfaces on metal substrates such as aluminium,[136] copper,[137-139] magnesium[81, 140, 141] and steel.[142, 143]

2. Drag reduction

The low fraction of contact between water and superhydrophobic surfaces enables a high mobility for water to travel on superhydrophobic surfaces. Therefore, superhydrophobic surfaces can be used for drag reduction. For example, the flow rate of water is much higher in a superhydrophobic tube/pipe than that in normal tubes/pipes.[144, 145] Superhydrophobic surfaces can be further treated on ships so that they could travel with less drag and less energy consumption in water.[146, 147]

3. Anti-icing

Icing of surfaces causes serious and recurrent problems in cold-climate regions,[148, 149] this is because the exposure of a surface to freezing rain (super-cooled water) leads to materials damage. Due to less fraction of water contact, superhydrophobic surfaces dramatically reduce

the ice formation upon impact of super-cooled water.[150] However, superhydrophobic surfaces are not able to stop the icing behaviour but to delay the ice formation.[151] That is, icing will eventually happen if the temperature is low enough, the atmospheric humanity is high enough, or the exposure time to cold temperature is long enough.

4. Anti-bacteria

The anti-bacterial property of superhydrophobic surfaces does not refer to inducing the death of bacteria; instead, superhydrophobic coatings greatly reduce the likelihood for bacteria to attach to the surface.[152] Due to the less contact and high mobility of water on superhydrophobic surfaces, it is difficult for bacteria to colonise the surface because the bacteria will be going with the rolling water droplets or their culture solution.[153-155]

5. Oil-water separation

In most cases, superhydrophobic surfaces can be easily wetted by liquid hydrocarbons with lower surface tensions than that of water, such as peanut oil and hexadecane.[76, 156, 157] On this point, superhydrophobic coatings can be treated on mesh, sponge or membrane for oil-water-separation, in a way that oil is able to pass through the mesh while water is stopped.[158, 159] The oil-water separation properties of superhydrophobic surfaces have great potential to be used for water purification and oil recycling.[160]

1.3.2 Applications of superoleophobic surfaces

Superoleophobic surfaces own most of the functions that superhydrophobic surfaces have, such as anti-corrosion, drag reduction, anti-bacterial, and anti-icing.[161, 162] Moreover, superoleophobic surfaces have superior self-cleaning properties compared with superhydrophobic surfaces. For example, superoleophobic surfaces repel cooking oils, which could readily stain a superhydrophobic surface. However, superoleophobic surfaces cannot usually be used for oil-water separation because in most cases they repel both water and oils. This is one exception – a superhydrophilic–superoleophobic coating.[163] This coating was treated onto a mesh to make a superhydrophilic–superoleophobic surface, which allows water to pass through the mesh while stops oil.

1.3.3 Applications of SLIPS surfaces

SLIPS surfaces repel most liquids including water and liquid hydrocarbons. Instead of using air pockets to support liquid, SLIPS apply a lubricating layer to fill the air pockets which are created by a highly textured surface morphology. The lubricating layer is usually a liquid with low surface tension and should not be miscible with the liquids that are expected to be repelled (testing liquids). The main advantage of SLIPS compared with "dry" super-repellent surfaces is that SLIPS surfaces will survive when high pressure is applied because the lubricating layer in SLIPS is more stable than the air cushion in "dry" super-repellent surfaces. Therefore, SLIPS is expected to have longer longevity than that of "dry" super-repellent surfaces when the surfaces are used in high atmospheric pressure or underwater. However, the disadvantage of SLIPS is that the surfaces would lose the repelling properties once the lubricating layer is dried. Apart from the above mentioned situations, SLIPS can be applied in most cases where superoleophobic and superhydrophobic surfaces are used, such as self-cleaning,[128, 164] anti-icing,[119, 165] and anti-biofouling.[117, 166]

1.4 Summary

In this "Introduction", the mechanism, synthesis and applications of superhydrophobic surfaces, superoloephobic surfaces and SLIPS have been introduced. Although these surfaces show different functions, they have two things in common: (1) they are designed to repel liquids; (2) their functions are dependent on their surface micro/nano morphologies. However, these micro/nano morphologies are mechanically weak and may be easily damaged by a finger print, resulting in the loss of their repelling functions. This thesis will present strategies regarding the improvement of surface robustness of repellent surfaces.

In the following chapter (Chapter 2), superhydrophobic coatings are treated onto steel surfaces (hard substrate) and some soft porous materials such as cotton, filter paper and scouring pad. Steel surface was chemically etched by $CuCl_2$ solution to create surface roughness, and the by-products in this reaction were deposited onto soft substrates. Both the steel and the soft materials became superhydrophobic after low surface energy modification. Moreover, the steel mesh was made superhydrophobic-oloephilic for oil-water separation, achieving a separation rate of 96%. However, the surface robustness of steel surface was comparatively weak; the surface lost superhydrophobicity after 6 cycles of sandpaper abrasion. Therefore, the synthesis of a more durable superhydrophobic surface is presented in Chapter 3.

In Chapter 3, a paint-like suspension was fabricated using dual scaled TiO_2 nanoparticles and an ethanol-based solution containing fluorosilane. This paint can be treated onto almost any solid surfaces such as glass, steel, cotton and paper. The superhydrophobic coating is highly compatible with commercial adhesives, and the surfaces retained superhydrophobicity after finger print, knife cut and even 40 cycles of sandpaper abrasion. The surface repelled water even after oil-contamination, however, it did not repel oil, therefore, a durable surface that repels both water and oil is introduced in Chapter 4.

In Chapter 4, a SLIPS coating was fabricated by lubricating a superhydrophobic paint treated substrate that was reported in Chapter 3. The SLIPS not only inherited most of the advantages from the superhydrophobic painted coatings (for example, it can be treated onto most solid substrates; it is highly durable etc.), but also repel various liquids such as water, coffee, red wine, cooking oil and hexadecane. Apart from mechanical tests, the SLIPS surfaces also retained omniphobicity after thermal and chemical durability tests such as low (-196 °C) and high temperatures (200 °C), and exposure to acid and base liquids.

This thesis performs facile and low cost methods to prepare robust superhydrophobic and SLIPS surfaces, hopefully one day this technique will benefit people's daily life at every aspect.

1.5 References

1. Barthlott, W.; Neinhuis, C. Purity of the sacred lotus, or escape from contamination in biological surfaces. *Planta* 1997, 202, 1-8.

2. Patankar, N. A. Mimicking the lotus effect: influence of double roughness structures and slender pillars. *Langmuir* 2004, 20, 8209-8213.

3. Bhushan, B.; Jung, Y. C.; Koch, K. Micro-, nano-and hierarchical structures for superhydrophobicity, self-cleaning and low adhesion. *Philosophical Transactions of the Royal Society of London A: Mathematical, Physical and Engineering Sciences* 2009, 367, 1631-1672.

4. Li, X.-M.; Reinhoudt, D.; Crego-Calama, M. What do we need for a superhydrophobic surface? A review on the recent progress in the preparation of superhydrophobic surfaces. *Chemical Society Reviews* 2007, 36, 1350-1368.

5. Su, Y.; Ji, B.; Zhang, K.; Gao, H.; Huang, Y.; Hwang, K. Nano to micro structural hierarchy is crucial for stable superhydrophobic and water-repellent surfaces. *Langmuir* 2010, 26, 4984-4989.

6. Cheng, Y. T.; Rodak, D. E.; Wong, C. A.; Hayden, C. A. Effects of micro-and nano-structures on the self-cleaning behaviour of lotus leaves. *Nanotechnology* 2006, 17, 1359.

7. Fürstner, R.; Barthlott, W.; Neinhuis, C.; Walzel, P. Wetting and self-cleaning properties of artificial superhydrophobic surfaces. *Langmuir* 2005, 21, 956-961.

8. Burton, Z.; Bhushan, B. Surface characterization and adhesion and friction properties of hydrophobic leaf surfaces. *Ultramicroscopy* 2006, 106, 709-719.

9. Nosonovsky, M.; Bhushan, B. Roughness optimization for biomimetic superhydrophobic surfaces. *Microsystem Technologies* 2005, 11, 535-549.

10. Feng, X.-Q.; Gao, X.; Wu, Z.; Jiang, L.; Zheng, Q.-S. Superior water repellency of water strider legs with hierarchical structures: experiments and analysis. *Langmuir* 2007, 23, 4892-4896.

11. Gao, X.; Jiang, L. Biophysics: water-repellent legs of water striders. *Nature* 2004, 432, 36-36.

12. Zheng, Y.; Gao, X.; Jiang, L. Directional adhesion of superhydrophobic butterfly wings. *Soft Matter* 2007, 3, 178-182.

13. Zhang, X.; Shi, F.; Niu, J.; Jiang, Y.; Wang, Z. Superhydrophobic surfaces: from structural control to functional application. *Journal of Materials Chemistry* 2008, 18, 621-633.

14. Bormashenko, E.; Bormashenko, Y.; Stein, T.; Whyman, G.; Bormashenko, E. Why do pigeon feathers repel water? Hydrophobicity of pennae, Cassie–Baxter wetting hypothesis and Cassie–Wenzel capillarity-induced wetting transition. *Journal of colloid and interface science* 2007, 311, 212-216.

15. Bormashenko, E.; Gendelman, O.; Whyman, G. Superhydrophobicity of lotus leaves versus birds wings: different physical mechanisms leading to similar phenomena. *Langmuir* 2012, 28, 14992-14997.

16. Bohn, H. F.; Federle, W. Insect aquaplaning: Nepenthes pitcher plants capture prey with the peristome, a fully wettable water-lubricated anisotropic surface. *Proceedings of the National Academy of Sciences of the United States of America* 2004, 101, 14138-14143.

17. Chen, H.; Zhang, P.; Zhang, L.; Liu, H.; Jiang, Y.; Zhang, D.; Han, Z.; Jiang, L. Continuous directional water transport on the peristome surface of Nepenthes alata. *Nature* 2016, 532, 85-89.

18. Braun, R. J. Dynamics of the tear film. *Annual Review of Fluid Mechanics* 2012, 44, 267-297.

19. Oatis, C. A. The mechanics and pathomechanics of human movement. 2003.

20. Federle, W.; Barnes, W. J. P.; Baumgartner, W.; Drechsler, P.; Smith, J. M. Wet but not slippery: boundary friction in tree frog adhesive toe pads. *Journal of The Royal Society Interface* 2006, 3, 689-697.

21. Parker, A. R.; Lawrence, C. R. Water capture by a desert beetle. *Nature* 2001, 414, 33-34.

22. Zhai, L.; Berg, M. C.; Cebeci, F. C.; Kim, Y.; Milwid, J. M.; Rubner, M. F.; Cohen, R. E. Patterned superhydrophobic surfaces: toward a synthetic mimic of the Namib Desert beetle. *Nano Letters* 2006, 6, 1213-1217.

23. Ju, J.; Bai, H.; Zheng, Y.; Zhao, T.; Fang, R.; Jiang, L. A multi-structural and multi-functional integrated fog collection system in cactus. *Nature communications* 2012, 3, 1247.

24. Lorenceau, É.; Quéré, D. Drops on a conical wire. *Journal of Fluid Mechanics* 2004, 510, 29-45.

25. Renvoisé, P.; Bush, J. W. M.; Prakash, M.; Quéré, D. Drop propulsion in tapered tubes. *EPL (Europhysics Letters)* 2009, 86, 64003.

26. Chaudhury, M. K.; Whitesides, G. M. How to make water run uphill. *Science* 1992, 256, 1539-1541.

27. Daniel, S.; Chaudhury, M. K.; Chen, J. C. Fast drop movements resulting from the phase change on a gradient surface. *Science* 2001, 291, 633-636.

28. Patankar, N. A. On the modeling of hydrophobic contact angles on rough surfaces. *Langmuir* 2003, 19, 1249-1253.

29. Feng, L.; Li, S.; Li, H.; Zhai, J.; Song, Y.; Jiang, L.; Zhu, D. Super‐hydrophobic surface of aligned polyacrylonitrile nanofibers. *Angewandte Chemie* 2002, 114, 1269-1271.

30. Feng, X.; Feng, L.; Jin, M.; Zhai, J.; Jiang, L.; Zhu, D. Reversible super-hydrophobicity to super-hydrophilicity transition of aligned ZnO nanorod films. *Journal of the American Chemical Society* 2004, 126, 62-63.

31. Young, T. An essay on the cohesion of fluids. *Philosophical Transactions of the Royal Society of London* 1805, 95, 65-87.

32. Cassie, A. B. D.; Baxter, S. Wettability of porous surfaces. *Transactions of the Faraday Society* 1944, 40, 546-551.

33. Cassie, A. B. D. Contact angles. *Discussions of the Faraday Society* 1948, 3, 11-16.

34. Wenzel, R. N. Resistance of solid surfaces to wetting by water. *Industrial & Engineering Chemistry* 1936, 28, 988-994.

35. Wenzel, R. N. Surface Roughness and Contact Angle. *The Journal of Physical Chemistry* 1949, 53, 1466-1467.

36. Ma, Y.; Cao, X.; Feng, X.; Ma, Y.; Zou, H. Fabrication of super-hydrophobic film from PMMA with intrinsic water contact angle below 90. *Polymer* 2007, 48, 7455-7460.

37. Yuan, Y.; Lee, T. R. Contact angle and wetting properties. In *Surface science techniques*, Springer: 2013; pp 3-34.

38. Antonini, C.; Villa, F.; Bernagozzi, I.; Amirfazli, A.; Marengo, M. Drop rebound after impact: the role of the receding contact angle. *Langmuir* 2013, 29, 16045-16050.

39. Berg, J. M.; Eriksson, L. G. T.; Claesson, P. M.; Borve, K. G. N. Three-component Langmuir-Blodgett films with a controllable degree of polarity. *Langmuir* 1994, 10, 1225-1234.

40. Guo, C.; Wang, S.; Liu, H.; Feng, L.; Song, Y.; Jiang, L. Wettability alteration of polymer surfaces produced by scraping. *Journal of Adhesion Science and Technology* 2008, 22, 395-402.

41. Wang, S.; Liu, K.; Yao, X.; Jiang, L. Bioinspired Surfaces with Superwettability: New Insight on Theory, Design, and Applications. *Chemical Reviews* 2015, 115, 8230-8293.

42. Vogler, E. A. Structure and reactivity of water at biomaterial surfaces. *Advances in colloid and interface science* 1998, 74, 69-117.

43. Rafiee, J.; Rafiee, M. A.; Yu, Z. Z.; Koratkar, N. Superhydrophobic to superhydrophilic wetting control in graphene films. *Advanced Materials* 2010, 22, 2151-2154.

44. Wang, J.; Wen, Y.; Hu, J.; Song, Y.; Jiang, L. Fine Control of the Wettability Transition Temperature of Colloidal‐Crystal Films: From Superhydrophilic to Superhydrophobic. *Advanced Functional Materials* 2007, 17, 219-225.

45. Zhang, X.; Jin, M.; Liu, Z.; Tryk, D. A.; Nishimoto, S.; Murakami, T.; Fujishima, A. Superhydrophobic TiO2 surfaces: Preparation, photocatalytic wettability conversion, and superhydrophobic-superhydrophilic patterning. *The Journal of Physical Chemistry C* 2007, 111, 14521-14529.

46. Dean, B.; Bhushan, B. Shark-skin surfaces for fluid-drag reduction in turbulent flow: a review. *Philosophical Transactions of the Royal Society of London A: Mathematical, Physical and Engineering Sciences* 2010, 368, 4775-4806.

47. Bechert, D. W.; Bruse, M.; Hage, W. Experiments with three-dimensional riblets as an idealized model of shark skin. *Experiments in fluids* 2000, 28, 403-412.

48. Ball, P. Engineering shark skin and other solutions. *Nature* 1999, 400, 507-509.

49. Koch, K.; Barthlott, W. Superhydrophobic and superhydrophilic plant surfaces: an inspiration for biomimetic materials. *Philosophical Transactions of the Royal Society of London A: Mathematical, Physical and Engineering Sciences* 2009, 367, 1487-1509.

50. Liu, X.; Zhou, J.; Xue, Z.; Gao, J.; Meng, J.; Wang, S.; Jiang, L. Clam's Shell Inspired High‐Energy Inorganic Coatings with Underwater Low Adhesive Superoleophobicity. *Advanced Materials* 2012, 24, 3401-3405.

51. Miwa, M.; Nakajima, A.; Fujishima, A.; Hashimoto, K.; Watanabe, T. Effects of the surface roughness on sliding angles of water droplets on superhydrophobic surfaces. *Langmuir* 2000, 16, 5754-5760.

52. Yan, Y. Y.; Gao, N.; Barthlott, W. Mimicking natural superhydrophobic surfaces and grasping the wetting process: A review on recent progress in preparing superhydrophobic surfaces. *Advances in colloid and interface science* 2011, 169, 80-105.

53. Verho, T.; Bower, C.; Andrew, P.; Franssila, S.; Ikkala, O.; Ras, R. H. A. Mechanically durable superhydrophobic surfaces. *Advanced Materials* 2011, 23, 673-678.

54. Lu, Y.; Sathasivam, S.; Song, J.; Crick, C. R.; Carmalt, C. J.; Parkin, I. P. Robust self-cleaning surfaces that function when exposed to either air or oil. *Science* 2015, 347, 1132-1135.

55. Nakajima, A.; Abe, K.; Hashimoto, K.; Watanabe, T. Preparation of hard super-hydrophobic films with visible light transmission. *Thin Solid Films* 2000, 376, 140-143.

56. Pierce, E.; Carmona, F. J.; Amirfazli, A. Understanding of sliding and contact angle results in tilted plate experiments. *Colloids and Surfaces A: Physicochemical and Engineering Aspects* 2008, 323, 73-82.

57. Han, D.; Steckl, A. J. Superhydrophobic and oleophobic fibers by coaxial electrospinning. *Langmuir* 2009, 25, 9454-9462.

58. Wang, M.-F.; Raghunathan, N.; Ziaie, B. A nonlithographic top-down electrochemical approach for creating hierarchical (micro-nano) superhydrophobic silicon surfaces. *Langmuir* 2007, 23, 2300-2303.

59. Koch, K.; Bhushan, B.; Jung, Y. C.; Barthlott, W. Fabrication of artificial Lotus leaves and significance of hierarchical structure for superhydrophobicity and low adhesion. *Soft Matter* 2009, 5, 1386-1393.

60. Ming, W.; Wu, D.; van Benthem, R.; De With, G. Superhydrophobic films from raspberry-like particles. *Nano letters* 2005, 5, 2298-2301.

61. Guo, Z.-G.; Liu, W.-M.; Su, B.-L. A stable lotus-leaf-like water-repellent copper. *Applied Physics Letters* 2008, 92, 063104.

62. Jin, M.; Feng, X.; Feng, L.; Sun, T.; Zhai, J.; Li, T.; Jiang, L. Superhydrophobic aligned polystyrene nanotube films with high adhesive force. *Advanced Materials* 2005, 17, 1977-1981.

63. Bhushan, B.; Her, E. K. Fabrication of superhydrophobic surfaces with high and low adhesion inspired from rose petal. *Langmuir* 2010, 26, 8207-8217.

64. Feng, L.; Zhang, Y.; Xi, J.; Zhu, Y.; Wang, N.; Xia, F.; Jiang, L. Petal effect: a superhydrophobic state with high adhesive force. *Langmuir* 2008, 24, 4114-4119.

65. Bormashenko, E.; Stein, T.; Pogreb, R.; Aurbach, D. “Petal Effect” on surfaces based on lycopodium: High-stick surfaces demonstrating high apparent contact angles. *The Journal of Physical Chemistry C* 2009, 113, 5568-5572.

66. Ebert, D.; Bhushan, B. Wear-resistant rose petal-effect surfaces with superhydrophobicity and high droplet adhesion using hydrophobic and hydrophilic nanoparticles. *Journal of colloid and interface science* 2012, 384, 182-188.

67. Liu, K.; Du, J.; Wu, J.; Jiang, L. Superhydrophobic gecko feet with high adhesive forces towards water and their bio-inspired materials. *Nanoscale* 2012, 4, 768-772.

68. Li, J.; Liu, X.; Ye, Y.; Zhou, H.; Chen, J. Gecko-inspired synthesis of superhydrophobic ZnO surfaces with high water adhesion. *Colloids and Surfaces A: Physicochemical and Engineering Aspects* 2011, 384, 109-114.

69. Cheng, Z.; Feng, L.; Jiang, L. Tunable adhesive superhydrophobic surfaces for superparamagnetic microdroplets. *Advanced Functional Materials* 2008, 18, 3219-3225.

70. Extrand, C. W.; Kumagai, Y. An experimental study of contact angle hysteresis. *Journal of Colloid and interface Science* 1997, 191, 378-383.

71. Ouchi, T.; Kontani, T.; Saito, T.; Ohya, Y. Suppression of cell attachment and protein adsorption onto amphiphilic polylactide-grafted dextran films. *Journal of Biomaterials Science, Polymer Edition* 2005, 16, 1035-1045.

72. Krishnan, A.; Liu, Y.-H.; Cha, P.; Woodward, R.; Allara, D.; Vogler, E. A. An evaluation of methods for contact angle measurement. *Colloids and Surfaces B: Biointerfaces* 2005, 43, 95-98.

73. Ma, M.; Hill, R. M. Superhydrophobic surfaces. *Current opinion in colloid & interface science* 2006, 11, 193-202.

74. Wang, S.; Feng, L.; Jiang, L. One‐Step Solution‐Immersion Process for the Fabrication of Stable Bionic Superhydrophobic Surfaces. *Advanced Materials* 2006, 18, 767-770.

75. Wang, H.; Xue, Y.; Ding, J.; Feng, L.; Wang, X.; Lin, T. Durable, Self‐Healing Superhydrophobic and Superoleophobic Surfaces from Fluorinated‐Decyl Polyhedral Oligomeric Silsesquioxane and Hydrolyzed Fluorinated Alkyl Silane. *Angewandte Chemie International Edition* 2011, 50, 11433-11436.

76. Yao, X.; Gao, J.; Song, Y.; Jiang, L. Superoleophobic surfaces with controllable oil adhesion and their application in oil transportation. *Advanced Functional Materials* 2011, 21, 4270-4276.

77. Pan, S.; Kota, A. K.; Mabry, J. M.; Tuteja, A. Superomniphobic surfaces for effective chemical shielding. *Journal of the American Chemical Society* 2012, 135, 578-581.

78. Wilson, P. W.; Lu, W.; Xu, H.; Kim, P.; Kreder, M. J.; Alvarenga, J.; Aizenberg, J. Inhibition of ice nucleation by slippery liquid-infused porous surfaces (SLIPS). *Physical Chemistry Chemical Physics* 2013, 15, 581-585.

79. Li, J.; Kleintschek, T.; Rieder, A.; Cheng, Y.; Baumbach, T.; Obst, U.; Schwartz, T.; Levkin, P. A. Hydrophobic liquid-infused porous polymer surfaces for antibacterial applications. *ACS applied materials & interfaces* 2013, 5, 6704-6711.

80. Manabe, K.; Nishizawa, S.; Kyung, K.-H.; Shiratori, S. Optical phenomena and antifrosting property on biomimetics slippery fluid-infused antireflective films via layer-by-layer comparison with superhydrophobic and antireflective films. *ACS applied materials & interfaces* 2014, 6, 13985-13993.

81. Xu, W.; Song, J.; Sun, J.; Lu, Y.; Yu, Z. Rapid fabrication of large-area, corrosion-resistant superhydrophobic Mg alloy surfaces. *ACS applied materials & interfaces* 2011, 3, 4404-4414.

82. Lu, Y.; Sathasivam, S.; Song, J.; Xu, W.; Carmalt, C. J.; Parkin, I. P. Water droplets bouncing on superhydrophobic soft porous materials. *Journal of Materials Chemistry A* 2014, 2, 12177-12184.

83. Richard, D.; Clanet, C.; Quéré, D. Surface phenomena: Contact time of a bouncing drop. *Nature* 2002, 417, 811-811.

84. Bird, J. C.; Dhiman, R.; Kwon, H.-M.; Varanasi, K. K. Reducing the contact time of a bouncing drop. *Nature* 2013, 503, 385-388.

85. Liu, Y.; Moevius, L.; Xu, X.; Qian, T.; Yeomans, J. M.; Wang, Z. Pancake bouncing on superhydrophobic surfaces. *Nat Phys* 2014, 10, 515-519.

86. Erbil, H. Y.; Demirel, A. L.; Avcı, Y.; Mert, O. Transformation of a simple plastic into a superhydrophobic surface. *Science* 2003, 299, 1377-1380.

87. Xue, C.-H.; Jia, S.-T.; Zhang, J.; Ma, J.-Z. Large-area fabrication of superhydrophobic surfaces for practical applications: an overview. *Science and Technology of Advanced Materials* 2016.

88. Qian, B.; Shen, Z. Fabrication of superhydrophobic surfaces by dislocation-selective chemical etching on aluminum, copper, and zinc substrates. *Langmuir* 2005, 21, 9007-9009.

89. Liao, R.; Zuo, Z.; Guo, C.; Yuan, Y.; Zhuang, A. Fabrication of superhydrophobic surface on aluminum by continuous chemical etching and its anti-icing property. *Applied Surface Science* 2014, 317, 701-709.

90. Song, J.; Xu, W.; Liu, X.; Lu, Y.; Wei, Z.; Wu, L. Ultrafast fabrication of rough structures required by superhydrophobic surfaces on Al substrates using an immersion method. *Chemical engineering journal* 2012, 211, 143-152.

91. Darmanin, T.; de Givenchy, E. T.; Amigoni, S.; Guittard, F. Superhydrophobic surfaces by electrochemical processes. *Advanced materials* 2013, 25, 1378-1394.

92. Lu, Y.; Xu, W.; Song, J.; Liu, X.; Xing, Y.; Sun, J. Preparation of superhydrophobic titanium surfaces via electrochemical etching and fluorosilane modification. *Applied Surface Science* 2012, 263, 297-301.

93. Lu, Y.; Song, J.; Liu, X.; Xu, W.; Sun, J.; Xing, Y. Loading capacity of a self-assembled superhydrophobic boat array fabricated via electrochemical method. *IET Micro & Nano Letters* 2012, 7, 786-789.

94. Crick, C. R.; Bear, J. C.; Kafizas, A.; Parkin, I. P. Superhydrophobic photocatalytic surfaces through direct incorporation of titania nanoparticles into a polymer matrix by aerosol assisted chemical vapor deposition. *Advanced Materials* 2012, 24, 3505-3508.

95. Crick, C. R.; Parkin, I. P. A single step route to superhydrophobic surfaces through aerosol assisted deposition of rough polymer surfaces: duplicating the lotus effect. *Journal of Materials Chemistry* 2009, 19, 1074-1076.

96. Liu, H.; Feng, L.; Zhai, J.; Jiang, L.; Zhu, D. Reversible wettability of a chemical vapor deposition prepared ZnO film between superhydrophobicity and superhydrophilicity. *Langmuir* 2004, 20, 5659-5661.

97. Wu, W.; Wang, X.; Liu, X.; Zhou, F. Spray-coated fluorine-free superhydrophobic coatings with easy repairability and applicability. *ACS applied materials & interfaces* 2009, 1, 1656-1661.

98. Ogihara, H.; Okagaki, J.; Saji, T. Facile fabrication of colored superhydrophobic coatings by spraying a pigment nanoparticle suspension. *Langmuir* 2011, 27, 9069-9072.

99. Hwang, H. S.; Kim, N. H.; Lee, S. G.; Lee, D. Y.; Cho, K.; Park, I. Facile fabrication of transparent superhydrophobic surfaces by spray deposition. *ACS applied materials & interfaces* 2011, 3, 2179-2183.

100. Han, J. T.; Jang, Y.; Lee, D. Y.; Park, J. H.; Song, S.-H.; Ban, D.-Y.; Cho, K. Fabrication of a bionic superhydrophobic metal surface by sulfur-induced morphological development. *Journal of Materials Chemistry* 2005, 15, 3089-3092.

101. Zhang, W.; Yu, Z.; Chen, Z.; Li, M. Preparation of super-hydrophobic Cu/Ni coating with micro-nano hierarchical structure. *Materials Letters* 2012, 67, 327-330.

102. Lu, Y.; Song, J.; Liu, X.; Xu, W.; Xing, Y.; Wei, Z. Preparation of Superoleophobic and Superhydrophobic Titanium Surfaces via an Environmentally Friendly Electrochemical Etching Method. *ACS Sustainable Chemistry & Engineering* 2013, 1, 102-109.

103. Tuteja, A.; Choi, W.; Ma, M.; Mabry, J. M.; Mazzella, S. A.; Rutledge, G. C.; McKinley, G. H.; Cohen, R. E. Designing superoleophobic surfaces. *Science* 2007, 318, 1618-1622.

104. Bellanger, H.; Darmanin, T.; Taffin de Givenchy, E.; Guittard, F. Chemical and physical pathways for the preparation of superoleophobic surfaces and related wetting theories. *Chemical reviews* 2014, 114, 2694-2716.

105. Zhou, H.; Wang, H.; Niu, H.; Gestos, A.; Lin, T. Robust, self‐healing superamphiphobic fabrics prepared by two‐step coating of fluoro‐containing polymer,

fluoroalkyl silane, and modified silica nanoparticles. *Advanced functional materials* 2013, 23, 1664-1670.

106. He, Z.; Ma, M.; Lan, X.; Chen, F.; Wang, K.; Deng, H.; Zhang, Q.; Fu, Q. Fabrication of a transparent superamphiphobic coating with improved stability. *Soft Matter* 2011, 7, 6435-6443.

107. Kang, S. M.; Kim, S. M.; Kim, H. N.; Kwak, M. K.; Tahk, D. H.; Suh, K. Y. Robust superomniphobic surfaces with mushroom-like micropillar arrays. *Soft Matter* 2012, 8, 8563-8568.

108. Ahuja, A.; Taylor, J. A.; Lifton, V.; Sidorenko, A. A.; Salamon, T. R.; Lobaton, E. J.; Kolodner, P.; Krupenkin, T. N. Nanonails: A simple geometrical approach to electrically tunable superlyophobic surfaces. *Langmuir* 2008, 24, 9-14.

109. Liu, T. L.; Kim, C.-J. C. Turning a surface superrepellent even to completely wetting liquids. *Science* 2014, 346, 1096-1100.

110. Ou, J.; Hu, W.; Liu, S.; Xue, M.; Wang, F.; Li, W. Superoleophobic textured copper surfaces fabricated by chemical etching/oxidation and surface fluorination. *ACS applied materials & interfaces* 2013, 5, 10035-10041.

111. Song, J.; Huang, S.; Hu, K.; Lu, Y.; Liu, X.; Xu, W. Fabrication of superoleophobic surfaces on Al substrates. *Journal of Materials Chemistry A* 2013, 1, 14783-14789.

112. Kota, A. K.; Li, Y.; Mabry, J. M.; Tuteja, A. Hierarchically structured superoleophobic surfaces with ultralow contact angle hysteresis. *Advanced Materials* 2012, 24, 5838-5843.

113. Deng, X.; Mammen, L.; Butt, H.-J.; Vollmer, D. Candle soot as a template for a transparent robust superamphiphobic coating. *Science* 2012, 335, 67-70.

114. Wong, T.-S.; Kang, S. H.; Tang, S. K. Y.; Smythe, E. J.; Hatton, B. D.; Grinthal, A.; Aizenberg, J. Bioinspired self-repairing slippery surfaces with pressure-stable omniphobicity. *Nature* 2011, 477, 443-447.

115. Charpentier, T. V. J.; Neville, A.; Baudin, S.; Smith, M. J.; Euvrard, M.; Bell, A.; Wang, C.; Barker, R. Liquid infused porous surfaces for mineral fouling mitigation. *Journal of colloid and interface science* 2015, 444, 81-86.

116. Sunny, S.; Vogel, N.; Howell, C.; Vu, T. L.; Aizenberg, J. Lubricant‐Infused Nanoparticulate Coatings Assembled by Layer‐by‐Layer Deposition. *Advanced Functional Materials* 2014, 24, 6658-6667.

117. Epstein, A. K.; Wong, T.-S.; Belisle, R. A.; Boggs, E. M.; Aizenberg, J. Liquid-infused structured surfaces with exceptional anti-biofouling performance. *Proceedings of the National Academy of Sciences* 2012, 109, 13182-13187.

118. Dai, X.; Stogin, B. B.; Yang, S.; Wong, T.-S. Slippery wenzel state. *ACS nano* 2015, 9, 9260-9267.

119. Liu, Q.; Yang, Y.; Huang, M.; Zhou, Y.; Liu, Y.; Liang, X. Durability of a lubricant-infused Electrospray Silicon Rubber surface as an anti-icing coating. *Applied Surface Science* 2015, 346, 68-76.

120. Kim, P.; Wong, T.-S.; Alvarenga, J.; Kreder, M. J.; Adorno-Martinez, W. E.; Aizenberg, J. Liquid-infused nanostructured surfaces with extreme anti-ice and anti-frost performance. *ACS nano* 2012, 6, 6569-6577.

121. Solomon, B. R.; Khalil, K. S.; Varanasi, K. K. Drag reduction using lubricant-impregnated surfaces in viscous laminar flow. *Langmuir* 2014, 30, 10970-10976.

122. Tsai, P. A. Slippery interfaces for drag reduction. *Journal of fluid mechanics* 2013, 736, 1-4.

123. Yang, S.; Qiu, R.; Song, H.; Wang, P.; Shi, Z.; Wang, Y. Slippery liquid-infused porous surface based on perfluorinated lubricant/iron tetradecanoate: Preparation and corrosion protection application. *Applied Surface Science* 2015, 328, 491-500.

124. Qiu, R.; Zhang, Q.; Wang, P.; Jiang, L.; Hou, J.; Guo, W.; Zhang, H. Fabrication of slippery liquid-infused porous surface based on carbon fiber with enhanced corrosion

inhibition property. *Colloids and Surfaces A: Physicochemical and Engineering Aspects* 2014, 453, 132-141.

125. Wang, P.; Lu, Z.; Zhang, D. Slippery liquid-infused porous surfaces fabricated on aluminum as a barrier to corrosion induced by sulfate reducing bacteria. *Corrosion Science* 2015, 93, 159-166.

126. You, I.; Lee, T. G.; Nam, Y. S.; Lee, H. Fabrication of a micro-omnifluidic device by omniphilic/omniphobic patterning on nanostructured surfaces. *ACS nano* 2014, 8, 9016-9024.

127. Manna, U.; Lynn, D. M. Fabrication of Liquid‐Infused Surfaces Using Reactive Polymer Multilayers: Principles for Manipulating the Behaviors and Mobilities of Aqueous Fluids on Slippery Liquid Interfaces. *Advanced Materials* 2015, 27, 3007-3012.

128. Zhang, J.; Wang, A.; Seeger, S. Nepenthes Pitcher Inspired Anti‐Wetting Silicone Nanofilaments Coatings: Preparation, Unique Anti‐Wetting and Self‐Cleaning Behaviors. *Advanced Functional Materials* 2014, 24, 1074-1080.

129. Wong, T.-S.; Sun, T.; Feng, L.; Aizenberg, J. Interfacial materials with special wettability. *MRS bulletin* 2013, 38, 366-371.

130. Liu, B.; Lange, F. F. Pressure induced transition between superhydrophobic states: configuration diagrams and effect of surface feature size. *Journal of colloid and interface science* 2006, 298, 899-909.

131. Forsberg, P.; Nikolajeff, F.; Karlsson, M. Cassie–Wenzel and Wenzel–Cassie transitions on immersed superhydrophobic surfaces under hydrostatic pressure. *Soft Matter* 2011, 7, 104-109.

132. Nosonovsky, M. Materials science: Slippery when wetted. *Nature* 2011, 477, 412-413.

133. Grinthal, A.; Aizenberg, J. Mobile Interfaces: Liquids as a Perfect Structural Material for Multifunctional, Antifouling Surfaces. *Chemistry of Materials* 2014, 26, 698-708.

134. Jenner, E.; D'Urso, B. Wetting states on structured immiscible liquid coated surfaces. *Applied Physics Letters* 2013, 103, 251606.

135. Mohamed, A. M. A.; Abdullah, A. M.; Younan, N. A. Corrosion behavior of superhydrophobic surfaces: A review. *Arabian Journal of Chemistry* 2015, 8, 749-765.

136. Li, S.-M.; Zhou, S.-Z.; Liu, J.-H. Fabrication and Anti-Corrosion Property of In situ Self-Assembled Super-Hydrophobic Films on Aluminum Alloys. *Acta Physico-Chimica Sinica* 2009, 25, 2581-2589.

137. Khorsand, S.; Raeissi, K.; Ashrafizadeh, F. Corrosion resistance and long-term durability of super-hydrophobic nickel film prepared by electrodeposition process. *Applied Surface Science* 2014, 305, 498-505.

138. Fan, Y.; Li, C.; Chen, Z.; Chen, H. Study on fabrication of the superhydrophobic sol–gel films based on copper wafer and its anti-corrosive properties. *Applied Surface Science* 2012, 258, 6531-6536.

139. Huang, Y.; Sarkar, D. K.; Gallant, D.; Chen, X. G. Corrosion resistance properties of superhydrophobic copper surfaces fabricated by one-step electrochemical modification process. *Applied surface science* 2013, 282, 689-694.

140. Wang, Z.; Li, Q.; She, Z.; Chen, F.; Li, L.; Zhang, X.; Zhang, P. Facile and fast fabrication of superhydrophobic surface on magnesium alloy. *Applied Surface Science* 2013, 271, 182-192.

141. She, Z.; Li, Q.; Wang, Z.; Li, L.; Chen, F.; Zhou, J. Researching the fabrication of anticorrosion superhydrophobic surface on magnesium alloy and its mechanical stability and durability. *Chemical engineering journal* 2013, 228, 415-424.

142. Chen, X.; Yuan, J.; Huang, J.; Ren, K.; Liu, Y.; Lu, S.; Li, H. Large-scale fabrication of superhydrophobic polyurethane/nano-Al 2 O 3 coatings by suspension flame spraying for anti-corrosion applications. *Applied Surface Science* 2014, 311, 864-869.

143. Wang, N.; Xiong, D.; Deng, Y.; Shi, Y.; Wang, K. Mechanically robust superhydrophobic steel surface with anti-icing, UV-durability, and corrosion resistance properties. *ACS applied materials & interfaces* 2015, 7, 6260-6272.

144. Shirtcliffe, N. J.; McHale, G.; Newton, M. I.; Zhang, Y. Superhydrophobic copper tubes with possible flow enhancement and drag reduction. *ACS applied materials & interfaces* 2009, 1, 1316-1323.

145. Watanabe, K.; Udagawa, Y.; Udagawa, H. Drag reduction of Newtonian fluid in a circular pipe with a highly water-repellent wall. *Journal of Fluid Mechanics* 1999, 381, 225-238.

146. Dong, H.; Cheng, M.; Zhang, Y.; Wei, H.; Shi, F. Extraordinary drag-reducing effect of a superhydrophobic coating on a macroscopic model ship at high speed. *Journal of Materials Chemistry A* 2013, 1, 5886-5891.

147. Jiang, C. G.; Xin, S. C.; Wu, C. W. Drag reduction of a miniature boat with superhydrophobic grille bottom. *AIP Advances* 2011, 1, 032148.

148. Frankenstein, S.; Tuthill, A. M. Ice adhesion to locks and dams: past work; future directions? *Journal of cold regions engineering* 2002, 16, 83-96.

149. Parent, O.; Ilinca, A. Anti-icing and de-icing techniques for wind turbines: Critical review. *Cold regions science and technology* 2011, 65, 88-96.

150. Cao, L.; Jones, A. K.; Sikka, V. K.; Wu, J.; Gao, D. Anti-icing superhydrophobic coatings. *Langmuir* 2009, 25, 12444-12448.

151. Kulinich, S. A.; Farhadi, S.; Nose, K.; Du, X. W. Superhydrophobic surfaces: are they really ice-repellent? *Langmuir* 2010, 27, 25-29.

152. Zhang, X.; Wang, L.; Levänen, E. Superhydrophobic surfaces for the reduction of bacterial adhesion. *RSC Advances* 2013, 3, 12003-12020.

153. Privett, B. J.; Youn, J.; Hong, S. A.; Lee, J.; Han, J.; Shin, J. H.; Schoenfisch, M. H. Antibacterial fluorinated silica colloid superhydrophobic surfaces. *Langmuir* 2011, 27, 9597-9601.

154. Crick, C. R.; Ismail, S.; Pratten, J.; Parkin, I. P. An investigation into bacterial attachment to an elastomeric superhydrophobic surface prepared via aerosol assisted deposition. *Thin Solid Films* 2011, 519, 3722-3727.

155. Berendjchi, A.; Khajavi, R.; Yazdanshenas, M. E. Fabrication of superhydrophobic and antibacterial surface on cotton fabric by doped silica-based sols with nanoparticles of copper. *Nanoscale research letters* 2011, 6, 1-8.

156. Darmanin, T.; Guittard, F. Super oil-repellent surfaces from conductive polymers. *Journal of Materials Chemistry* 2009, 19, 7130-7136.

157. Steele, A.; Bayer, I.; Loth, E. Inherently superoleophobic nanocomposite coatings by spray atomization. *Nano letters* 2008, 9, 501-505.

158. Wang, C.-F.; Lin, S.-J. Robust superhydrophobic/superoleophilic sponge for effective continuous absorption and expulsion of oil pollutants from water. *ACS applied materials & interfaces* 2013, 5, 8861-8864.

159. Wu, L.; Zhang, J.; Li, B.; Wang, A. Mechanical-and oil-durable superhydrophobic polyester materials for selective oil absorption and oil/water separation. *Journal of colloid and interface science* 2014, 413, 112-117.

160. Song, J.; Huang, S.; Lu, Y.; Bu, X.; Mates, J. E.; Ghosh, A.; Ganguly, R.; Carmalt, C. J.; Parkin, I. P.; Xu, W. Self-driven one-step oil removal from oil spill on water via selective-wettability steel mesh. *ACS applied materials & interfaces* 2014, 6, 19858-19865.

161. Chu, Z.; Seeger, S. Superamphiphobic surfaces. *Chemical Society Reviews* 2014, 43, 2784-2798.

162. Jiang, T.; Guo, Z.; Liu, W. Biomimetic superoleophobic surfaces: focusing on their fabrication and applications. *Journal of Materials Chemistry A* 2015, 3, 1811-1827.

163. Yang, J.; Zhang, Z.; Xu, X.; Zhu, X.; Men, X.; Zhou, X. Superhydrophilic–superoleophobic coatings. *Journal of Materials Chemistry* 2012, 22, 2834-2837.

164. Huang, X.; Chrisman, J. D.; Zacharia, N. S. Omniphobic slippery coatings based on lubricant-infused porous polyelectrolyte multilayers. *ACS Macro Letters* 2013, 2, 826-829.

165. Kreder, M. J.; Alvarenga, J.; Kim, P.; Aizenberg, J. Design of anti-icing surfaces: smooth, textured or slippery? *Nature Reviews Materials* 2016, 1, 15003.

166. Leslie, D. C.; Waterhouse, A.; Berthet, J. B.; Valentin, T. M.; Watters, A. L.; Jain, A.; Kim, P.; Hatton, B. D.; Nedder, A.; Donovan, K. A bioinspired omniphobic surface coating on medical devices prevents thrombosis and biofouling. *Nature biotechnology* 2014, 32, 1134-1140.

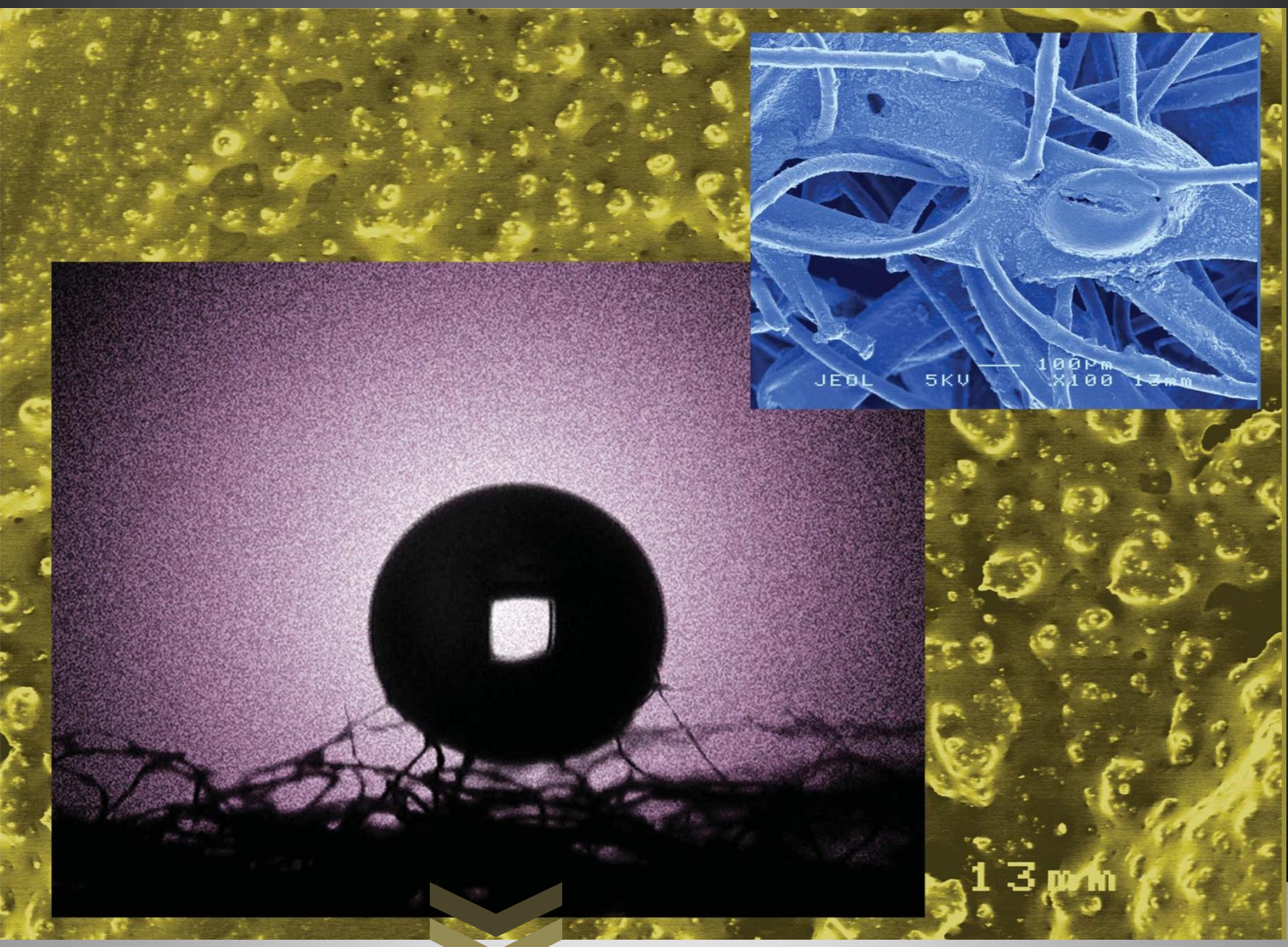

Chapter 2

Making superhydrophobic surfaces *via* chemical methods

Yao Lu

UCL CHEM

About the cover image of Chapter 2

A water droplet was supported by the threads of a superhydrophobic sponge as a perfect sphere.

This image is reproduced with permission from Ref. "*J. Mater. Chem. A* 2014, 2, 12601-12601"

About the figures in this chapter

All the figures except for Fig. 2.2 in Chapter 2 are reproduced with permission from Refs.

"Y. Lu et al., *J. Mater. Chem. A* 2014, 2, 11628-11634 " and

"Y. Lu et al., *J. Mater. Chem. A* 2014, 2, 12177-12184"

Chapter 2
Making superhydrophobic surfaces *via* chemical methods

2.1 Introduction

The substrates of a coating can be divided into two types - hard and soft surfaces.[1] A hard surface refers to a material that is difficult to change its shape under the conditions of room temperature and ordinary pressure, e.g. glass and steel surfaces etc.;[2, 3] a soft substrate means that the nature of the material is flexible and deformable, which usually refers to a fabric/textile (e.g. cotton and cloth) or paper.[4, 5] It is of great practical significance to make superhydrophobic surfaces on both hard and soft materials, for example, to protect carbon steel or mild steel from corrosion, to make water-proofing garments, and to separate oil and water.

2.1.1 Superhydrophobic mild steel

Mild steel, which is considered to be a hard substrate, is one of the most widely used forms of steel because it provides material properties that are acceptable for many applications with a comparatively low price. However, there is an extremely high cost to repair and replace the rusted mild steel every year. The corrosion of mild steel is mainly because of the contact with air and moisture,[6, 7] therefore, making the steel surface superhydrophobic is a potential method to reduce or even stop the rusting.

Zhang *et al.*[3, 8] fabricated superhydrophobic coatings on steel substrates by immersing steel into a mixture of HNO_3 and H_2O_2 solution, followed by low-surface-energy polymer treatments. Hess *et al.*[9] used a 48–51% hydrofluoric acid solution to etch steel surface and make superhydrophobic surfaces. However, the use of strong acids would have an influence to the environment if the abovementioned methods were applied to large scale productions. Tesler *et al.*[10] used electrochemical deposition of nanoporous tungsten oxide to create surface structures to make superhydrophobic and SLIPS steel surfaces, the prepared surfaces were robust but this method cannot be used to make a large-scale object due to the technical limitations. Therefore, a method that avoids strong acid and alkali, and has the potential for large scale applications is needed.

2.1.2 Superhydrophobic soft porous materials

In our daily life, soft porous materials are everywhere, such as our clothes, a piece of paper, and a cleaning sponge. These materials are usually considered to be hydrophilic due to the presence of partially hydroxylated surfaces, so that they are very easy to get wet and stained by rain, mud, ink, coffee etc. For water proofing and self-cleaning purposes, making superhydrophobic surfaces on soft porous substrates such as fabrics, textiles and paper are of great importance.

There are lots of methods to make superhydrophobic cotton fabrics,[11-13] sponges,[14, 15] and paper.[5, 16, 17] However, a simple and general method is still needed to enable fabrics to become superhydrophobic.

2.1.3 Oil-water separation

The technique of oil-water separation is one of the most important applications of superhydrophobic surfaces for water purification and spilt oil collection.[18, 19] The oil–water separation methods using superhydrophobic–superoleophilic mesh/membrane can be briefly classified as three systems: tube-membrane/mesh-container [Fig. 2.1(a) and (b)], mesh-oil container–water container [Fig. 2.1(c) and (d)], and membrane/mesh sealed vessel-water container [Fig. 2.1(e) and (f)]. Here, light oil or organic solvent refers to oil or organic solvent with lower density than that of water; while heavy oil or organic solvent means the oil or organic solvent has a larger density than that of water.

The tube-membrane/mesh-container devices can be used to separate water and heavy oils as well as heavy organic solvents, for example chloroform,[20] dichloromethane,[21] and heavy crude oil.[19] In this system, heavy oils or heavy organic solvents in an oil-water mixture stay on the bottom of the tube; such a condition enables heavy oils or organic solvents to get into contact with the separating mesh or membrane so that they can be filtered. However, this system might not work efficiently if the mixture is made of water and light oil. As shown in Fig. 2.1(a) and (b), the oil-water mixture has to be poured carefully to make sure that oil contacts the separating mesh first and then followed by water. When the light oil-water mixture was poured fast to the tube, or the mixture was not layered clearly, there would be some oil left to float on the water in the tube. In this case, the contact between floating oil and separating mesh was stopped by the water layer in the middle, resulting in a lower oil-water separation rate or a low oil collection rate.

The mesh-oil container-water container system is as shown in Fig. 2.1(c). When the oil-water mixture was poured onto the separating mesh, oil goes through the mesh and get into the beaker underneath, and water rolls to the end of the mesh and get into the further beaker[22]. After this process, oil and water are separated into different beakers as shown in Fig. 2.1(d). This system can be used for both light and heavy oils, but it is subject to spills that would influence the oil-water separation rate.

The system of membrane/mesh sealed vessel-water container uses a superhydrophobic-superoleophilic mesh to cover a vessel,[23-25] which is then positioned into a larger container as

shown in Fig. 2.1(e). When the oil-water mixture was poured onto the separating mesh, oil passes through the mesh and is then collected in the vessel, and water is stopped by the mesh and then goes into the container outside. After the separating process, oil and water are collected into the vessel and the outside container respectively as shown in Fig. 2.1(f). In this system, although the collected oil can be in a high purity, the spills of the mixture would influence the collection rate of water.

Overall, the three oil-water separating systems described have the same drawback, that is, the oil-water mixture has to go very slowly and carefully onto the separating mesh. When the mixture goes quickly, the separation would not be complete, resulting in that some oil goes with water droplets and eventually get into the container for water collection.

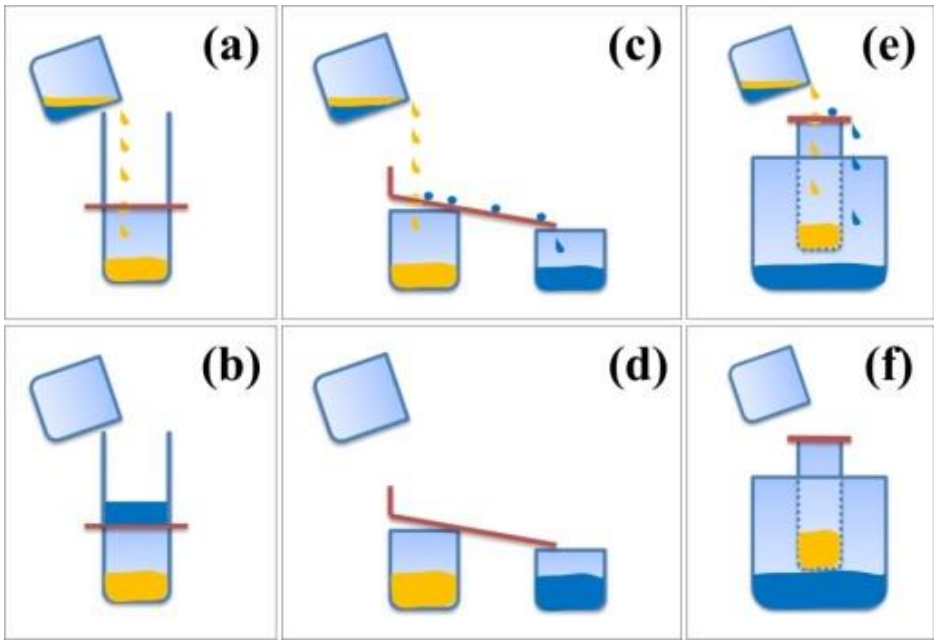

Fig. 2.1 Oil-water separation systems. (a) and (b) are the schematics of the tube-membrane/mesh-container system; (c) to (f) are the schematics of the mesh-oil container-water-container systems. Yellow and blue liquids are oil and water, respectively. Here light oil is used as an example that floats on water. The separating meshes/membranes in the middle are superhydrophobic-superoleophilic.

In this chapter, a "green" route was created to prepare superhydrophobic surfaces on both hard and soft porous materials. First, mild steel was chemically etched by $CuCl_2$ solution to create surface roughness; then the products such as CuCl(OH) and $Cu_2Cl(OH)_3$ were deposited on soft porous substrates including cotton wool, scouring pad, filter paper, sponge etc. to build surface structures. Finally, both hard and soft surfaces with micron roughness

were treated with hydrophobic agents to lower the surface energy. Here, using the products in the former process to contribute to the latter fabrication is an idea that reduces waste in reactions and minimizes the pressure on the environment – this shows the spirit of green chemistry according to American Chemical Society.

The coated steel plates had a water contact angle (WCA) greater than 150° and the treated soft porous materials, such as scouring pad and cotton wool, were able to support the water droplet as a perfect sphere by their threads. The mechanical durability of the treated steel plates was also tested through sandpaper abrasion.

The coated superhydrophobic steel surfaces can not only be used to protect mild steel from rusting, but can also be used for oil-water separations through making a superhydrophobic-superoleophilic mesh. The separation is repeatable and oil collection rate can reach >96%.

2.2 Experimental

2.2.1 Materials

Carbon steel plates (from Goodman) and meshes (0.16 mm diameter, from Mesh UK) were used. Soft porous materials such as scouring pad (from a sponge), filter paper, and cotton wool were used for substrates and were purchased from Aldrich Chemical Co. Cupric chloride (98.0% $CuCl_2 \cdot 2H_2O$) was used for creating surface roughness of carbon steel. 1H, 1H, 2H, 2H-perfluorooctyltriethoxysilane (Fluorosilane, short for FAS, $C_8F_{13}H_4Si(OCH_2CH_3)_3$) and Sylgard 184 Silicone Elastomer were used for reducing the surface energy, as shown in Fig. 2.2. Laboratory solvents (ethanol and chloroform) were at the highest possible grade. All of these chemicals were purchased from Sigma-Aldrich.

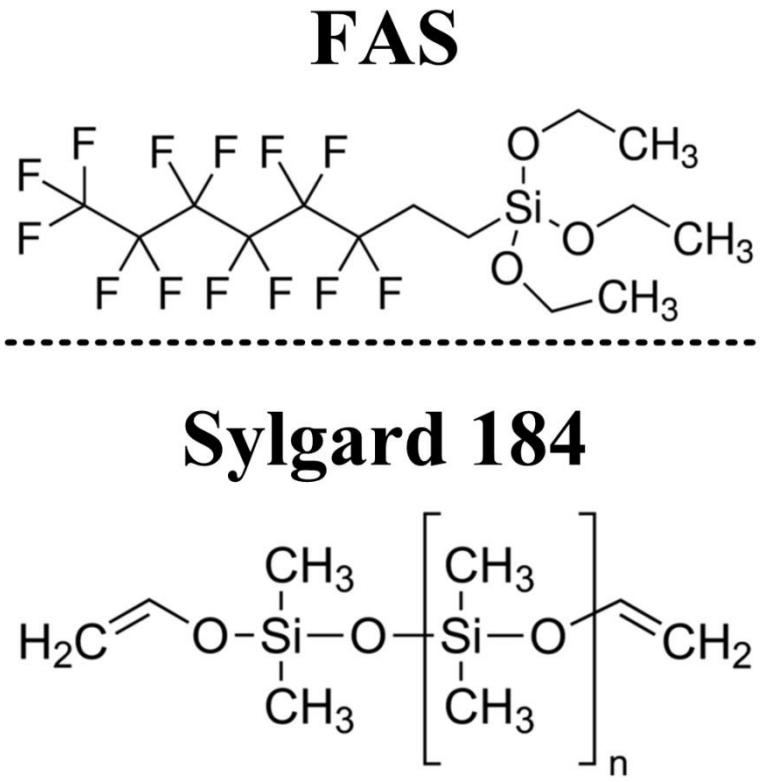

Fig. 2.2 Chemical structures of FAS and Sylgard 184.

2.2.2 Creation of surface micro-nano morphology on hard substrates

Carbon steel plates and meshes were immersed into a solution of $CuCl_2$ (0.2 mol/L; this concentration was arbitrarily chosen, it was effective in this experiment so that alternative concentrations were not tested) in distilled water for 3 min, followed by a 30-min ultrasonical cleaning in distilled water. Then the cleaned carbon steel plates and meshes were dried at 90 °C for 30 min.

2.2.3 Deposition of produced powder on soft materials to make surface roughness

Scouring pad, filter paper, and cotton wool were immersed into the solution used in the previous step; the products after etching steel were left for deposition of micro-nano-scale roughness on soft porous substrates. The solution containing these substrates was stirred at 300 r/min for 10 min and then exposed to air for 2 days. The samples were then dried at 90 °C for 24 hours.

2.2.4 Low surface energy modification

Fluorosilane (FAS) and Sylgard 184 Silicone Elastomer were used as solutions for surface energy reduction.

The method of making FAS: 1.0 wt % 1H, 1H, 2H, 2H-perfluorooctyltriethoxysilane (1 g) was put into an absolute ethanol solvent (99 g) and then the solution was magnetically stirred for 2 hours.

The method of making Sylgard 184 Silicone Elastomer: this elastomer consists of two parts, the first is the elastomer and the second a curing agent to encourage cross linking and hardening to generate a heat resistant polymer. Both polymer and cross link agent (10:1 ratio, here, 10 mL and 1 mL were used) were dissolved in chloroform (50 mL) by rapid stirring for 5 min to make a solution.[26]

The method of coating with FAS or Sylgard 184: samples were imersed into FAS or Sylgard 184 solution for 2 hours and then were dried for 2 hours at 90 °C.

Note: the aformentioned steel plate samples were treated with FAS and Sylgard 184, respectively. The steel mesh samples were treated only with Sylgard 184 while the soft porous samples were only treated by FAS.

2.2.5 Characterizations

Scanning electron microscopy (SEM) was performed to determine surface morphology using a JEOL JSM-6301F Field Emission SEM. The X-ray patterns were examined using STOE SEIFERT (Mo source radiation, 2-40° 2θ range, 0.495°/step) in a transmission mode X-ray diffractometer (XRD). Surface chemical compositions were investigated using X-ray photoelectron spectroscopy (XPS, Thermo Scientific K-alpha photoelectron spectrometer, the XPS spectra were referenced to carbon and the photon source was aluminium) and attenuated total reflectance Fourier transform infrared spectroscopy (ATR-FTIR, BRUKER, platinum-ATR, measurements were taken over a range of 1000 to 4000 cm^{-1}). The water contact angles (WCAs) were measured at ambient temperature *via* the sessile-drop method using an optical contact angle meter (FTA 1000, water droplet is 5 µL).

2.2.6 Robustness tests

The treated steel plate was longitudinally and transversely abraded by sand paper (Grade Grit no. 240).[27] Two experiments were performed on this sample: (1) Variation of weights — different weights (0, 20 g, 50 g, 80 g and 100 g, respectively) were positioned on the sample that was faced to the sand paper; the sample was then moved for 10 cm on the sand paper longitudinally and transversely (20 cm totally travelled per weight load); WCAs were measured after each weight test. (2) Cycles of mechanical abrasion tests were carried out on the same sample after the weight tests, here we defined one cycle for sample weighing 100 g was moved for 10 cm in the longitudinal and transverse paths respectively (20 cm in total); 30 cycles were tested on the sample and WCAs were measured after each test.

2.2.7 Oil-water separation

The mild steel mesh was treated using the above mentioned method to make it superhydrophobic. The surface energy of the $CuCl_2$ solution etched mesh was lowered by the Sylgard polymer. The treated mesh was bent as a “V” shape in cross section to hold the separating liquids. Mixed liquids containing random masses of oil and water were poured onto the mesh. A beaker was placed under the mesh to collect the separated oil. The collection rate is the ratio of mass of collected oil divided by the mass of the oil that was put into the original oil–water mixture. The first 10 separations were used to take images and the 11^{th} – 25^{th} separations were used to calculate the separation rate.

2.3 Results and discussion

To make a surface superhydrophobic, two factors are required – creation of surface roughness and reduction of the surface energy. Superhydrophobic steel surfaces were fabricated in two stages consisting of a $CuCl_2$ solution etch to create surface roughness and then FAS and Sylgard was used respectively to lower the surface energy. Surface roughness of superhydrophobic soft porous materials was obtained through the deposition of the produced particles from the reaction of $CuCl_2$ etching steel, and then FAS was used to reduce their surface energy.

In this section, a discussion of results is given in terms of wettability, surface morphology, surface compositions. Robustness and oil-water separation applications are also presented.

2.3.1 Wettability

The wettability of a surface is characterized *via* water contact angles (WCAs). The untreated mild steel plate was partially wetted with a WCA of 102° as shown in Fig. 2.3(a). The mild steel surface was firstly etched by $CuCl_2$ solution and then treated with FAS [Fig. 2.3(b)] and Sylgard 184 [Fig. 2.3(c)], respectively. The WCAs for the two treated samples were 156° [Fig. 2.3(b)] and 157° [Fig. 2.3(c)] respectively showing their superhydrophobicity. Here, either FAS or Sylgard was able to reduce the surface energy of the etched steel, and hence the FAS treated and the Sylgard treated samples had similar contact angles.

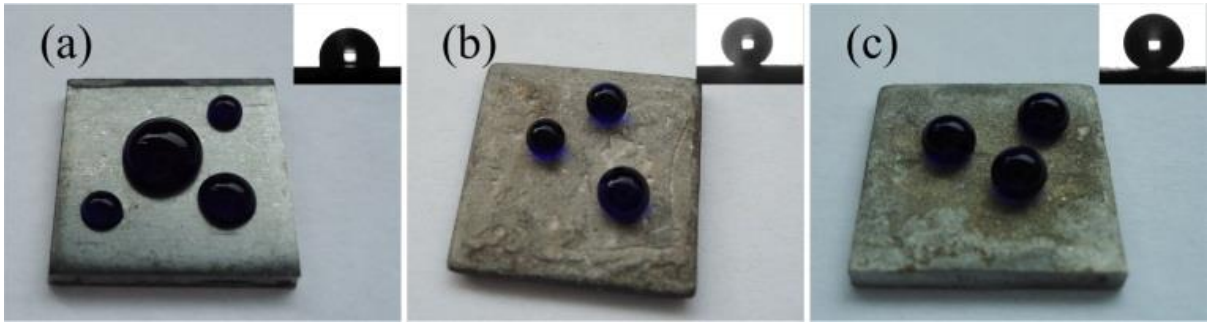

Fig. 2.3 Water droplets (dyed blue) on the surfaces of (a) untreated mild steel, (b) mild steel etched by $CuCl_2$ solution followed by FAS modification and (c) mild steel etched by $CuCl_2$ solution followed by Sylgard treatment. Inserts show the horizontal views of a water droplet contacted these surfaces.

Fig. 2.4 shows water droplets on a treated scouring pad [Fig. 2.4(a) and (b)], filter paper [Fig. 2.4(c) and (d)], and cotton wool [Fig. 2.4(e) and (f)], respectively. These hydrophilic soft materials were made superhydrophobic after treatments with the products from the reaction of $CuCl_2$ solution etching of mild steel followed by surface energy reduction. The treated scouring pad, filter paper and cotton wool supported water droplets as a perfect sphere, indicating their superhydrophobicity. This method can also be used to treat other textiles to make superhydrophobic surfaces, such as sponge and cloths, as shown in Fig. 2.5.

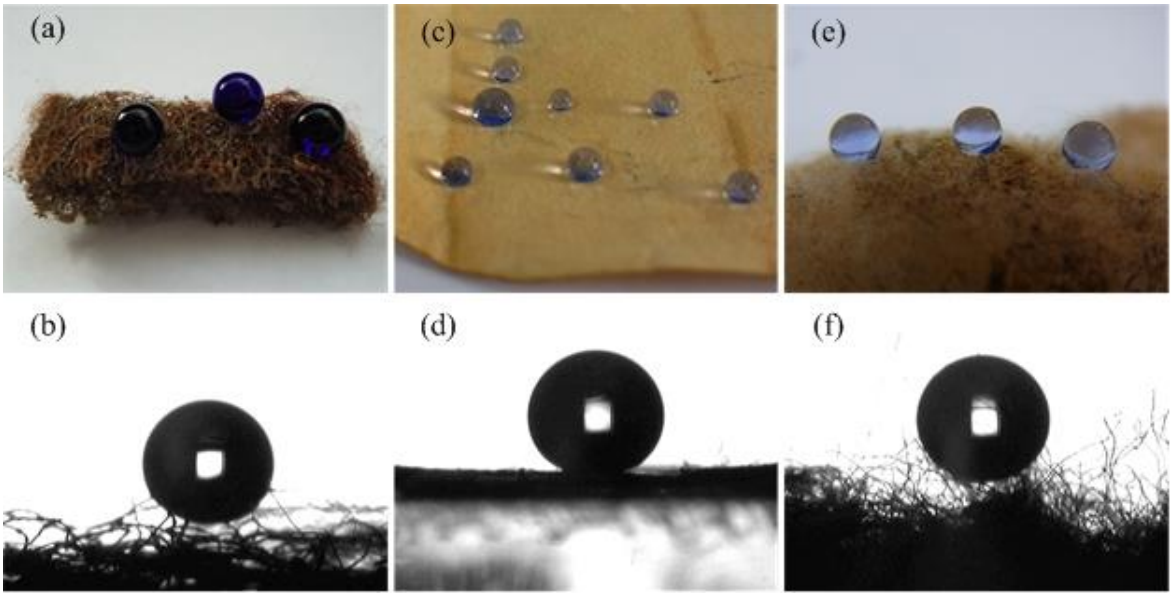

Fig. 2.4 Water droplets on treated scouring pad [(a) and (b)], filter paper [(c) and (d)], and cotton wool [(e) and (f)], respectively.

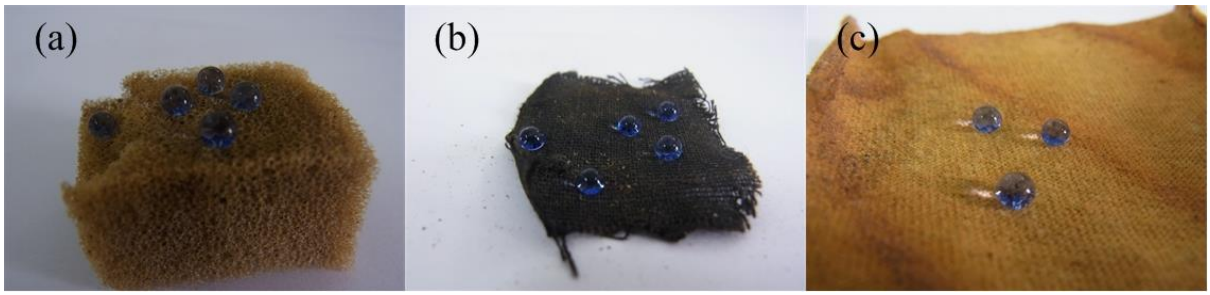

Fig. 2.5 Images of superhydrophobic (a) sponge, (b) cloth A and (c) cloth B.

2.3.2 Surface morphology

Surface micron structures were characterized using SEM. Fig. 2.6 shows the side view SEM images of untreated steel plate [Fig. 2.6 (a) and (b)] and $CuCl_2$ solution etched steel surface [Fig. 2.6 (c) and (d)], respectively. The etched surface is more textured than the untreated mild steel surface. It is seen that the chemical etching made a big difference to the mild steel surface. After the $CuCl_2$ etching process, FAS and Sylgard polymers were respectively treated. In this thesis, surface roughness was not quantified; this is because the distribution of surface morphology was quite random. Occasionally, lower surface roughness data might lead better hydrophobicity. It is more likely to quantify the relationship between wettability (water contact angles) and uniform surface roughness such as micro/nano scaled arrays of posts, needles and re-entrant structures as shown in Fig. 1.14(c).

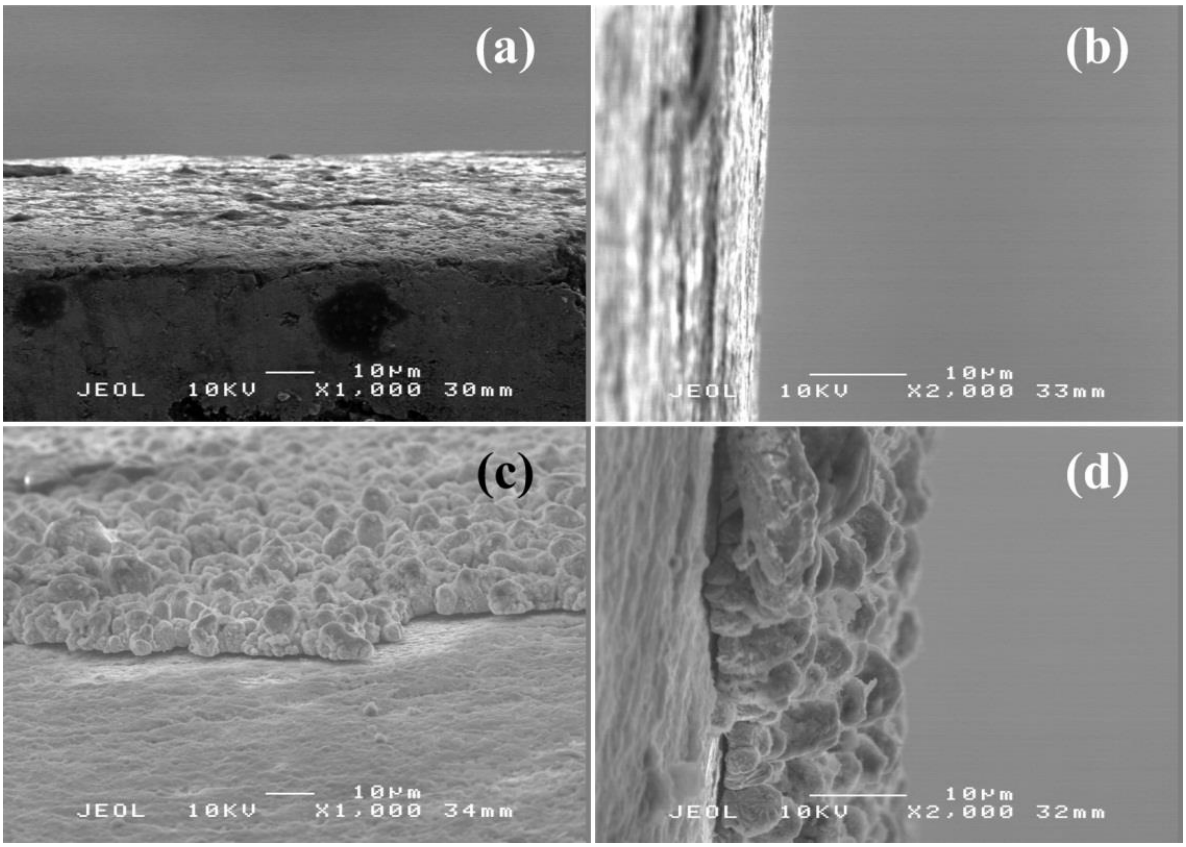

Fig. 2.6 Side view SEM images of [(a) and (b)] untreated steel and [(c) and (d)] $CuCl_2$ solution etched steel surfaces.

Fig. 2.7 shows the top view SEM images of untreated steel [Fig. 2.7(a) and (b)], $CuCl_2$-FAS treated steel [Fig. 2.7(c) and (d)] and $CuCl_2$-Sylgard treated steel surfaces [Fig. 2.7(e) and (f)], respectively. Although in low magnification [x 5000, Fig. 2.7(a)], the untreated surface presented a rough morphology in some areas, most areas were plain and less structured; at the high magnification [x 30000, Fig. 2.7(b)], nano scaled structures can be observed, and this is why the chemical etching is necessary to make the surface rougher than the untreated one. Fig. 2.7(c) and (d) shows the surfaces etched by the $CuCl_2$ solution followed by FAS treatment. These surfaces showed much more textured morphologies than those on the original steel surfaces, and also it is noted that FAS did not greatly change the surface morphology. The case is different if Sylgard polymer is applied to reduce the energy of a surface. Fig. 2.7(e) and (f) shows the $CuCl_2$ solution etched surface followed by Sylgard treatment. At the magnification of x 5000, as shown in Fig. 2.7(e), the surface was textured as it had been chemically etched; at a higher magnification [x 30000, Fig. 2.7(f)], the surface presented a bamboo-like morphology. The formation of the bamboo-like morphology is because the Sylgard polymer was deposited on the etched surface, which shows that Sylgard also contributed to make a surface rougher.

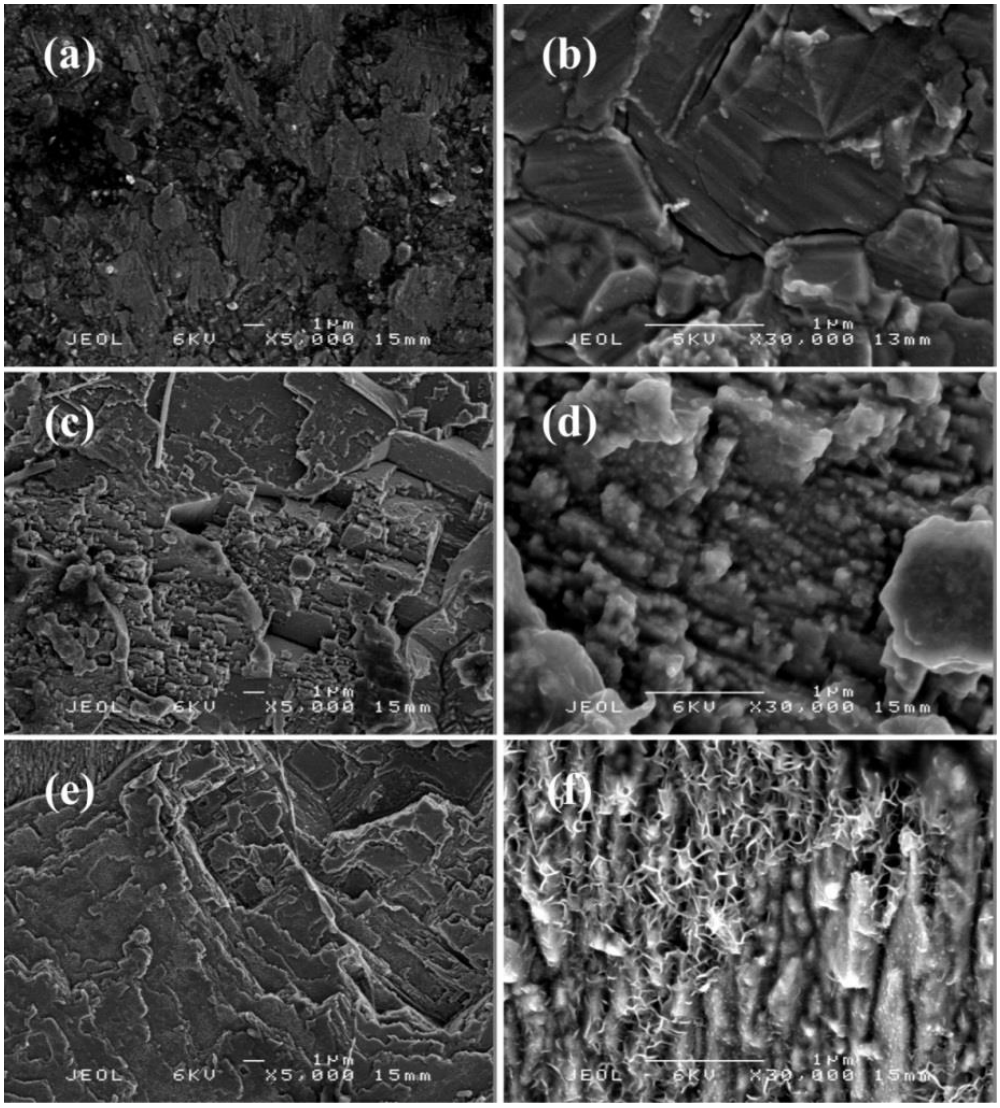

Fig. 2.7 Top view SEM images of [(a) and (b)] untreated steel, [(c) and (d)] $CuCl_2$-FAS treated steel and [(e) and (f)] $CuCl_2$-Sylgard treated steel surfaces, respectively.

The structures on steel surfaces formed due to $CuCl_2$ solution etching. The products left in the solution after etching the steel surfaces were then used to create micro and nano roughness on soft porous materials. After the deposition, these surfaces obtained micro and nano structures; and further become superhydrophobic after FAS modification. Figs. 2.8 to 2.11 show the SEM images of scouring pad, filter paper, cotton wool, sponge and cloths, before and after the product-treatments. These produced particles, which were embedded into the textiles, presented very rough surface morphologies. This surface roughness is necessary for these soft porous substrates to obtain superhydrophobicity. The untreated surfaces presented smooth morphologies at high magnifications (x10000) indicating that they do not originally have nanoscale structures.

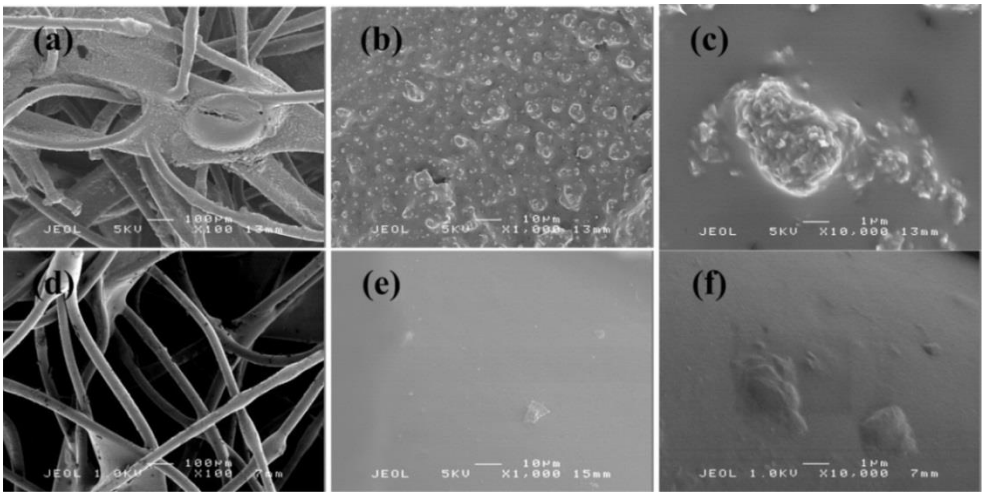

Fig. 2.8 SEM images of (a-c) treated and (d-f) untreated scouring pads, respectively.

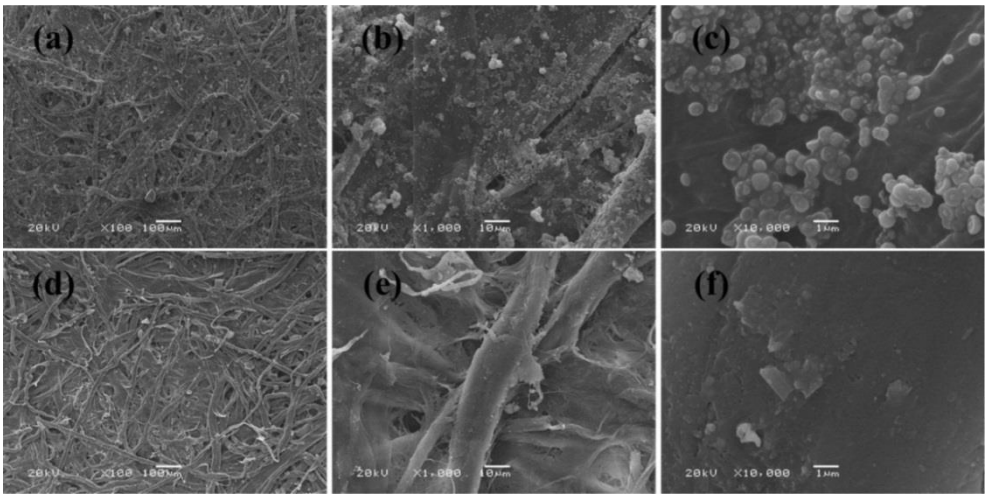

Fig. 2.9 SEM images of (a-c) treated and (d-f) untreated filter papers, respectively.

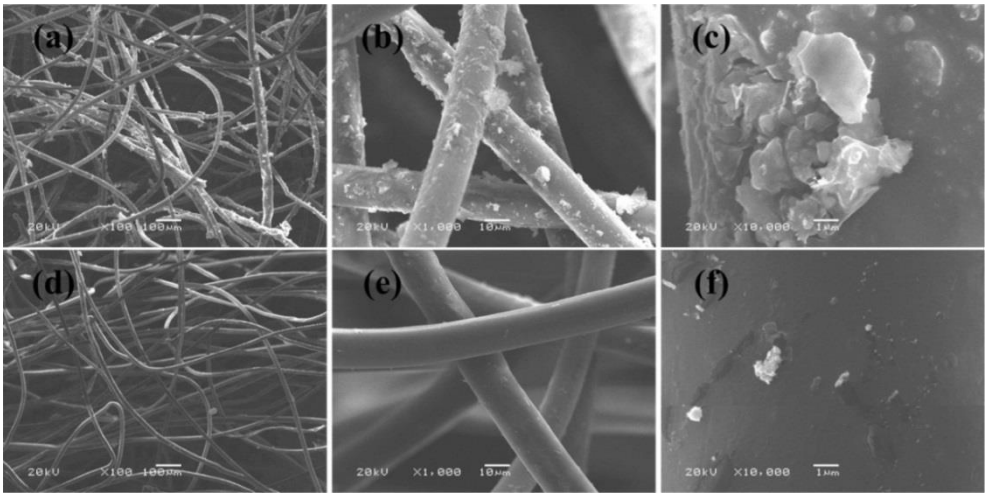

Fig. 2.10 SEM images of (a-c) treated and (d-f) untreated cotton wool, respectively.

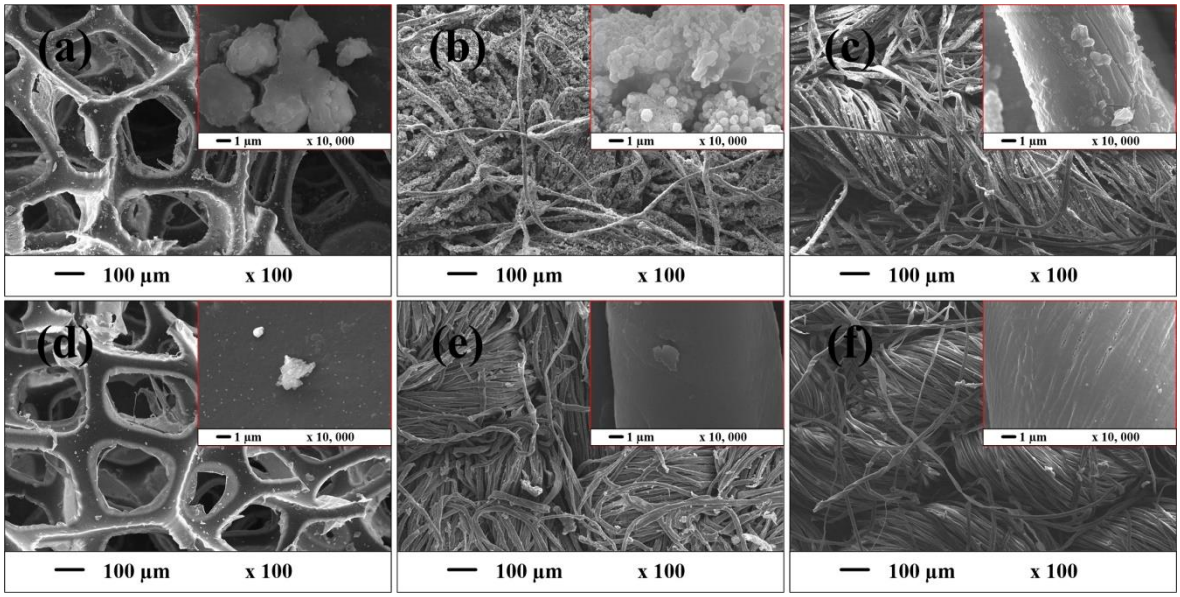

Fig. 2.11 SEM images of superhydrophobic (a) sponge, (b) cloth A and (c) cloth B; and untreated (d) sponge, (e) cloth A and (f) cloth B. Inserts are in 10000X magnification.

2.3.3 Surface compositions

Both hard (steel) and soft (scouring pad, filter paper and cotton wool) surfaces became superhydrophobic according to the optical images and wettability characterizations. From SEM images, it is seen that either hard or soft surfaces were successfully roughened to gain micro and nano structures by chemical treatment. Here, characterizations regarding surface compositions including crystal structures and chemistry compositions are reported.

XRD was used to probe the crystallinity of the surface. Here, XRD was only carried out on the soft porous samples because they were made from the products of $CuCl_2$ etched steel, therefore, analysis of these surfaces could gain a better understanding of the reactions involved. Fig. 2.12 shows the XRD patterns of treated and untreated scouring pad, filter paper and cotton wool. Peaks at 7.4°, 14.8° and 18.1° 2θ corresponding to paratacamite [$Cu_2Cl(OH)_3$] were present on the treated scouring pad, filter paper, and cotton wool (PDF NO. 01-070-0821 25-1427,[28]). The XRD pattern for treated cotton wool also shows reflections at 7.4°, 16.2°, 18.1° 2θ corresponding to [CuCl(OH)] (PDF NO. 01-074-1650 23-1063,[29]). The paratacamite was produced from the reaction of steel in a $CuCl_2$/water solution. It was formed in three steps – first, a metathesis reaction occurred as shown in Equation 2.1; second, the produced Cu was then oxidized by the exposure of air as shown in Equation 2.2; finally, the produced copper hydroxide carbonate hydrolyzed in the $CuCl_2$ solution,[30] as shown in Equations 2.3 and 2.4; the pH of the solution at the end of the reaction turned to 4.34 indicating the production of H^+, as shown in Equation (2.4). In addition, Fe_3O_4[31] and FeO(OH)[32] were also detected on some of the samples, however, CuCl(OH), Fe_3O_4 or FeO(OH) were not observed on all treated superhydrophobic samples, indicating that the absence of these compounds does not affect the growth of micro-nano structures. The surface structures were then most likely to be created from paratacamite because this was observed on all the treated samples. Here the products of steel etching were recycled and used to create micro and nano roughness on soft porous substrates; this reduces the waste chemicals to the environment. Hence we were able to use the generated waste products to make texturing on soft porous materials.

$$Fe + CuCl_2 \rightarrow FeCl_2 + Cu \quad (2.1)$$

$$2Cu + O_2 + CO_2 + H_2O \rightarrow Cu_2(OH)_2CO_3 \quad (2.2)$$

$$CuCl_2 + H_2O \rightarrow CuCl(OH) + HCl \quad (2.3)$$

$$Cu_2(OH)_2CO_3 + HCl + H_2O \rightarrow Cu_2Cl(OH)_3 + 2H^+ + HCO_3^- \quad (2.4)$$

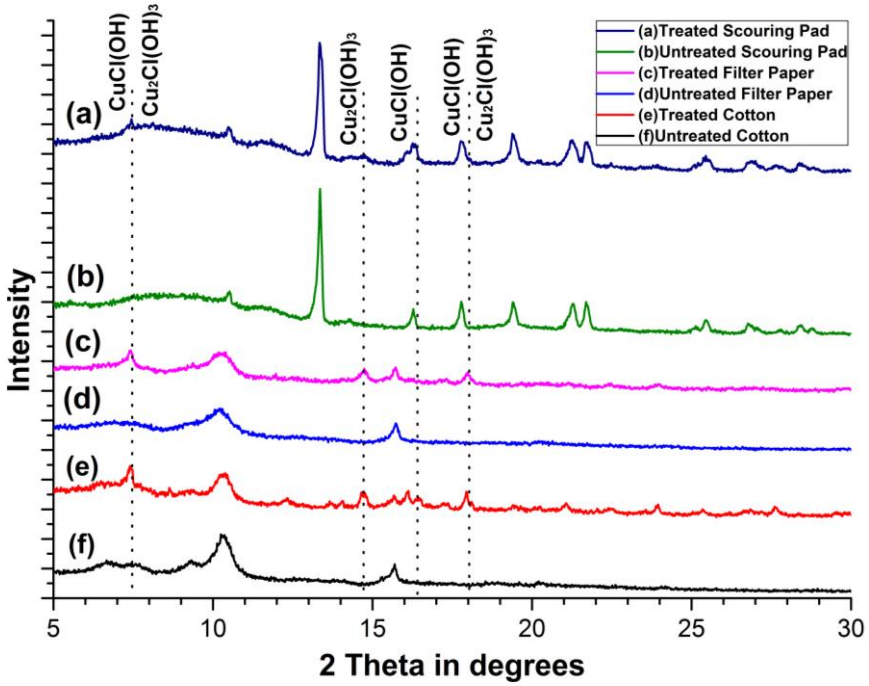

Fig. 2.12 XRD patterns of (a) treated scouring pad, (b) untreated scouring pad, (c) treated filter paper, (d) untreated filter paper, (e) treated cotton wool, and (f) untreated cotton wool, respectively.

ATR-FTIR was used to characterize the chemical compounds on untreated and treated steel surfaces. Fig. 2.13 shows the ATR-FTIR spectra of (a) original steel, (b) mild steel etched by $CuCl_2$ solution followed by FAS modification, (c) FAS in ethanol solution, (d) mild steel etched by $CuCl_2$ solution and then followed by Sylgard treatment and (e) Sylgard in chloroform. No absorption peaks were observed on the original mild steel [Fig. 2.13(a)], which indicates that the untreated control sample was not coated with any detectable organic material. The sample coated with FAS [Fig. 2.13(b)] shows bands at 1374, 1239, 1151 cm^{-1} that can be assigned to the C–F stretching vibration with respect of the $–CF_2–$ and $–CF_3$ groups in FAS. The absorption bands at 1056 and 2962 cm^{-1} correspond to Si–O and C–H stretches, respectively. Fig. 2.13(c) shows the ATR-FTIR spectrum of FAS in ethanol

solution for comparison, peaks at 1378, 1330, 1271 cm^{-1} corresponding to C–F stretching vibration of the $–CF_2–$ and $–CF_3$ groups, and the vibrations that were observed at 1089 and 2972 cm^{-1} corresponding to Si–O and C–H chemical bonds, respectively can be seen. The peak at 3325 cm^{-1} refers to ethanol (O-H stretch). Fig. 2.13(a)–(c) show that FAS was successfully adhered onto the mild steel, which was etched by $CuCl_2$ solution. Fig. 2.13(d) and (e) show the ATR-FTIR spectra of mild steel etched by $CuCl_2$ solution followed by Sylgard treatment and Sylgard in chloroform, respectively, both of which have an absorption peak at 2962 cm^{-1} corresponding to C–H vibrations. Comparison of Fig. 2.13(d) with (a/e), shows that the Sylgard has been successfully applied to the etched mild steel.

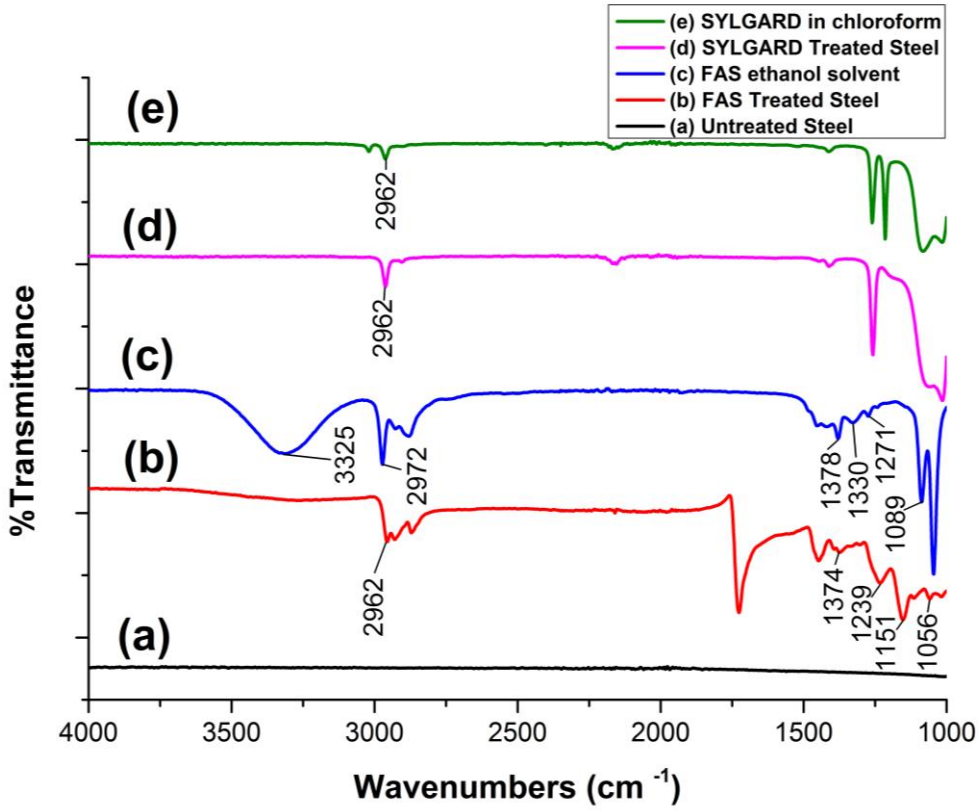

Fig. 2.13 ATR-FTIR spectra of (a) original mild steel, (b) $CuCl_2$ solution etched mild steel, followed by FAS treatment, (c) FAS dissolved in ethanol, (d) $CuCl_2$ solution etched mild steel, followed by Sylgard treatment and (e) Sylgard dissolved in chloroform.

XPS was used to detect surface elements on soft surfaces. Fig. 2.14 shows the XPS spectra of the surfaces of the scouring pad, filter paper, and cotton wool, respectively. For both treated and untreated samples, C 1s (between 280 and 290 eV) and O 1s (between 528 and 536 eV) were detected, indicating that the soft porous substrates contain C and O. Two peaks at 930 and 960 eV correspond to Cu 2p and the peak around 200 eV agrees well with literature values for Cl 2p. The Cu and Cl can be found on treated samples due to the presence of paratacamite, while on untreated samples, neither Cu nor Cl were detected. F was only detected on treated samples (F 1s, peak between 680 and 690 eV) revealing the presence of FAS.

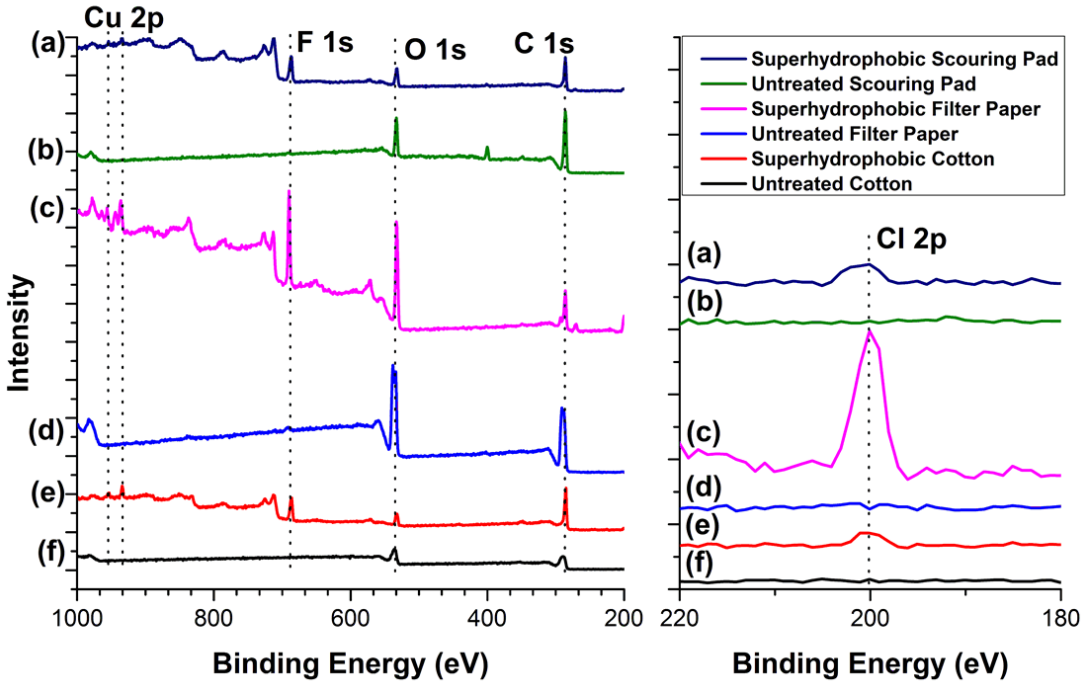

Fig. 2.14 XPS spectra of scouring pad [(a) treated and (b) untreated], filter paper [(c) treated and (d) untreated], and cotton wool [(e) treated and (f) untreated], respectively.

2.3.4 Robustness tests

Surface robustness of treated mild steel was tested through sandpaper abrasion. Fig. 2.15 shows water contact angles after (a) variation of weights and (b) multi-cycles of sandpaper abrasion tests. Water contact angles did not significantly change during one abrasion cycle when the sample was loaded 0, 20, 50, 80 and 100 g, respectively, as shown in Fig. 2.15(a). During the multi-cycles of sandpaper abrasion tests, as shown in Fig. 2.15(b), water contact angles showed some fluctuations during the first 20 cycles, this is because the contact angle measuring points were randomly selected on the rough treated surface, some taller areas on the surface was preferentially damaged while the lower plateaus were protected as shown in Fig. 2.16. The protected parts showed comparatively greater contact angles. However, with increasing abrasion cycles, the contact angles noticeably reduced, indicating that the surface micron structures were damaged.

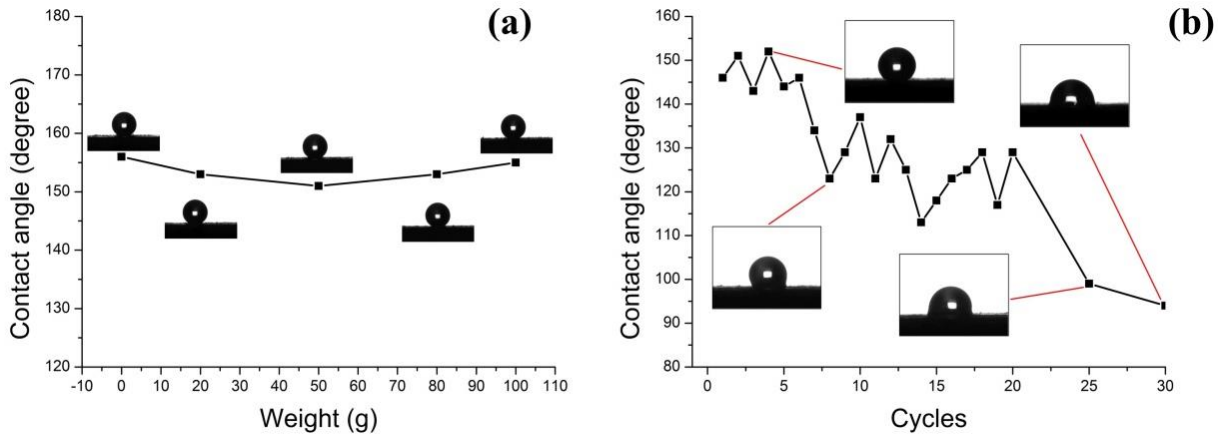

Fig. 2.15 Sandpaper abrasion tests. (a) Water contact angles after weight load abrasion tests. (b) Water contact angles after circles of mechanical abrasion tests.

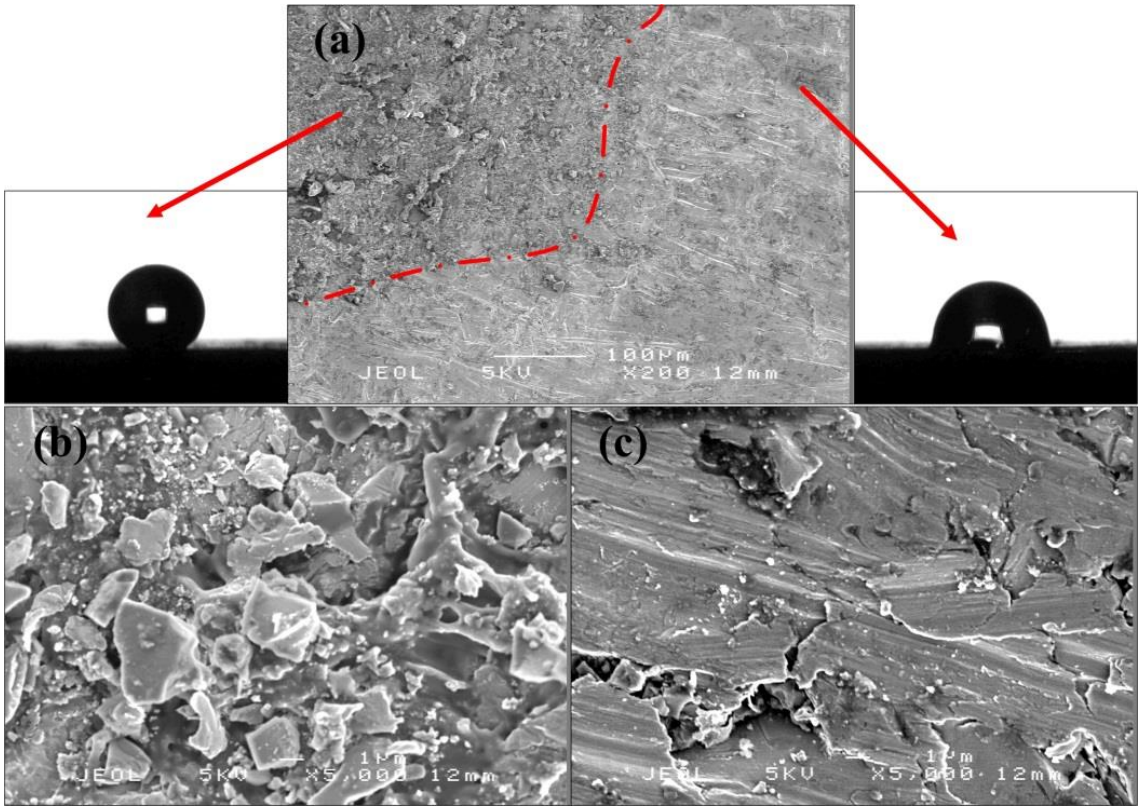

Fig. 2.16 SEM images of the steel surface after the 30-cycle mechanical abrasion tests. (a) Some taller parts were scratched while lower parts were protected, resulting in some areas of the sample still showed hydrophobicity. In 5000 X, (b) the micro structures of lower areas were protected by taller areas in the hydrophobic area; (c) the structures were damaged in the taller parts.

2.3.5 Oil-water separation

Oil-water separation has many potential applications in spilt oil clean up and the food industry.[33] One of the strategies for oil-water separation is to make a superhydrophobic-superolephilic mesh or membrane to let oil go through but to stop water getting into the mesh. Here, mild steel mesh was used as a substrate; $CuCl_2$ solution and Sylgard polymer was used to etch surface roughness and lower the surface energy (see experimental section). Fig. 2.17(a) shows that a water droplet (dyed blue) beaded on the treated mesh, while the oil droplet could easily go through the mesh as shown in Fig. 2.17(b). SEM images show that the mesh was highly textured after chemical etching and Sylgard polymer treatments as shown in Fig. 2.17(c). The original mesh, however, showed smoother morphologies than those on the treated sample as shown in Fig. 2.17(d).

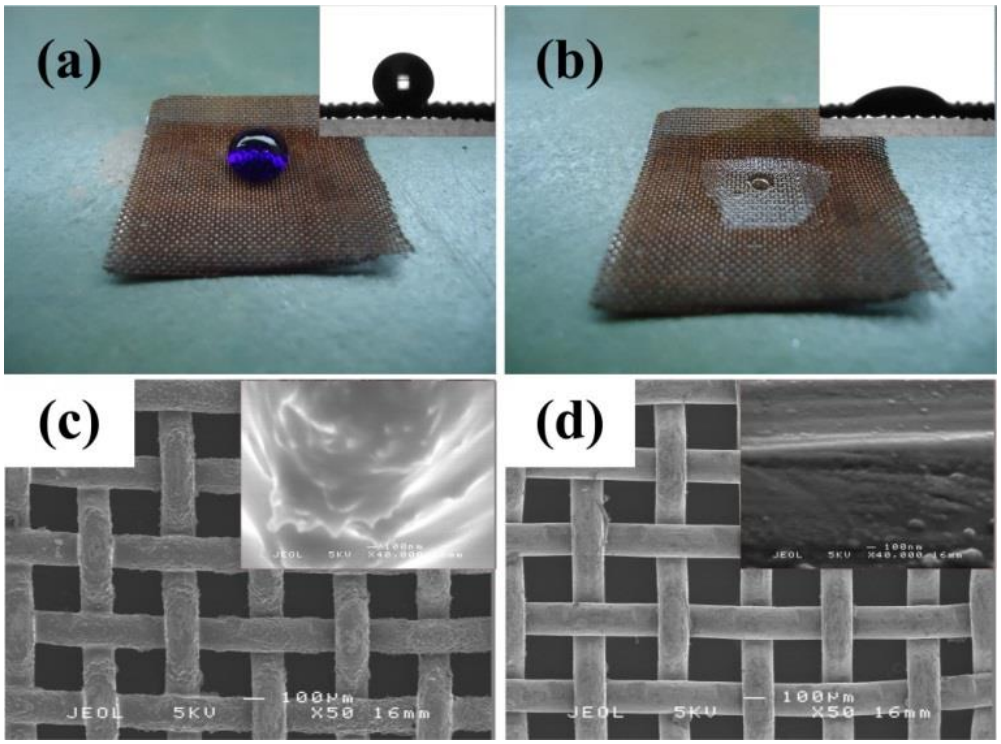

Fig. 2.17 (a) A water droplet and (b) an oil droplet on superhydrophobic-superoleophilic mild steel mesh. (c) and (d) are SEM images of treated and untreated mild steel.

The fabricated superhydrophobic-superoleophilic mild steel mesh was bent into a "V" shape in cross section (this mesh can also be made into baskets and vessels etc.) to enable floating oils on water to always be in contact with the mesh area as shown in Fig. 2.18. This mesh was used for oil-water separation tests as shown in Table 2.1. The first ten tests were used for taking pictures. The oil-water separation data was collected from the 11th to 25th separation.

The separation rate was the average value of the 15 repeat separation tests, which could reach > 96%. The method was facile, reusable and had a stable separation rate each time.

Fig. 2.18 Yellow and blue liquids refer to oil and water, respectively. Here, light oil is used as an example that is floating on water. The meshes or membranes in the middle are superhydrophobic-superoleophilic, which can stop water and let oil pass through.

Table 2.1 Oil water separating tests of the treated mild steel mesh. Here we chose different mass compositions of oil-water mixtures. The separation rate = oil collection (g)/oil (g) x 100%.

Round	Oil (g)	Water (g)	Oil collection (g)	Separation rates
11	20.64	7.95	20.31	98.4%
12	15.99	12.54	15.5	96.9%
13	13.27	11.6	12.69	95.6%
14	13.6	15.35	13.37	98.3%
15	8.94	7.39	8.53	95.4%
16	8.46	6.42	7.97	94.2%
17	7.76	9.18	7.53	97.1%
18	8.42	11.62	8.11	96.3%
19	10.34	7.32	9.86	95.4%
20	9.14	12.06	8.74	95.6%
21	7.27	11.59	6.86	94.4%
22	8.2	10.48	7.72	94.2%
23	9.42	14.5	9.06	96.2%
24	15.05	11.24	14.63	97.2%
25	10.83	12.78	10.71	98.9%

2.4 Conclusions

In the literature, $CuCl_2$ solution was usually used to roughen steel surfaces to make superhydrophobic coatings such as the work reported in Ref. 33, however, the produced Cu was used to create the rough surface morphology with the disposal of the produced solution. In this chapter, a "green" method was designed to make superhydrophobic surfaces both on hard and soft surfaces. $CuCl_2$ solution was used to etch mild steel surface to build the surface micro-nano roughness, the produced solution after etching was used to coat the soft porous materials. The deposited particles from the produced solution contributed to the creation of the surface structures on soft substrates such as cotton wool, filter paper and scouring pad etc. These etched mild steel and deposited soft materials were then treated with either FAS or Sylgard to lower the surface energy, and they became superhydrophobic after the drying processes. The prepared surfaces showed remarkable water repellence, the droplets on the superhydrophobic scouring pad and cotton wool were supported by the threads of these materials and even shaped as perfect spheres (Fig. 2.4).

The weak robustness of superhydrophobic surfaces on hard substrates is a big issue that hinders their industrial applications. Sandpaper abrasion was used to test the robustness of superhydrophobic mild steel plate. The hydrophobicity began to go down after 6 cycles of abrasion and the surface completely lost its function after 30 cycles of abrasion. Therefore, this method of superhydrophobic surface fabrication is not durable enough to be used in abrasive conditions.

However, this method of making superhydrophobic surfaces can still be used in some cases where mechanical abrasion is not necessary, for example, oil-water separation. Mild steel mesh was treated with $CuCl_2$ etching and Sylgard polymer modification. The prepared mesh had a separation rate over 96% from the 11^{th} to 25^{th} separation.

2.5 References

1. F. Chen, J. Song, Y. Lu, S. Huang, X. Liu, J. Sun, C. J. Carmalt, I. P. Parkin and W. Xu, *Journal of Materials Chemistry A*, 2015, **3**, 20999-21008.

2. X. Deng, L. Mammen, Y. Zhao, P. Lellig, K. Müllen, C. Li, H. J. Butt and D. Vollmer, *Advanced Materials*, 2011, **23**, 2962-2965.

3. Q. Wang, B. Zhang, M. Qu, J. Zhang and D. He, *Applied Surface Science*, 2008, **254**, 2009-2012.

4. J. Zimmermann, F. A. Reifler, G. Fortunato, L.-C. Gerhardt and S. Seeger, *Advanced Functional Materials*, 2008, **18**, 3662-3669.

5. H. Ogihara, J. Xie, J. Okagaki and T. Saji, *Langmuir*, 2012, **28**, 4605-4608.

6. M. Yamashita, H. Miyuki, Y. Matsuda, H. Nagano and T. Misawa, *Corrosion Science*, 1994, **36**, 283-299.

7. T. Misawa, K. Asami, K. Hashimoto and S. Shimodaira, *Corrosion Science*, 1974, **14**, 279-289.

8. M. Qu, B. Zhang, S. Song, L. Chen, J. Zhang and X. Cao, *Advanced Functional Materials*, 2007, **17**, 593-596.

9. L. Li, V. Breedveld and D. W. Hess, *ACS applied materials & interfaces*, 2012, **4**, 4549-4556.

10. A. B. Tesler, P. Kim, S. Kolle, C. Howell, O. Ahanotu and J. Aizenberg, *Nat Commun*, 2015, **6**.

11. B. Deng, R. Cai, Y. Yu, H. Jiang, C. Wang, J. Li, L. Li, M. Yu, J. Li and L. Xie, *Advanced Materials*, 2010, **22**, 5473-5477.

12. Y. Zhao, Y. Tang, X. Wang and T. Lin, *Applied Surface Science*, 2010, **256**, 6736-6742.

13. X. Zhou, Z. Zhang, X. Xu, F. Guo, X. Zhu, X. Men and B. Ge, *ACS applied materials & interfaces*, 2013, **5**, 7208-7214.

14. Q. Zhu, Y. Chu, Z. Wang, N. Chen, L. Lin, F. Liu and Q. Pan, *Journal of Materials Chemistry A*, 2013, **1**, 5386-5393.

15. C. Ruan, K. Ai, X. Li and L. Lu, *Angewandte Chemie International Edition*, 2014, **53**, 5556-5560.

16. O. Werner, C. Quan, C. Turner, B. Pettersson and L. Wågberg, *Cellulose*, 2010, **17**, 187-198.

17. M. Elsharkawy, T. M. Schutzius and C. M. Megaridis, *Lab on a Chip*, 2014, **14**, 1168-1175.

18. Z. Chu, Y. Feng and S. Seeger, *Angewandte Chemie International Edition*, 2015, **54**, 2328-2338.

19. X. Zhang, Z. Li, K. Liu and L. Jiang, *Advanced Functional Materials*, 2013, **23**, 2881-2886.

20. B. Wang, J. Li, G. Wang, W. Liang, Y. Zhang, L. Shi, Z. Guo and W. Liu, *ACS applied materials & interfaces*, 2013, **5**, 1827-1839.

21. Y. Shang, Y. Si, A. Raza, L. Yang, X. Mao, B. Ding and J. Yu, *Nanoscale*, 2012, **4**, 7847-7854.

22. Q. Pan, M. Wang and H. Wang, *Applied Surface Science*, 2008, **254**, 6002-6006.

23. C. R. Crick, J. A. Gibbins and I. P. Parkin, *Journal of Materials Chemistry A*, 2013, **1**, 5943-5948.

24. C. Wang, T. Yao, J. Wu, C. Ma, Z. Fan, Z. Wang, Y. Cheng, Q. Lin and B. Yang, *ACS applied materials & interfaces*, 2009, **1**, 2613-2617.

25. D. Tian, X. Zhang, X. Wang, J. Zhai and L. Jiang, *Physical Chemistry Chemical Physics*, 2011, **13**, 14606-14610.

26. C. R. Crick and I. P. Parkin, *Journal of Materials Chemistry*, 2009, **19**, 1074-1076.

27. Y. Lu, W. Xu, J. Song, X. Liu, Y. Xing and J. Sun, *Applied Surface Science*, 2012, **263**, 297-301.

28. M. E. Fleet, *Acta Crystallographica Section B: Structural Crystallography and Crystal Chemistry*, 1975, **31**, 183-187.

29. Y. Iitaka, S. Locchi and H. R. Oswald, *Helvetica Chimica Acta*, 1961, **44**, 2095-2103.

30. J. B. Sharkey and S. Z. Lewin, *American Mineralogist*, 1971, **56**, 179.

31. M. E. Fleet, *Journal of Solid State Chemistry*, 1986, **62**, 75-82.

32. H. Christensen and A. N. Christensen, Acta Chemica Scandinavica Series A-Physical And Inorganic Chemistry, 1978, vol. 32, pp. 87-88.

33. J. Song, S. Huang, Y. Lu, X. Bu, J. E. Mates, A. Ghosh, R. Ganguly, C. J. Carmalt, I. P. Parkin and W. Xu, *ACS applied materials & interfaces*, 2014, **6**, 19858-19865.

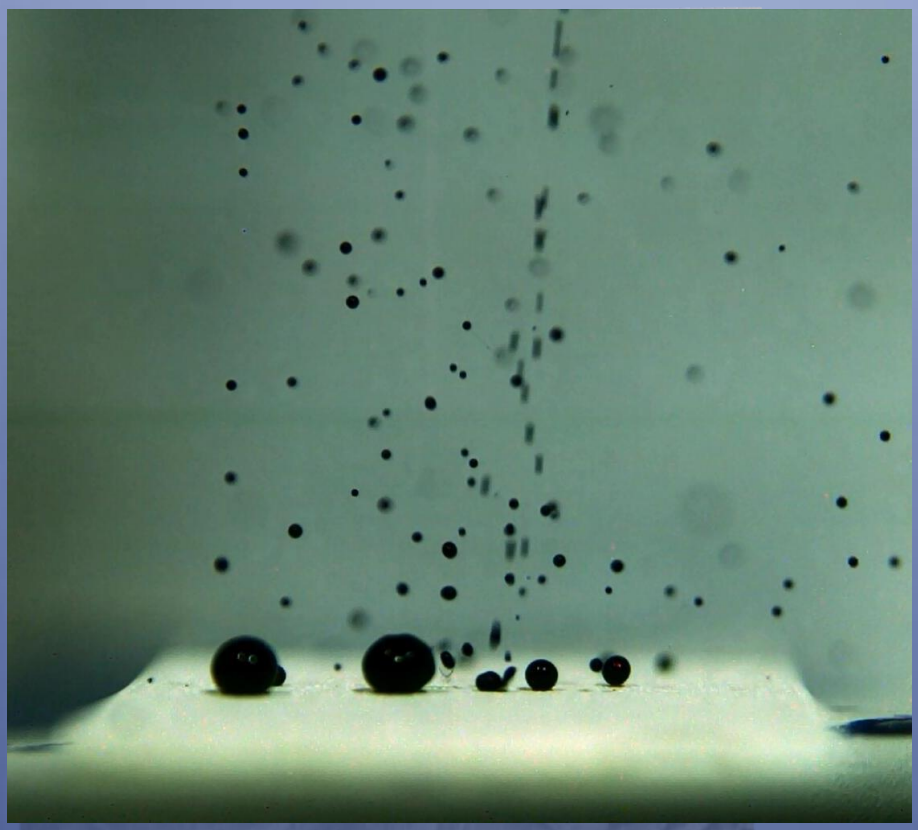

Chapter 3 Making robust superhydrophobic paint that can be treated on various substrates

Yao Lu

UCL CHEM

About the cover image of Chapter 3

Water spill (dyed blue) was repelled by a superhydrophobic paint treated surface.

This image is reproduced with permission from Ref.

“Y. Lu et al., *Science* 2015, 347, 1132-1135”

About the figures in this chapter

All the figures except for Figs. 3.1, 3.17, 3.24, 3.25 in Chapter 3 are reproduced with permission from Ref. “Y. Lu et al., *Science* 2015, 347, 1132-1135”

Chapter 3

Making robust superhydrophobic paint that can be treated on various substrates

3.1 Introduction

A comparatively "green" method to fabricate superhydrophobic surfaces was demonstrated in Chapter 2, however, as a solvent-based reaction, there were still some waste solvent discharged to the environment. In this chapter, a paint-like suspension is developed to make superhydrophobic surfaces. This paint was made of dual-scaled TiO_2 nanoparticles and fluoropolymer-ethanol-based solution. Different from the chemical method, this paint was fabricated though physically mixing the particles and solvent, such that the particles could form a coating to repel water, resulting in less discharge to the environment. In addition, the use of the superhydrophobic paint shows some advantages to previous methods of making superhydrophobic surfaces, for example, the paint can be applied to most solid substrates, superior mechanical robustness was achieved simply by bonding the surface with commercial adhesives, and it would even function under oil.

3.1.1 A general method to coat superhydrophobic surface

Fabrication of superhydrophobic surfaces usually depends on the nature of the substrates and needs two steps (roughen the surface, and then lower the surface energy). For example, when making superhydrophobic surfaces on metallic substrates, the first step is to create the surface roughness. In Chapter 2, $CuCl_2$ solutions were used to etch mild steel surfaces to create surface micro and nano structures.[1] However, this method is more like a "one solution – one substrate" design, and would not work if given a copper substrate. Similar ideas of material-removal are subject to the same limitation, such as chemical etching[2, 3] and electrochemical etching methods.[4, 5] However, the above mentioned methods would not work if roughening a non-metallic substrate (for example, on glass substrates). To make a superhydrophobic surface on glass substrates, aerosol-assisted chemical vapour deposition (AACVD) can be used to deposit hydrophobic polymers onto the substrates.[6-8] This method enables the polymer aerosols to form micro and nano scaled structures on glass substrates using one single step to prepare superhydrophobic surfaces. However, this step usually requires high temperatures (350 – 400 °C), where cellulose-based substrates such as paper and cotton wool will carbonize. Therefore, the aforementioned methods could not be generally used to form superhydrophobic surfaces on a variety of substrates.

3.1.2 Mechanical robustness

It is generally accepted that the preparation of superhydrophobic surfaces requires building surface micro and/or nano roughness.[9, 10] However, no matter how hard and durable a material can be on the macro scale, they become much weaker in the micro and nano scale, and can be destroyed even sometimes with a slight touch from a tissue. In this case, the surfaces would lose superhydrophobicity once the surface morphologies got damaged. In Chapter 2, the fabricated superhydrophobic steel surface could tolerate several sandpaper abrasion tests, due to the variation in height of the surface structures of the superhydrophobic steel, resulting in some areas losing superhydrophobicity whereas other areas were protected by the taller parts. Comparatively durable superhydrophobic Si and Ti surfaces were previously reported with the same mechanism.[11, 12] However, these surfaces will be eventually destroyed when the taller parts together with the bottom structures are worn out. Superhydrophobic soft materials (such as textiles, sponge etc.) are usually fabricated by deposition of superhydrophobic particles.[13-15] These soft materials are more robust than the hard surfaces because the fabric surfaces have a larger surface area and most of the area will not be directly abraded, this is a form of protection.[16-18] Hence the softness of these materials would absorb some of the applied force. The bonding between the threads of the soft substrates and the superhydrophobic particles plays an important role in their robustness. However, a general method to fabricate robust superhydrophobic surfaces on both hard and soft surfaces is still required.

3.1.3 Oil contamination

Although superhydrophobic surfaces have shown remarkable water-proofing and self-cleaning properties, they lose their functions once being contaminated by liquids with a lower surface tension (such as oil) than that of water.[19-21] The Lotus leaf is one of the best-known examples of a superhydrophobic surface,[22-24] however the Lotus leaf surface can be readily wetted by hexadecane (surface tension of 27.5 mN/m, the surface tension of water is 72.1 mN/m) with a contact angle of ~0°.[25] Designing silanized micron re-entrant surface structures enables a surface to repel both water and oil,[25, 26] and according to a recent discovery, micron double re-entrants structures are able to repel extremely wetting liquids such as perfluorohexane (surface tension of ~10 mN/m), without low surface energy treatments.[27] However, these surfaces are not applicable for lubricating components, for example, the gears and bearings of an automobile. Therefore, a surface that repels water before and after oil contamination is more suitable to be used for lubricating surfaces.

In this chapter, a superhydrophobic paint was developed aiming at overcoming the aforementioned three problems: the diversity of the applied substrates, mechanical robustness and oil contamination. The paint was simply made by dispersing TiO_2 nanoparticles into a fluorosilane-ethanol solution to make a suspension, this suspension could be treated on various substrates such as glass, steel, cotton and paper to make superhydrophobic surfaces. The surface robustness could be greatly improved and the surfaces retained their superhydrophobicity even after finger-print, knife-scratch and 40 cycles of sandpaper abrasion when bonding the paint to substrates using commercially available adhesives. The coated surfaces remained water repellent when contaminated by oil and even after immersion in oil.

3.2 Experimental

3.2.1 Materials

To develop the superhydrophobic paint, two types of titanium dioxide nanoparticles were used. Titanium dioxide (anatase) nanoparticles (diameter, ~ 60 - 200 nm, which was estimated through scanning electron microscopy and transmission electron microscopy images) were purchased from Sigma-Aldrich; in the following text, these TiO_2 nanoparticles will be called Sigma-TiO_2 to distinguish with the other type of titanium oxide. TiO_2 P25 (diameter, ~ 21 nm) was purchased from Degussa. 1H, 1H, 2H, 2H-perfluorooctyltriethoxysilane (also known as fluorosilane, or FAS, $C_8F_{13}H_4Si(OCH_2CH_3)_3$) was purchased from Sigma-Aldrich. All the laboratory solvents were purchased from Fisher Scientific and used as received.

Substrates including glass slides, cotton wool and filter paper were purchased from Fisher Scientific, and steel was purchased from the Goodman.

3.2.2 Making superhydrophobic paint and coating methods

1 g of FAS was dissolved into 99 g of ethanol solvent, and the resulting solution was mechanically stirred for 2 hours. 6 g of Sigma-TiO_2 and 6 g of TiO_2 P25 nanoparticles were then dispersed into the resulting FAS-ethanol solution to make a suspension. Note that these TiO_2 nanoparticles were used to create surface roughness, sole Sigma-TiO_2 and sole TiO_2 P25 nanoparticles dispersed into the FAS-ethanol solution were also tried at the initial stage; dual scaled surface morphology that was presented in this thesis gave better hydrophobicity and surface durability. Within the dual scaled surface morphology system, alternative particle sizes ranging from 20 nm to 10 μm would achieve a similar function.

To apply the suspension onto the substrates (glass, steel, cotton wool and filter paper), several coating methods were used.

Syringe coating – the suspension was extruded from a syringe onto a surface.

Spray coating – the suspension was sprayed onto a surface using an artist's spray gun.

Dip-coating – the sample was fixed on a dip-coater and inserted into the suspension, and then the sample was pulled out of the suspension at a rate of 120 mm/min.

After the paint was coated onto the substrates, the samples were dried in air at room temperature. It takes ~ 3-6 mins to dry on the hard substrates (e.g. glass and steel surfaces), ~

10-15 mins on filter paper surfaces and 30 mins or even longer on cotton wool surfaces. The drying time could be reduced if higher drying temperatures (60-80 °C) were applied.

3.2.3 Characterization

Surface morphologies were detected *via* scanning electron microscopy (SEM, JEOL JSM-6301F Field Emission) and transmission electron microscopy (TEM, JEOL JEM 2100 microscope at a beam acceleration of 200 kV). X-ray diffractometers (XRD) were used to characterize the surface crystal structures. For hard substrates (glass and steel), D4 Endeavor (Cu source, 10-60° 2θ range, 0.05°/step) was used in glancing angle mode (5^{o}); for soft substrates (cotton wool and filter paper), STOE Seifert (Mo source radiation, 2-40° 2θ range, 0.495°/step) was used in transmission mode. Surface chemical compositions were investigated using an X-ray photoelectron spectroscopy (XPS, Thermo Scientific K-alpha photoelectron spectrometer, the XPS spectra were referenced to carbon and the photon source was aluminium). The water contact angles were measured at room temperature *via* the sessile-drop method using an optical contact angle meter (FTA 1000, water droplet is 5 µL). Water droplet bouncing videos and images were taken by a Phantom V7.1 colour high speed camera at 2900 frame/s.

3.2.4 Water dropping tests

Water droplets were dropped from a 30-gauge dispensing tip that was fitted 40 mm high (tip to surface, Fig. 3.1), and the impact velocity (v) was ~ 0.89 m/s estimated by the law of free fall, $v^2 = 2gh$, where g is the acceleration due to gravity (~ 9.8 m/s^2 near the surface of the earth), h is the height from the syringe tip to the sample surface. The size of water droplets was ~ 6.3 ± 0.2 µL and they were detached under their own weight. Original and coated glass, steel, cotton wool and filter paper were used as substrates; here, coated samples were prepared *via* dip-coating. Water droplets were dyed blue with methylene blue to gain better visualization.

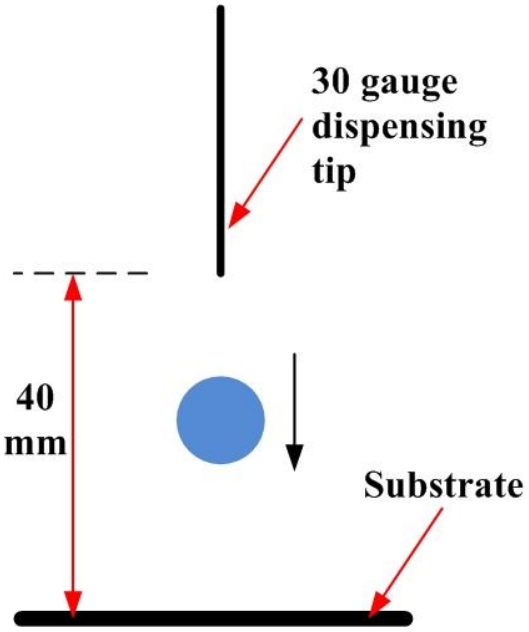

Fig. 3.1 Scheme of water dropping tests.

3.2.5 Self-cleaning tests in air

Self-cleaning of a superhydrophobic surface means two things – first, the surface repels "dirty" and coloured water, such as the mixture of mud and water and water-based ink. Second, foreign bodies such as dust can be removed easily by rolling water.

"Dirty" water repellent test: dip-coated cotton wool (white) was put into methylene blue dyed water and then removed. It is to test if the treated cotton wool could be dyed blue (Fig. 3.2).

Dirt-removal test: in this test, MnO powder was used as a mimic for dirt.

1. Two filter papers (one was spray coated, the other was untreated) were applied in this test. The treated filter paper was positioned on top at ~ 30° relative to the untreated sample. Dirt was placed onto the upper filter paper, and then water was applied to clean the upper piece of paper (the treated sample) as shown in Fig. 3.2.

2. Dirt-removal tests were also carried out on dip-coated glass and steel samples, the tests were to use a single water droplet to clean the dirt on the treated samples using the high speed camera. This is to understand how self-cleaning works among water, dirt and superhydrophobic surfaces.

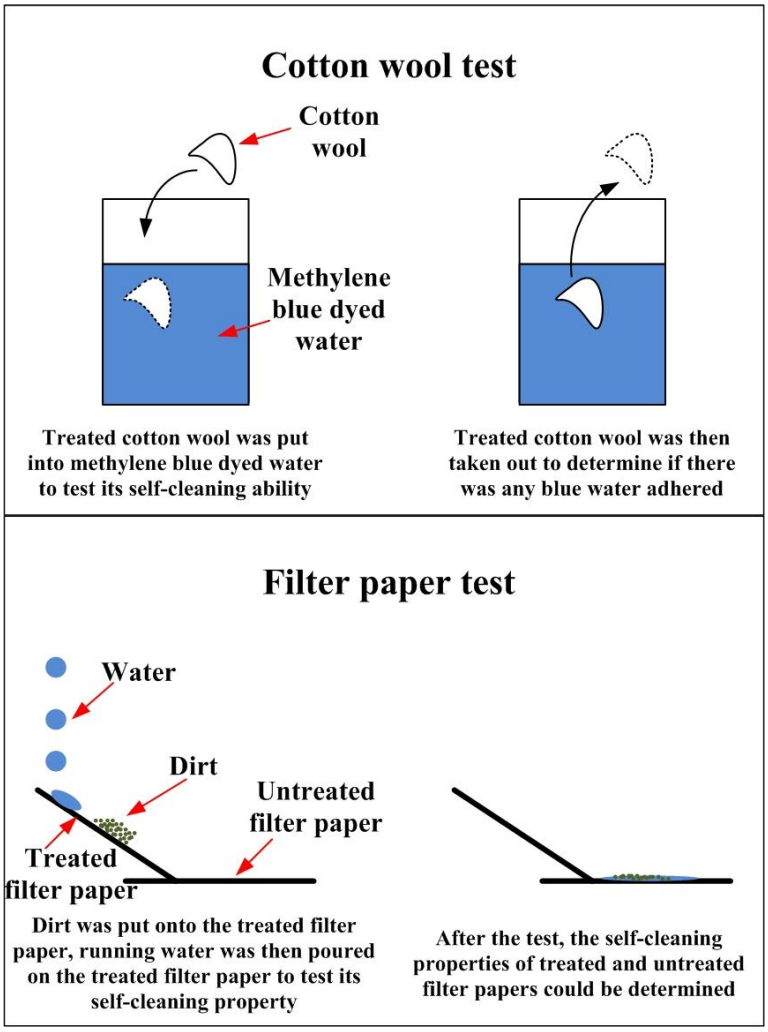

Fig. 3.2 Scheme of self-cleaning tests in air. The upper panel shows “dirty” water repellent test on dip-coated cotton wool, and the lower panel shows the dirt-removal test on the spray-coated filter paper.

3.2.6 Oil contamination tests

Oil contamination tests include two types of tests – first, the surface was immersed into oil to get contaminated, and then removed to test the self-cleaning properties in air. Second, the surface was immersed into oil and then self-cleaning properties were tested in oil. Hexadecane was used in the "oil contamination tests" as oil. The self-cleaning properties were also tested in two ways that were similar to those in air, including "dirty" water repellence and dirt-removal. Then a "2 × 2" experiment was set up as follows:

1. "Dirty" water repellence: methylene blue dyed water acted as "dirty" water.

1a. On oil immersion: a half treated (dip-coated) glass slide was immersed into oil; "dirty" water was dropped onto both untreated and treated parts to compare their water repellence in oil [Fig. 3.3(a)].

1b. In-air test: the spray-coated glass slide was firstly immersed into oil and then removed to air; "dirty" water was then dropped onto the surface to test its water repellence [Fig. 3.3(b)].

2. Dirt-removal tests: methylene blue dyed water acted as "dirty" water and MnO powder acted as dirt. The spray-coated glass slide was firstly contaminated by oil and then partly inserted into oil. Dirt was then positioned onto the surface of the sample; half of the dirt was immersed into oil while the other half was exposed to air as shown in Fig. 3.3(c). This is to test the dirt-removal properties either in air or oil phase.

2a. In-air test: "dirty" water was dropped onto the surface to remove the dirt exposed to air.

2b. On oil immersion: "dirty" water in 2a was used to remove the dirt immersed in oil.

In practical consideration, dirt-removal tests were carried out using cooking oil, soil (from Gordon Square, London) and dust (from offices, kitchens and labs) picked up and used as dirt in the experiment.

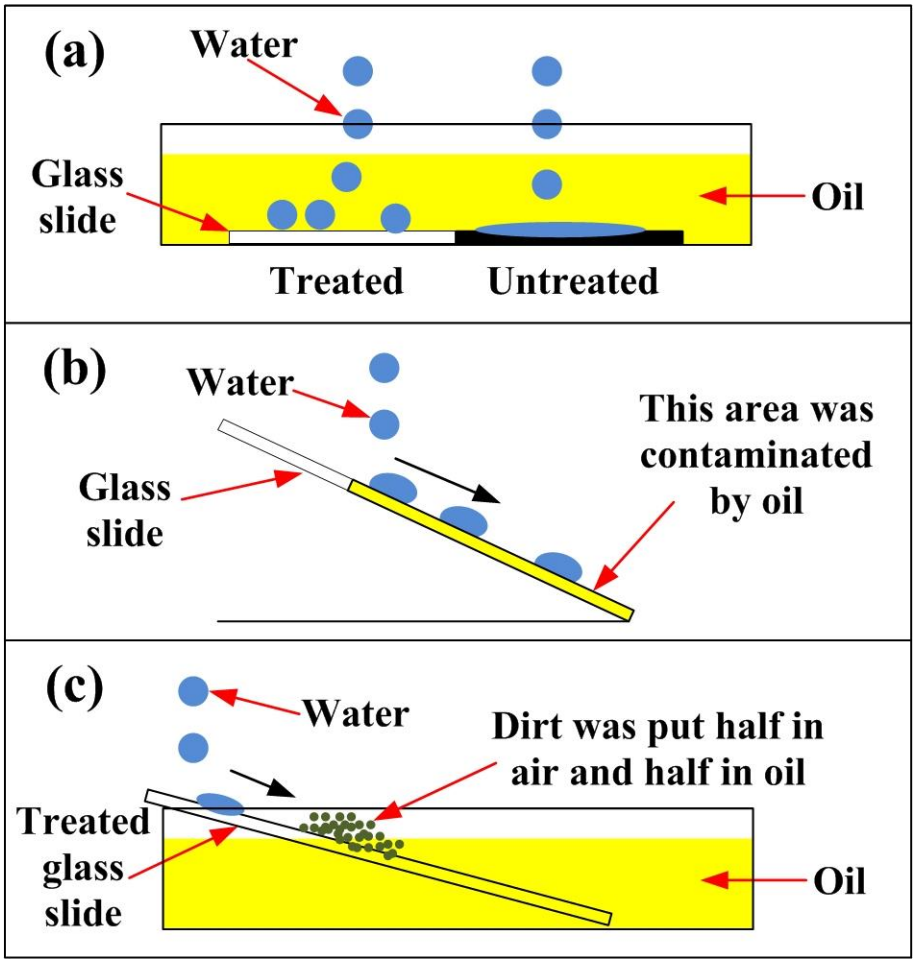

Fig. 3.3 Self-cleaning tests in oil. (a) "Dirty" water repellence – on oil immersion. A half dip-coated glass slide was immersed into oil; "dirty" water was dropped onto both untreated and treated parts. (b) "Dirty" water repellence – in air test. The spray-coated glass slide was firstly immersed into oil and then removed to air; "dirty" water was then dropped onto the surface. (c) Dirt-removal tests. The spray-coated glass slide was firstly contaminated by oil and then partly inserted into oil. Dirt was then positioned onto the surface of the sample; half of dirt was immersed into oil while the other half was exposed to air. "Dirty" water was dropped and expected to remove dirt either in air or oil on the treated surface.

3.2.7 Methods to test the robustness of superhydrophobic surfaces

The robustness of a superhydrophobic surface is one of the most important factors that determine if the surface is applicable in practical conditions. In our daily life, physical contact of a surface/coating can be hand touch (e.g. touch the wall), scratch (e.g. a car got scratched) or abrasion (e.g. sandpaper abrasion). To mimic practical conditions, finger-print, knife-scratch and sandpaper abrasion tests were carried out on the superhydrophobic paint treated substrates. In these tests, commercial adhesives (the Niceday double sided tape or the EVO-STIK spray adhesive) were used to bond the paint and the substrates and to aid surface robustness. Sample preparation and relevant robustness tests were as follows:

1. Sample preparation

1a. Glass substrate: the glass slide was firstly coated with adhesives (either double sided tape or spray adhesive) and then dip-coated into the superhydrophobic paint as shown in Fig. 3.4(a).

1b. Steel substrate: the steel plate was firstly bonded onto a glass slide using double sided tape to aid preparation and robustness tests, and then adhesives (either double sided tape or spray adhesive) were applied onto the steel surface, finally the steel surface was dip-coated into the superhydrophobic paint as shown in Fig. 3.4(b).

1c. Cotton wool and filter paper substrates: the sample preparation processes are the same between cotton wool and filter paper, here those of cotton wool are described as an example. The piece of cotton wool was firstly bonded onto a glass slide using double sided tape to aid preparation and robustness tests, and then adhesives (for soft substrates, double sided tapes are not applicable to bond the surfaces and the superhydrophobic paint, so only spray adhesives were used) were sprayed onto the cotton wool and then the cotton wool was dip-coated into the superhydrophobic paint as shown in Fig. 3.4(b). The same processes were used to prepare filter paper samples.

2. Robustness tests

2a. Finger-print: Fig. 3.4(c) shows the scheme of the finger-print tests. The surfaces were (from left to right) untreated, paint treated and paint + adhesive treated. Then the finger print was applied from left to right and it was expected that the superhydrophobic coatings would be removed from the substrates or adhesive bonded substrates. Water was then used to test the superhydrophobicity of the finger wiped surfaces.

2b. Knife-scratch: a knife (Sterile disposable scalpels from the Swann-Morton) was used to scratch the treated surfaces along the red dashed pattern as shown in Fig. 3.4(d). Water was then dropped onto the scratched samples to test their superhydrophobicity.

2c. Sandpaper abrasion: three steps were applied in this test. Fig 3.4(e) shows the side view of the test. The sample was face down to the sandpaper (Grit No. 240) and loaded by a 100 g weight. The sample and the weight were then guided to travel for 10 cm along a rule as shown in Fig. 3.4(f), Step 1. Then the sample was kept face down and rotated for 90° in Step 2. In Step 3, the sample was weighted with 100 g and guided to travel for 10 cm along the ruler. The three steps constituted one cycle of abrasion, and this is to guarantee the sample was abraded longitudinally and transversely.

To quantify the robustness of the superhydrophobic coatings, multiple cycles of abrasion tests were performed on a paint + double sided tape + glass substrate. Water contact angles were measured after each cycle of abrasion; however, water contact angles do not provide conclusive evidence regarding the superhydrophobicity of the whole area. As it was discussed in Chapter 2, superhydrophobic surfaces are so rough that it is inevitable to have taller plateaus that protect the lower parts from abrasion. Then the points or areas responsible for high water contact angles might only be on the taller or lower parts. To detect the superhydrophobicity of the whole abraded area, a water droplet was guided by a needle tip to travel around the surface after every 10 abrasion cycles.

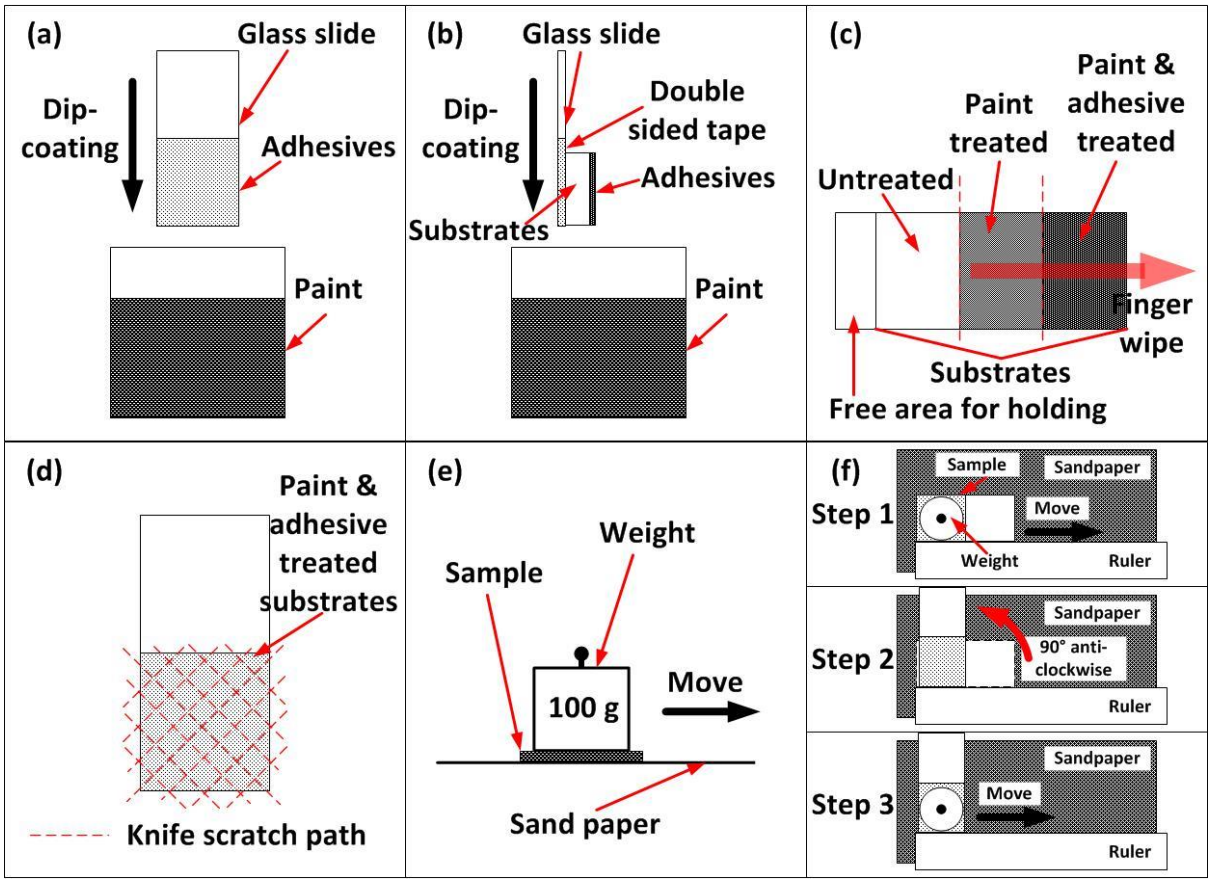

Fig. 3.4 Sample preparation and mechanical robustness tests. (a) Preparation of superhydrophobic paint + adhesive glass surface. Adhesives were applied onto the glass substrate followed by dip-coating of the superhydrophobic paint. (b) Preparation of superhydrophobic paint + adhesives + substrates (including steel, cotton wool and filter paper). Substrates were initially bonded onto glass slides using double sided tapes to aid further experiments, then adhesives were applied to treat the substrates followed by dip-coating of the superhydrophobic paint. (c) Finger-print test. Finger was used to wipe the untreated, superhydrophobic paint treated and superhydrophobic paint + adhesive treated surfaces, respectively, from left to right. (d) Knife-scratch test. The superhydrophobic paint + adhesive treated samples were scratched by a knife along the path of the red dashed line. (e) Side view of sandpaper abrasion tests of superhydrophobic paint + adhesive treated samples. The superhydrophobic surfaces that were faced to the sandpaper were weighted with a 100 g weight, then the samples were guided to move along a ruler for 10 cm as shown in Step 1 (f), then the sample was rotated for 90° with facing to the sandpaper as Step 2, in Step 3, the sample was guided to move for 10 cm along the ruler, the 3 steps are defined as one cycle of sandpaper abrasion. In a cycle of abrasion, the sample was abraded longitudinally and transversely.

3.3 Results and discussion

A superhydrophobic paint-like suspension was developed *via* dispersing dual scaled TiO_2 nanoparticles into a fluorosilane-ethanol solution. Experimental details were presented in the previous section including materials preparation, characterization, water dropping tests, self-cleaning tests either in air or oil, and mechanical robustness tests. In this section, results and relevant discussions will be presented.

3.3.1 Wettability on painted substrates

The paint can be easily coated to make superhydrophobic surfaces on most solid substrates including both hard and soft materials as shown in Fig. 3.5. Water droplets with methylene blue could wet the left (untreated) parts of glass [Fig. 3.5(a)], metal [Fig. 3.5(b)], cotton wool [Fig. 3.5(c)] and filter paper [Fig. 3.5(d)]; while for the right (treated) areas, water droplets were marble-shaped on the surfaces. Here, the glass and steel were coated *via* spray, the cotton wool was coated *via* dip-coating, and the filter paper was merely treated by a syringe coating. The coating methods were flexible based on various substrates, and high water repellent ability can be achieved by using dip-coating, spray or even simply with a syringe needle.

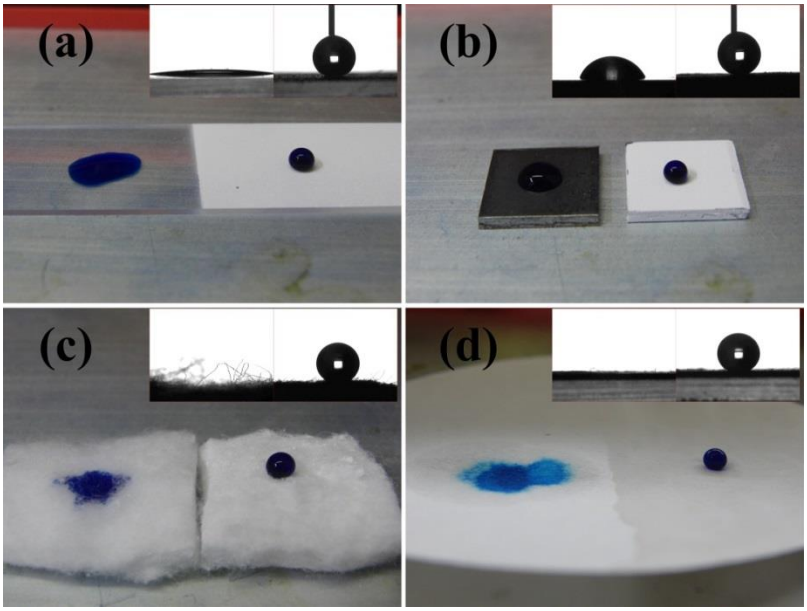

Fig. 3.5 Untreated (left) and treated (right) areas of hard (glass and steel) and soft (cotton wool and filter paper) materials, it is clearly seen that the treated areas have a superior surperhydrophobicity [Inserts are the images of untreated (left) and treated (right) materials taken by the water contact angle measuring machine].

3.3.2 Surface morphology

With respect to the superhydrophobic paint, two different sized TiO_2 nanoparticles enabled the surface roughness to be increased, and the fluorosilane-ethanol solution was used to lower the surface energy of the TiO_2 particles. SEM and TEM were used for characterization of the surface structures. Fig. 3.6(a) and (b) shows the SEM images of the TiO_2 coating. The surface has a binary-texture due to two types of nanoparticles as shown in Fig. 3.6(b). Fig. 3.6(c) and (d) shows the TEM images of the coating, it is seen that the coating consisted of two different sized nanoparticles. The diameters of bigger particles varied from 60 nm to 200 nm, while the sizes of smaller particles were around in 21 nm. This binary texture enhances the self-cleaning ability of surfaces.

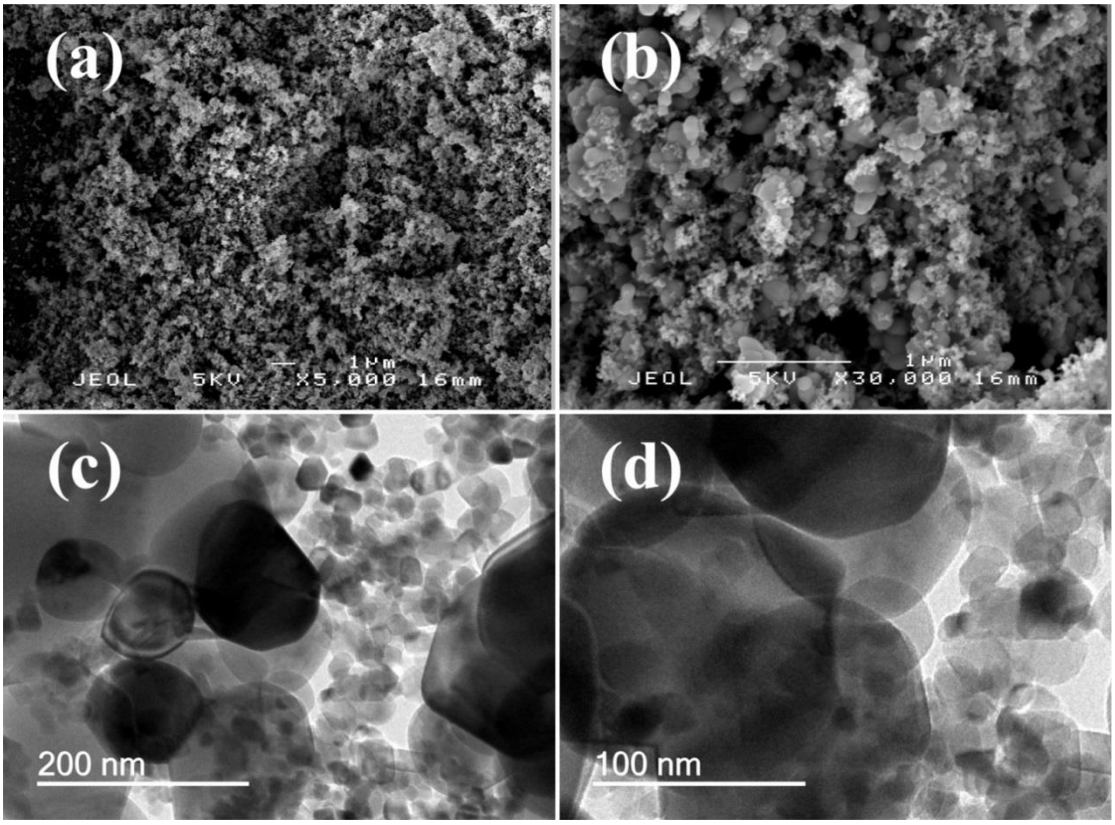

Fig. 3.6 (a) and (b) are SEM images of the coating in 5000 X and 30000 X magnifications, respectively. (c) and (d) are TEM images of the coating. Both bigger and smaller nanoparticles could be seen and measured *via* TEM images.

3.3.3 Surface crystals and chemistry

The paint can be applied to both hard and soft substrates. Two kinds of XRDs were used to detect the coatings treated on hard (glass and steel) and soft (cotton wool and filter paper) substrates, respectively, as shown in Fig. 3.7. Compared with the XRD patterns of standard anatase[28] and the untreated surfaces, glass, steel, cotton wool and filter paper surfaces were successfully treated with the fabricated coating. The experimental XRD patterns were compared with respective standard patterns for TiO_2 anatase based on the radiation source used.

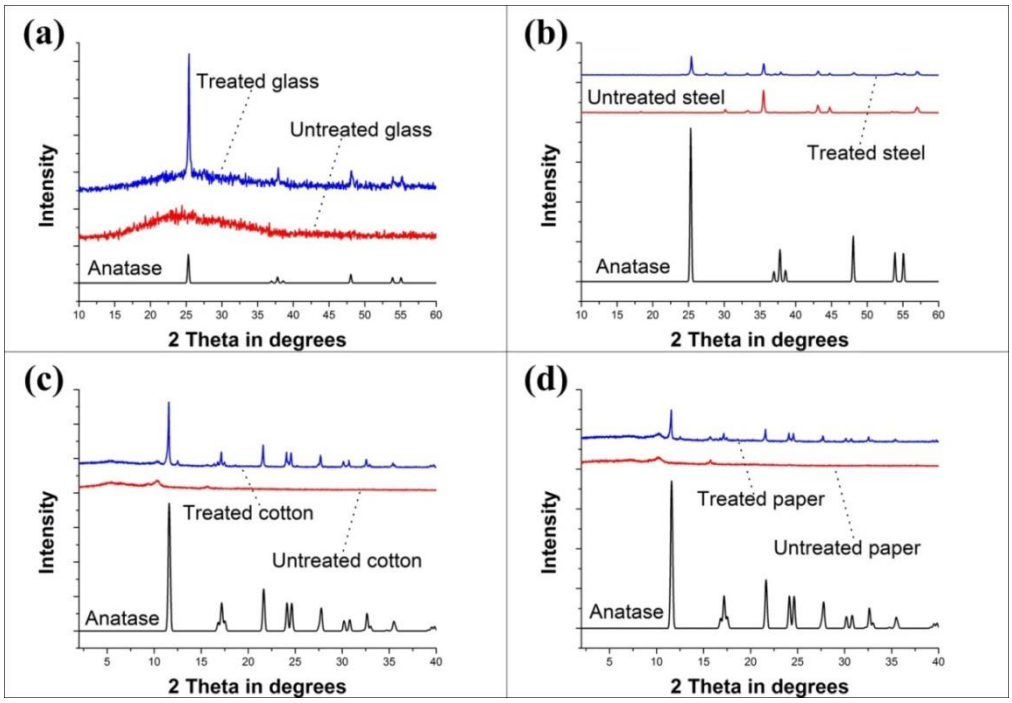

Fig. 3.7 XRD patterns of standard anatase, untreated and treated substrates, which were (a) glass, (b) steel, (c) cotton wool and (d) filter paper, respectively (glass is amorphous and no peaks on untreated glass).

For the paint, XPS was used to confirm the presence of Ti and F on the surface of the coatings as shown in Fig. 3.8. A $2p_{3/2}$ peak at binding energy 458.1 eV corresponding to Ti in the 4+ oxidation state was observed and matched to literature values.[29] Two F 1s environments were observed at 687.1 eV and 684.6 eV in a ratio of 5 to 1 respectively. This suggests that the peak at 687.1 eV corresponds to F in the $–CF_2$ groups while the 684.6 eV peak corresponds to F in the $–CF_3$ groups of the perfluorooctyltriethoxysilane compound used in coating the TiO_2 powders.

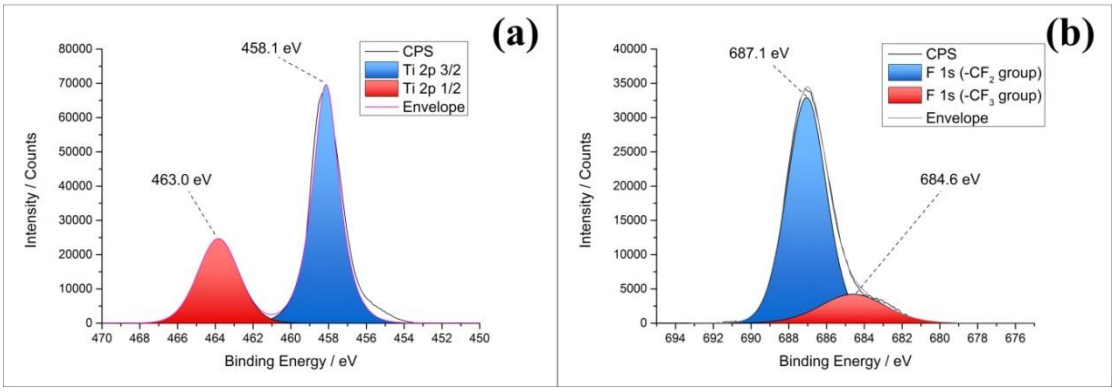

Fig. 3.8 XPS spectra of the self-cleaning coating. (a) and (b) show the presence of Ti and F on the surface, respectively.

3.3.4 Water droplet bouncing

Water dropping tests were carried out on untreated and superhydrophobic paint treated (*via* dip-coating) surfaces. When a surface shows an extremely high non-wetting property, water droplets tend to bounce instead of wetting the surface,[30, 31] no matter if the substrate is hard or soft. Fig. 3.9 shows the water bouncing process on the treated glass, steel, cotton wool and filter paper surfaces. The contact moment of water droplets and the solid surfaces is defined as 0, so the water bouncing processes could be seen from -2.41 ms to 13.45 ms. Here water droplets could completely leave the surface without wetting or even contaminating the surfaces (dyed blue), indicating that good superhydrophobicity and self-cleaning properties of the treated surfaces were obtained. Compared with treated samples, the untreated surfaces of glass, steel, cotton wool and filter paper stayed at their original wettability. Fig. 3.10 shows the water dropping tests on untreated glass, steel, cotton wool and filter paper from -2.41 ms to 13.45 ms (the water impacting moment is 0 and the last column is for the static status after the water drops).

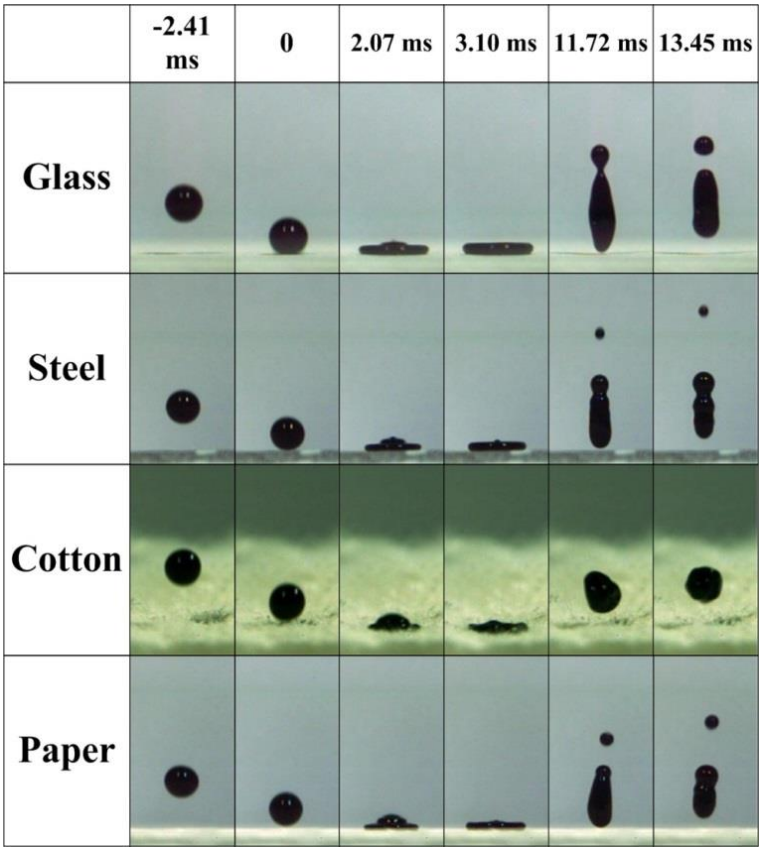

Fig. 3.9 Water droplets bouncing on the treated glass, steel, cotton wool and filter paper (droplet size: ~ 6.3 ± 0.2 μL).

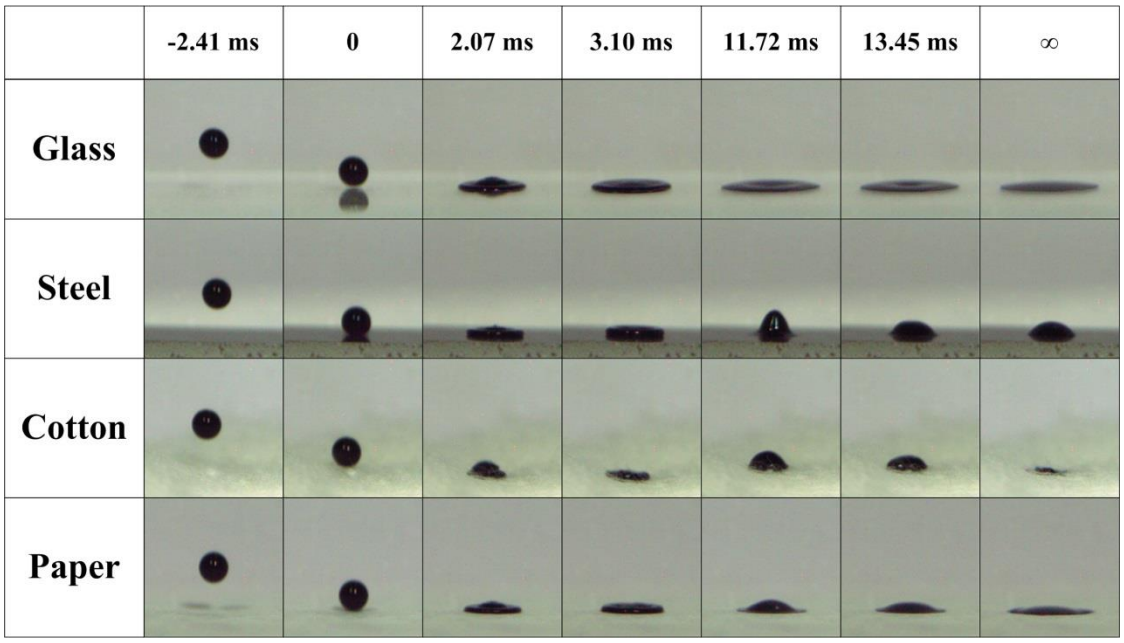

Fig. 3.10 Water dropping tests on untreated glass, steel, cotton wool and filter paper, respectively (droplet size: ~ 6.3 ± 0.2 μL).

3.3.5 Water proofing and dirt removal properties in air

The paint had good self-cleaning properties when treated with various substrates, especially for soft porous materials, which are widely used in making clothes and paper. The coating shows water proofing properties by the aforementioned water bouncing tests. Further tests on cotton wool can be seen in Fig. 3.11, which shows that the treated cotton wool inserted into the methylene blue dyed water, formed a negative meniscus on the solid-liquid-air interfaces due to the hydrophobicity. After the experiment, the cotton wool was taken out of the water, and it remained fully white with no trace of contamination by the blue water.

Dirt removal tests were carried out on the treated and original filter paper surfaces, as shown in Fig. 3.12. Dirt (MnO powder) was positioned onto the superhydrophobic paint treated filter paper, which was placed above an untreated filter paper sample. Water droplets were firstly applied to remove the dirt, and then water was poured continuously to remove the dirt onto the treated surface. After the test, the superhydrophobic sample was dry and clean while the untreated simple was wetted and contaminated.

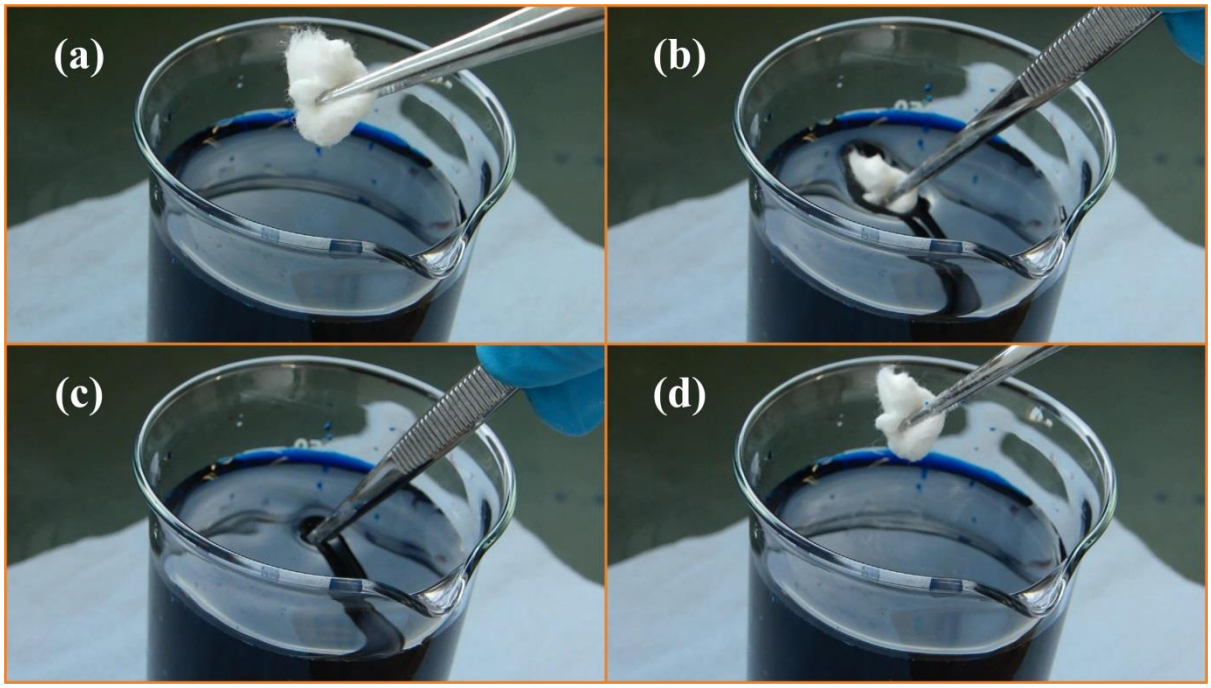

Fig. 3.11 “Dirty” water repellence tests on superhydrophobic paint treated cotton wool. (a) Before dipping into “dirty” water. (b) The cotton wool was dipped into “dirty” water. (c) The cotton wool was immersed into “dirty” water. (d) The cotton wool was removed from “dirty” water, and remained clean without any blue contaminated traces.

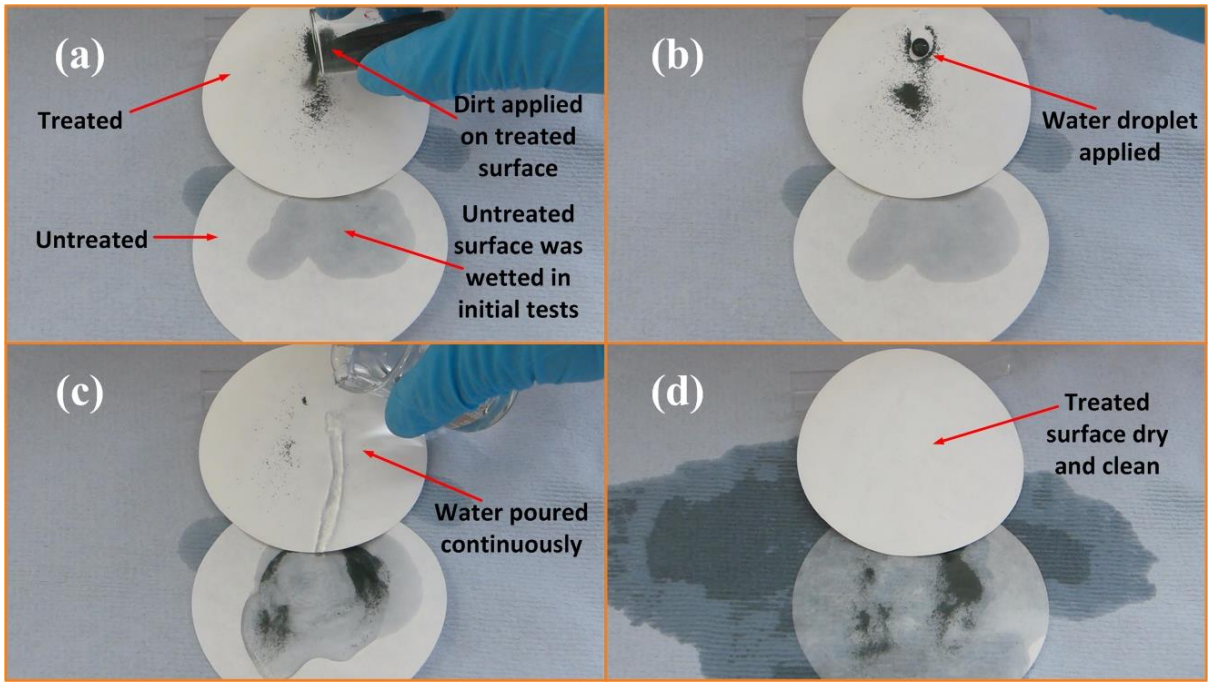

Fig. 3.12 Dirt-removal tests on superhydrophobic paint treated filter paper. The upper piece of filter paper was paint treated while the original filter paper was positioned under the treated sample. Initial water dropping tests on both samples were performed, the untreated filter paper was wetted and the treated sample was dry and clean. (a) Dirt was placed onto the treated filter paper. (b) Water droplets were applied to remove the dirt on the treated filter paper. (c) Water was poured continuously to remove the dirt on the treated filter paper. (d) After the water cleaning, the treated sample was dry and clean, while the untreated sample was wet and contaminated by the dirt.

A single water droplet was used to remove the dirt on the superhydrophobic painted treated glass and steel surfaces as shown by a high speed camera (Fig. 3.13), this is to understand how self-cleaning works among water, dirt and superhydrophobic surfaces. When the water droplet rolled into the dirt area, it picked up dirt and left a dry and clean trace on the superhydrophobic surfaces of either glass or steel.

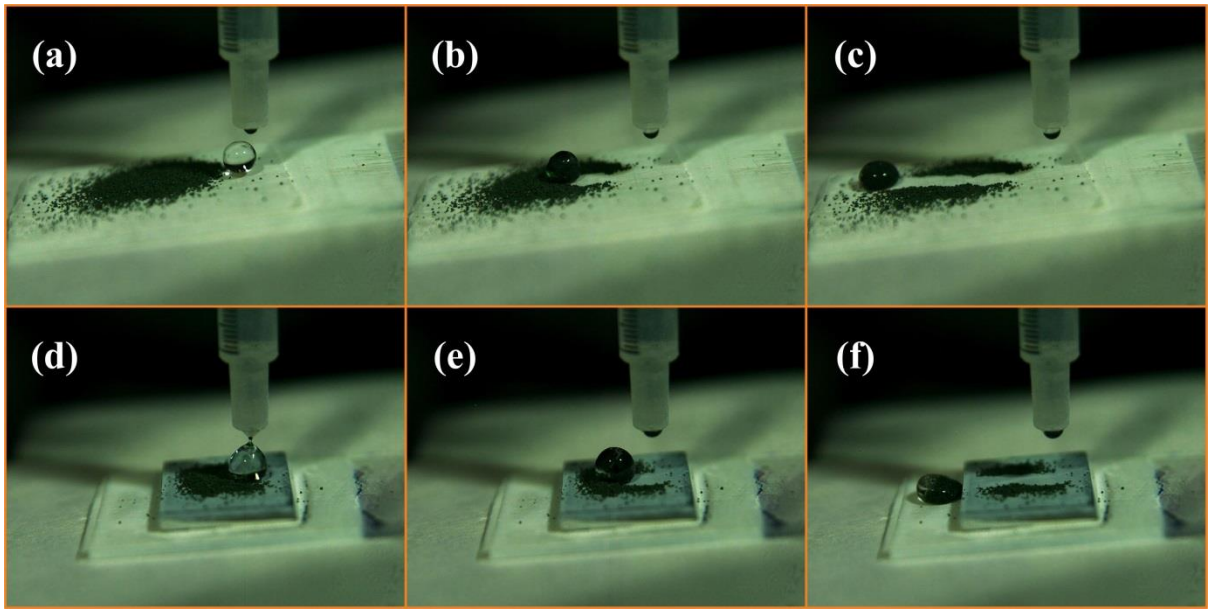

Fig. 3.13 High speed: dirt-removal tests on superhydrophobic paint treated glass and steel. (a) A water droplet was placed onto the treated glass surface. (b) The water droplet was half-way down removing the dirt on the treated glass surface. (c) The water droplet passed the dirt area, picked up the dirt and left a clean trace from the dirt area. (d) A water droplet was placed onto the treated steel surface. (e) The water droplet was half-way of removing the dirt on the treated steel surface. (f) The water droplet passed the dirt area, picked up the dirt and left a clean trace on the dirt area.

3.3.6 Self-cleaning tests after oil contamination and oil immersion

The treated surfaces show remarkable "Louts effect" in air as demonstrated by the water bouncing and self-cleaning tests. However, few reports have shown self-cleaning tests in oil as most superhydrophobic surfaces easily lose their water repellent ability when polluted by oil. This is because the surface tensions of most oils are smaller than that of water, resulting in oils more easily penetrating through the micro-nano morphologies of the superhydrophobic surfaces. Creating surface micro re-entrant structures to prepare superamphiphobic surfaces is an effective way to solve this problem as such surfaces repel both water and oils.[19, 25] However, there are still some conditions requiring both oil treatments and self-cleaning such as gears and bearings, in that condition, superamphiphobic surfaces cannot be treated with oil due to their oil-repellent properties. Here, the functional paint can be used for self-cleaning in oil.

Fig. 3.14 shows that water droplets still formed marble shapes on the coated surface when immersed in oil, thus it implies that the surfaces will retain their self-cleaning properties after oil-contamination on immersion due to the rolling motion of water droplets. For the untreated areas of the glass slide, water droplets spread and wet the surfaces.

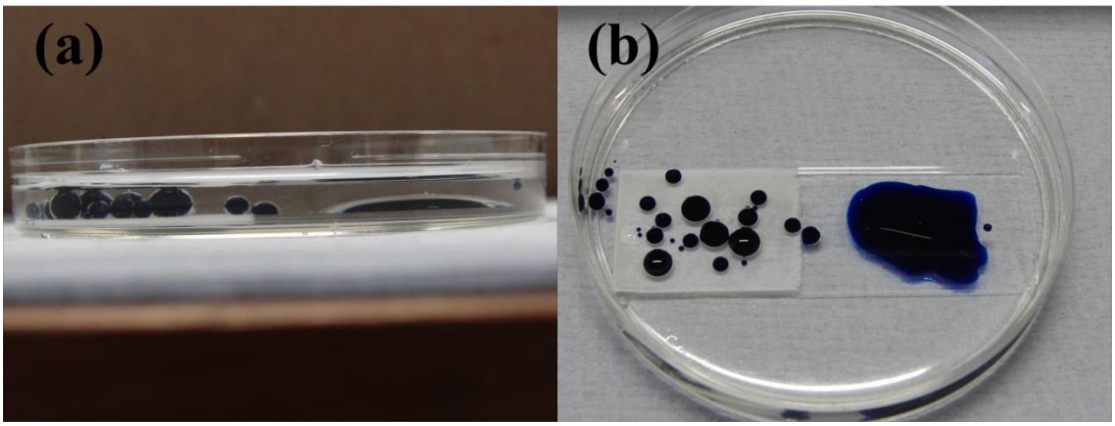

Fig. 3.14 Water droplets still shaped as marbles when placed on the coated surface that was immersed in oil (left part), and spread on the untreated areas (right part). (a) and (b) are the side and top views respectively.

Fig. 3.15(a) shows the side view of a tilted superhydrophobic painted treated glass surface which was partly immersed in oil (hexadecane), a water droplet (dye blue) was dropped into oil and repelled by the treated surface. Fig. 3.15(b) and (c) shows that water droplets were dropped onto an oil-contaminated superhydrophobic painted glass surface. The test was in air,

and water droplets were still repelled even though these droplets were no longer marble-shaped [insert of Fig. 3.15(b)]. Fig. 3.15(d) to (f) shows the dirt-removal tests either in air or oil on an oil-contaminated superhydrophobic painted treated glass surface. Dirt in either air and oil phases was removed by "dirty" water droplets indicating that the superhydrophobic coating had remarkable self-cleaning properties (including "dirty" water repellence and dirt-removal) either in air or oil.

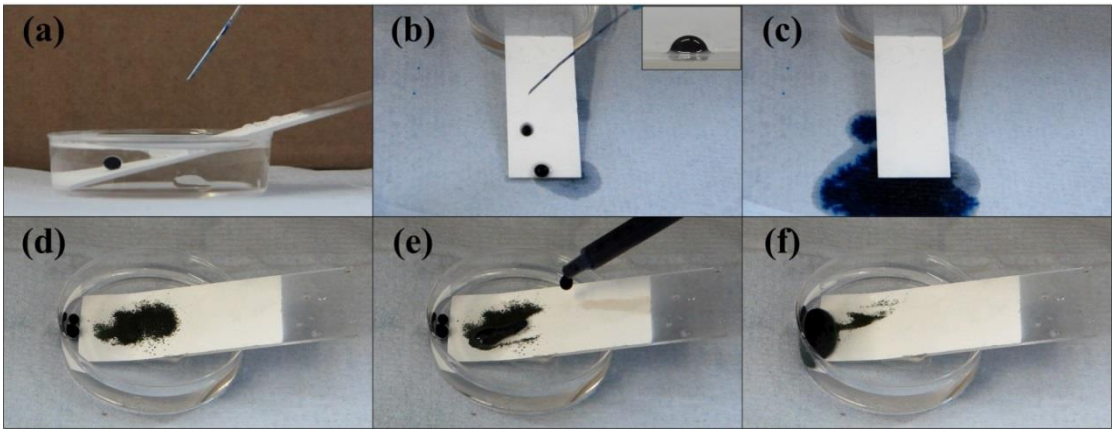

Fig. 3.15 Self-cleaning tests after oil contamination and oil immersion. (a) "Dirty" water droplet was repelled by a superhydrophobic painted treated glass surface that was immersed in oil (hexadecane). (b) and (c) "Dirty" water repellence of the oil contaminated treated surface, the insert in (b) shows a water droplet stays on the oil-contaminated treated surface. (d) to (f) Dirt-removal of the oil contaminated treated surface either in air or oil. Dirt was positioned onto the oil-contaminated treated surface with partly in air and partly in oil, "dirty" water was then dropped and removed the dirt.

The dirt-removal properties after oil-contamination were shown from the aforementioned tests, however, practical conditions must be taken into consideration. For example, our clothes might get stained by soil outside the house, or get dusty inside the house; they might get stained by chemicals from the lab, or from cooking oil at home. To mimic the practical conditions, soil (outdoor environment) and dust (indoor environment) were selected as dirt; hexadecane (chemical in the lab) and cooking oil (from home) were selected as oil in the dirt-removal experiment in either air or oil, as shown in Fig. 3.16. The superhydrophobic paint treated samples were initially pre-contaminated by respective oils and then partly inserted into the respective oils. It is seen that dirt (either in air or oil) was removed by "dirty" water from the superhydrophobic paint treated surfaces, indicating that the surfaces are also applicable to practical conditions for self-cleaning purposes.

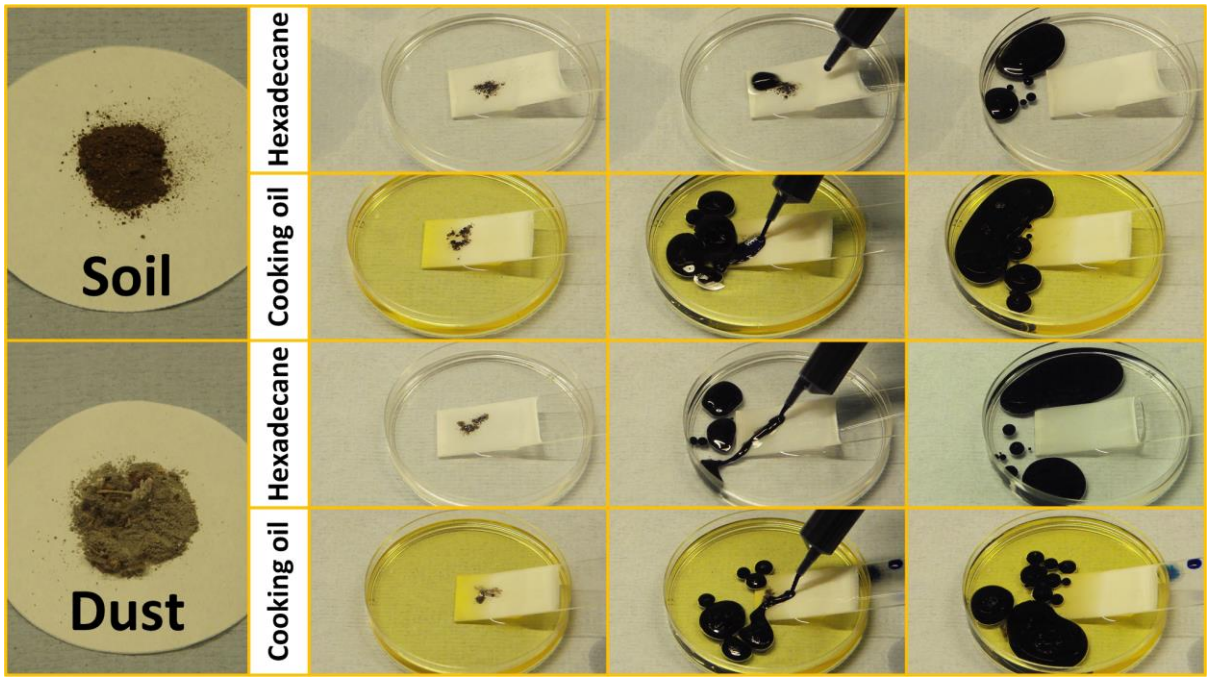

Fig. 3.16 Dirt-removal test on the superhydrophobic paint treated glass surface that was pre-contaminated by respective oils. Soil and dust were used as dirt, and hexadecane and cooking oil were used as oil. Dirt was placed partly in air and partly in oil on the treated surface, then "dirty" water was applied to remove dirt.

In air, water droplets were supported by the nano particles and air pockets in between, resulting in a high water contact angle and a low contact angle hysteresis. With the rolling motion, the coated surfaces achieved a self-cleaning ability. When the coated surfaces were immersed in hexadecane, the oil would gradually penetrate into the surface structures, and the oily molecules fill in air pockets and carry on supporting the water droplet; on the other hand, the particles (Sigma-TiO_2 and TiO_2 P25) forming the nano structures remained hydrophobic, so that they could still support the water droplet. In addition, these hydrophobic particles were positioned at the interface of oil-water, as shown in Fig. 3.17; in this condition, self-assembly of the particles occurred because it minimizes the area of the interface between particles and solution.[32-34] The particles then attracted each other and made water unable to penetrate; this is why the surface retained its water repellent ability after oil contamination. On oil immersion, water droplets were still marble-shaped on the coated surface [Fig. 3.14] and retained the rolling motion when tilted [Fig. 3.15(a)]. In this condition, the self-cleaning behaviour in oil is similar to that in vapour, thus it is not surprising that the coated surface retained its water repellency and dirt removal properties when immersed in oil [Fig. 3.15 (d) to (f)]. In air, the water droplet was no longer marble-shaped on the oil-contaminated treated

surface. Even losing the high water contact angle, a low contact angle hysteresis remained and still contributed to dirt removal due to the slippery motion.[35, 36] For these reasons, the coated surface still kept the self-cleaning properties when being contaminated by oil and even immersed.

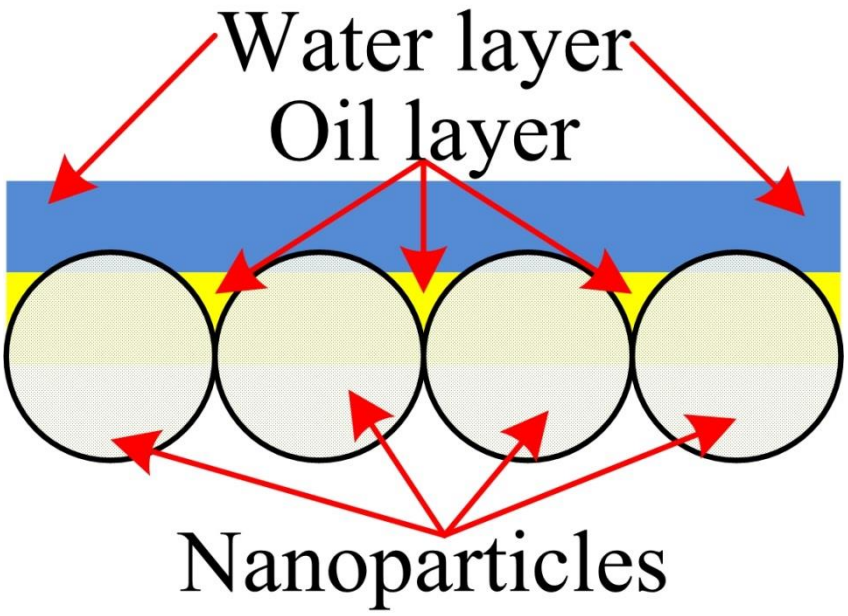

Fig. 3.17 The hydrophobic particles were positioned at an interface of oil-water, here, self-assembly of the particles occurred and then they attracted each other, making water unable to penetrate, this is why the surface retained water repellent ability after oil contamination.

3.3.7 Robust superhydrophobic surfaces

Mechanical robustness significantly affects the longevity of a superhydrophobic surface in practical conditions. In this section, surface robustness tests will include the finger-print, knife-scratch and sandpaper abrasion tests on superhydrophobic paint and adhesives (double sided tape or spray adhesive) and substrates (glass, steel, cotton wool or filter paper).

1. Finger-print: finger wiped the sample from the untreated area to superhydrophobic paint and then superhydrophobic paint and adhesive treated surface.

1a. Superhydrophobic paint and double sided tape + glass/steel (Fig 3.18). The original, superhydrophobic paint treated, and superhydrophobic paint + double sided tape treated glass and steel were wiped by the finger. “Dirty” water (methylene blue dyed) was dropped onto these surfaces before and after the experiment to test their self-cleaning properties.

Before finger printing, the original glass and steel got stained blue after the water dropping test; superhydrophobic paint treated, and superhydrophobic paint and double sided tape treated substrates remained dry and clean.

After finger printing, the superhydrophobic paint, which was directly coated onto the substrates, were removed, while the coatings remained on the adhesive bonded samples. “Dirty” water was then applied, it is seen that the areas where superhydrophobic paint got removed were stained while the superhydrophobic paint + double sided tape treated substrates remained dry and clean.

From this test, it is seen how mechanically weak a superhydrophobic surface can be, and how its robustness can be improved.

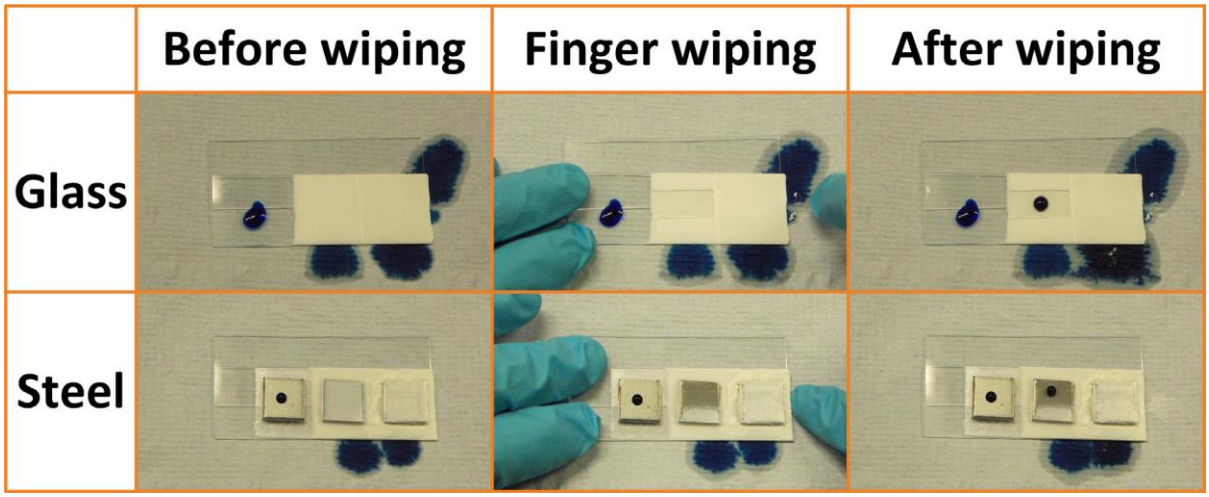

Fig. 3.18 On the glass and steel samples, surfaces from left to right are original, superhydrophobic paint treated, and superhydrophobic paint + double sided tape treated. After a finger-wipe, "dirty" water was dropped before and after the finger-print to test the self-cleaning properties of these surfaces.

1b. Superhydrophobic paint + spray adhesive + glass/steel/cotton wool/filter paper (Fig 3.19). The original, superhydrophobic paint treated, and superhydrophobic paint + spray adhesive treated substrates (glass, steel, cotton wool and filter paper) were wiped by a finger. "Dirty" water (methylene blue dyed) was dropped onto these surfaces before and after the experiment to test their self-cleaning properties.

Before finger printing, the original glass, steel, cotton wool and filter paper got stained blue after the water dropping test; superhydrophobic paint treated, and superhydrophobic paint and double sided tape treated substrates remained dry and clean.

After finger printing, the superhydrophobic paint, which was directly coated onto the hard substrates (glass and steel) were removed, while the coatings remained on the adhesive bonded samples. "Dirty" water was then applied and it can be seen that the areas where superhydrophobic paint got removed were stained while the superhydrophobic paint + double sided tape treated substrates remained dry and clean. However, superhydrophobic paint treated soft substrates (cotton wool and filter paper) retained superhydrophobicity even after one finger-print.

From this test, it is seen that superhydrophobic soft porous materials are more mechanically stable than the hard surfaces, this is due to the larger surface areas on porous materials, and

the superhydrophobic coatings in the grooves can be partly protected from applied mechanical impacts which are not very aggressive.

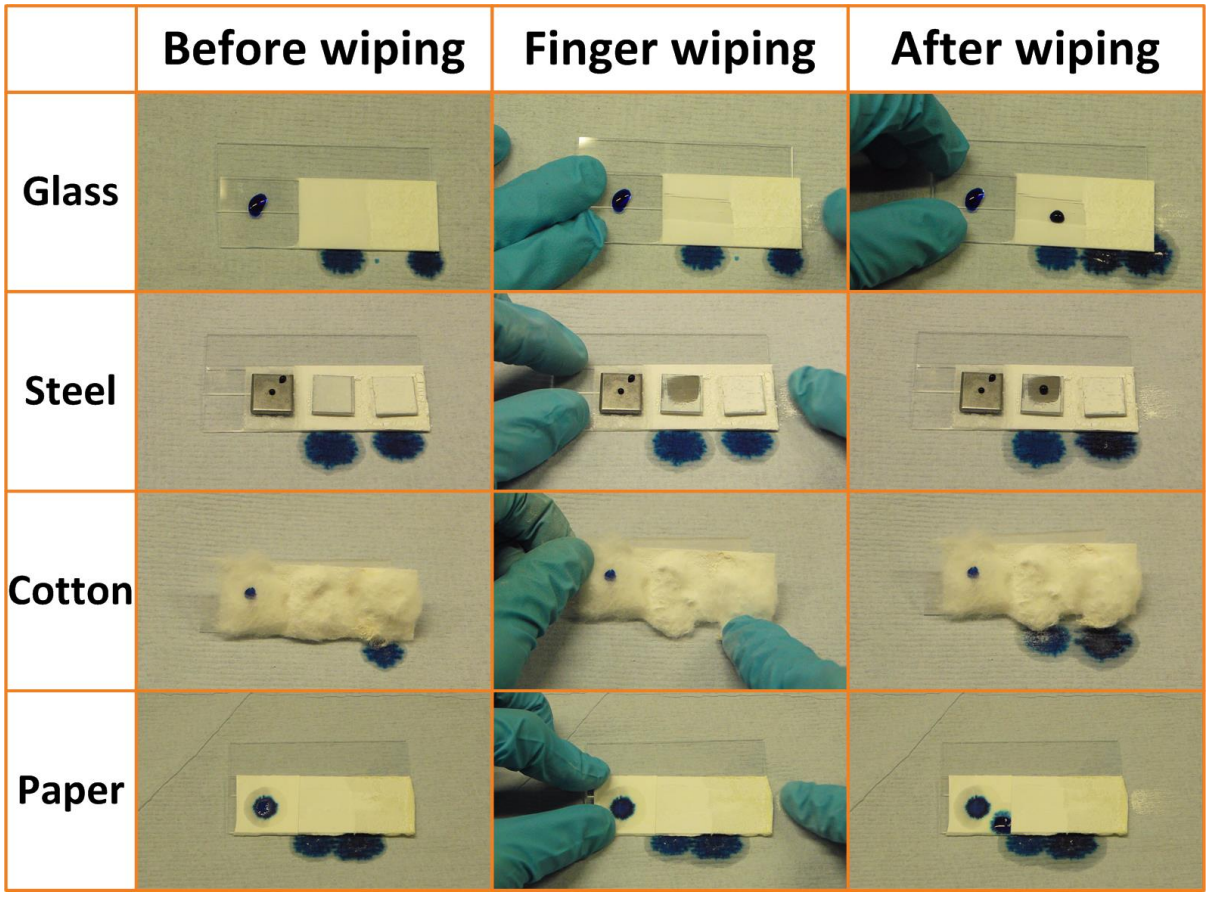

Fig. 3.19 Surfaces are original, superhydrophobic paint treated, and superhydrophobic paint + spray adhesive treated from left to right. After a finger-wipe, "dirty" water was dropped before and after the finger-print to test the self-cleaning properties of these surfaces.

2. Knife-scratch: a knife was used to scratch superhydrophobic paint and adhesive treated surfaces, "dirty" water was then dropped after scratching to test their self-cleaning properties.

2a. Knife-scratch on the "superhydrophobic paint + double sided tape + glass" surface, "dirty" water was then applied to test the superhydrophobicity after the knife-scratch (Fig. 3.20). As double sided tapes are not applicable to all the substrates, glass was used as an example of the substrate. After the knife-scratch, "dirty" water was still repelled away, indicating this surface is able to tolerate the knife-scratch.

Fig. 3.20 Knife-scratch on the superhydrophobic paint + double sided tape + glass substrate, water was then applied to test the superhydrophobicity after the knife-scratch.

2b. Superhydrophobic paint + spray adhesive + glass/steel/cotton wool/filter paper (Fig. 3.21). These substrates were firstly coated with spray adhesives and then dip-coated with superhydrophobic paint. After knife-scratch, "dirty" water was dropped onto these surfaces. The surfaces remained dry and clean after the tests indicating that the idea of bonding superhydrophobic paint and adhesives could greatly improve the robustness of superhydrophobic coatings.

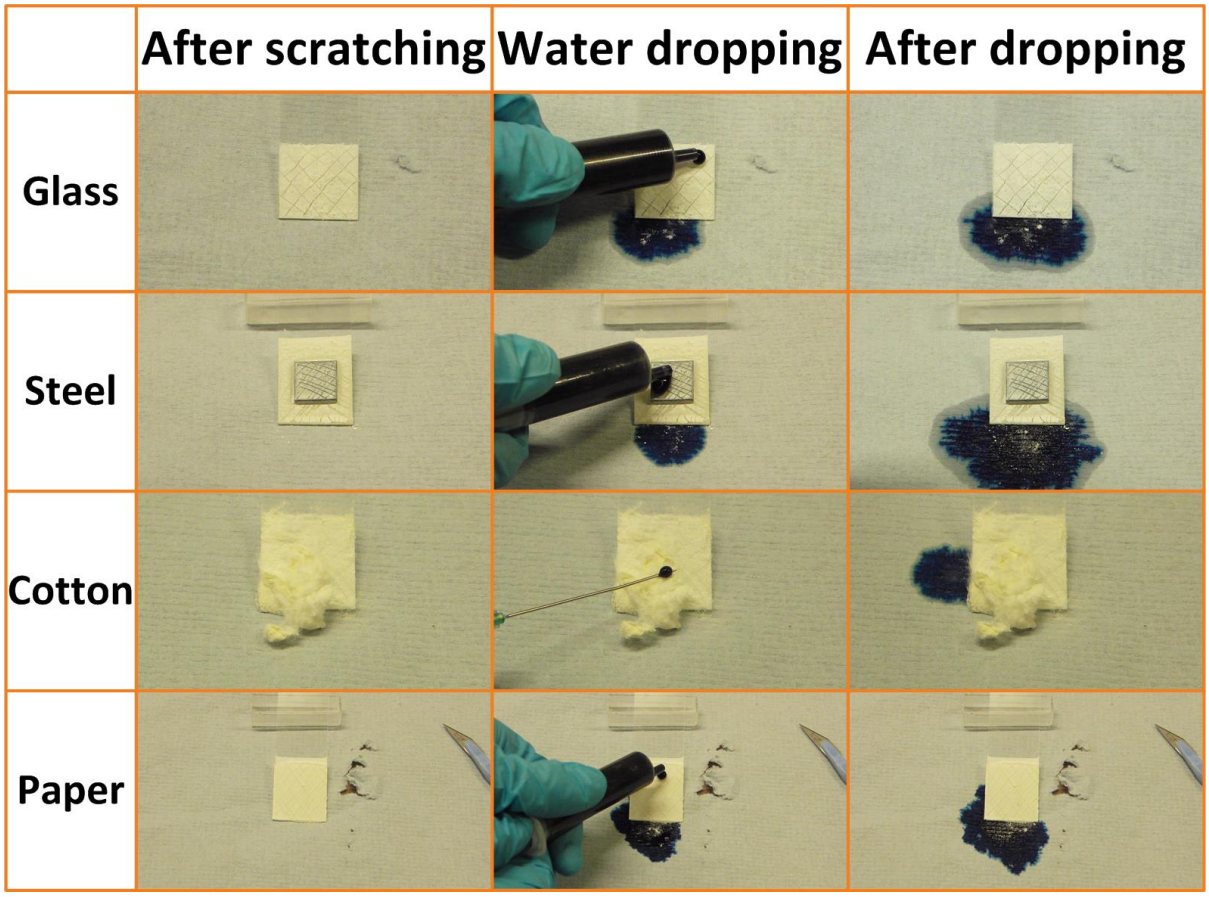

Fig. 3.21 Knife-scratch tests on superhydrophobic paint + spray adhesive + glass/steel/cotton wool/filter paper surfaces. Water was then applied to test the superhydrophobicity after the knife-scratch.

3. Sandpaper abrasion: coated surfaces were sandwiched between the weight and the sandpaper and then guided to travel with the coatings facing to the sandpaper.

It has been shown that the robustness of superhydrophobic coatings was greatly improved by combining adhesives and superhydrophobic paint, through the finger-print and knife-scratch tests. However, it is also required to quantify how robust a superhydrophobic surface is; so multiple cycles of sandpaper abrasion tests were carried out on the superhydrophobic paint + adhesive treated samples.

3a. Multiple cycles of sandpaper abrasion tests on superhydrophobic paint + double sided tape + glass substrates (Fig. 3.22). As double sided tapes are not applicable to all substrates, glass was used as an example of the substrate. Fig. 3.22(a) and (b) shows one cycle of sandpaper abrasion test, and this guarantees that the superhydrophobic surfaces got abraded longitudinally and transversely for 10 cm in each direction (20 cm in total) in one abrasion

cycle. Fig. 3.22(c) shows the plot of mechanical abrasion cycles and water contact angles after each cycle of the abrasion tests. The contact angle measuring points were picked up randomly on the abraded superhydrophobic surface, it is seen that the lowest contact angle is still greater than 156°, indicating that the surfaces remained superhydrophobic after abrasions even for 40 cycles. However, the randomly picked contact angle measuring points are not enough to prove that the whole area was able to tolerate multi-cycles of abrasion. Further a water droplet was guided to travel on the abraded surface as shown in Fig. 3.22(d). Fig. 3.23 shows that the water droplet was guided to travel on the superhydrophobic glass surface after sandpaper abrasion (travel direction, to left) for the 11th, 20th, 30th and 40th cycles. The droplet retained its marble-shape while travelling on the abraded surface indicating that the whole area of the surface retained superhydrophobicity.

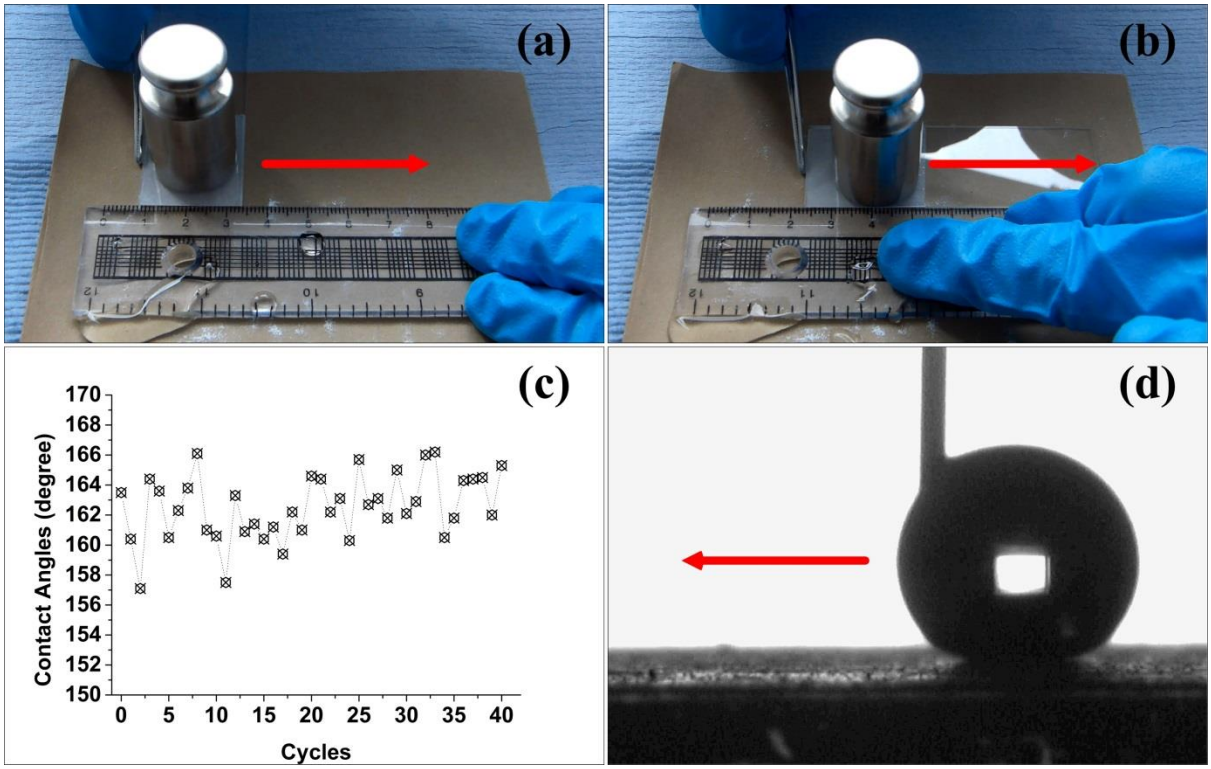

Fig. 3.22 (a) and (b) the treated surface with a weight of 100 g was moved longitudinally and transversely for 10 cm, respectively. (c) The plot of mechanical abrasion cycles and water contact angles after each abrasion test. (d) Water droplet travelling test after 40th cycle abrasion.

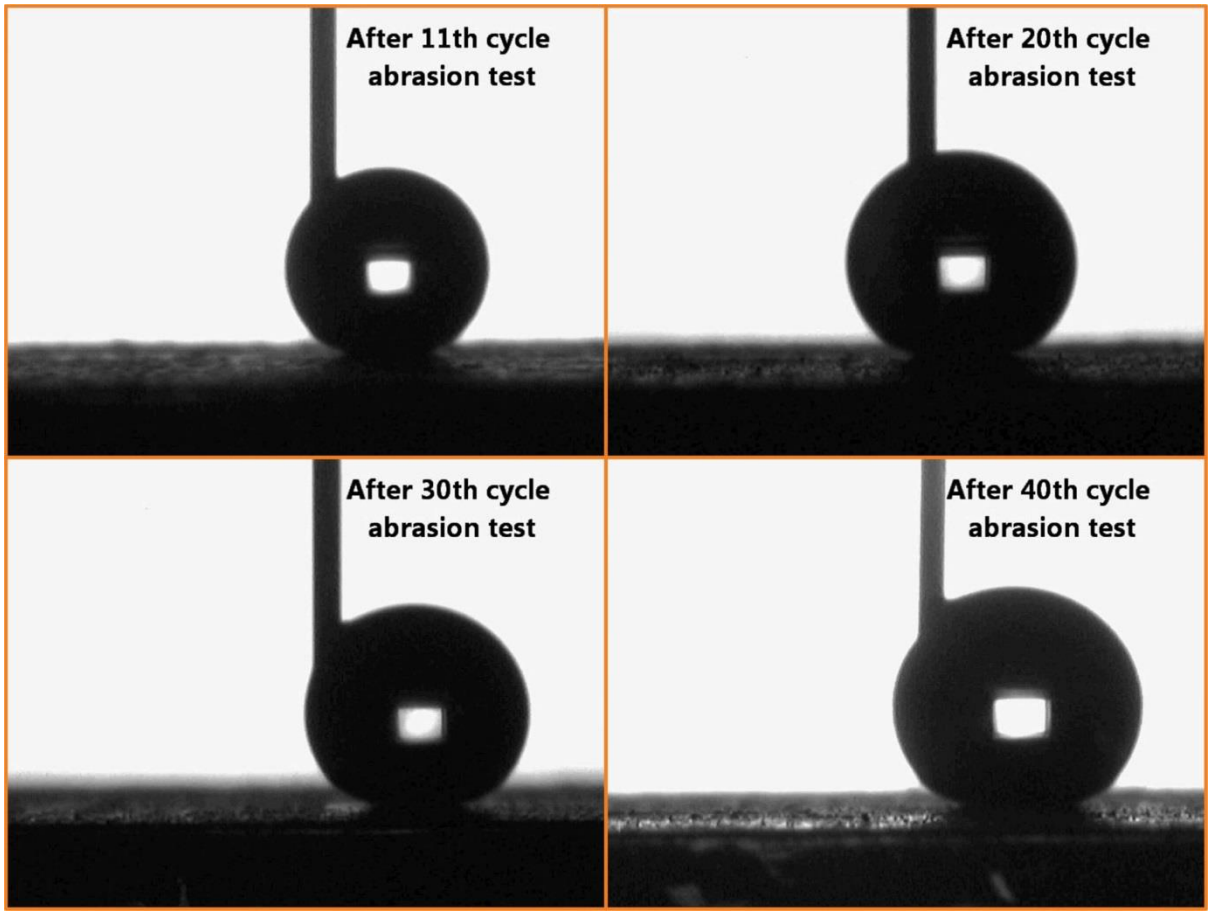

Fig. 3.23 A water droplet was guided to travel on the superhydrophobic glass surface after sandpaper abrasion (travel direction, to left).

So how does double sided tape help? Fig. 3.24 shows the SEM images of bare tape, painted tape and the painted tape after 1 cycle abrasion in magnifications of x 1000, x 5000 and x 30000 (rows are magnifications and columns are cycles of abrasion). Bare tape did not have any discernible surface roughness; after painting, the tape substrate was covered by dual nanoparticles; after 1 cycle of abrasion, some nanoparticles were removed and some scratches on the surface could be seen through SEM, however, in high magnification (x 30000), there were still some nanoscale roughness left and the surface did not change much both in morphology and wettability.

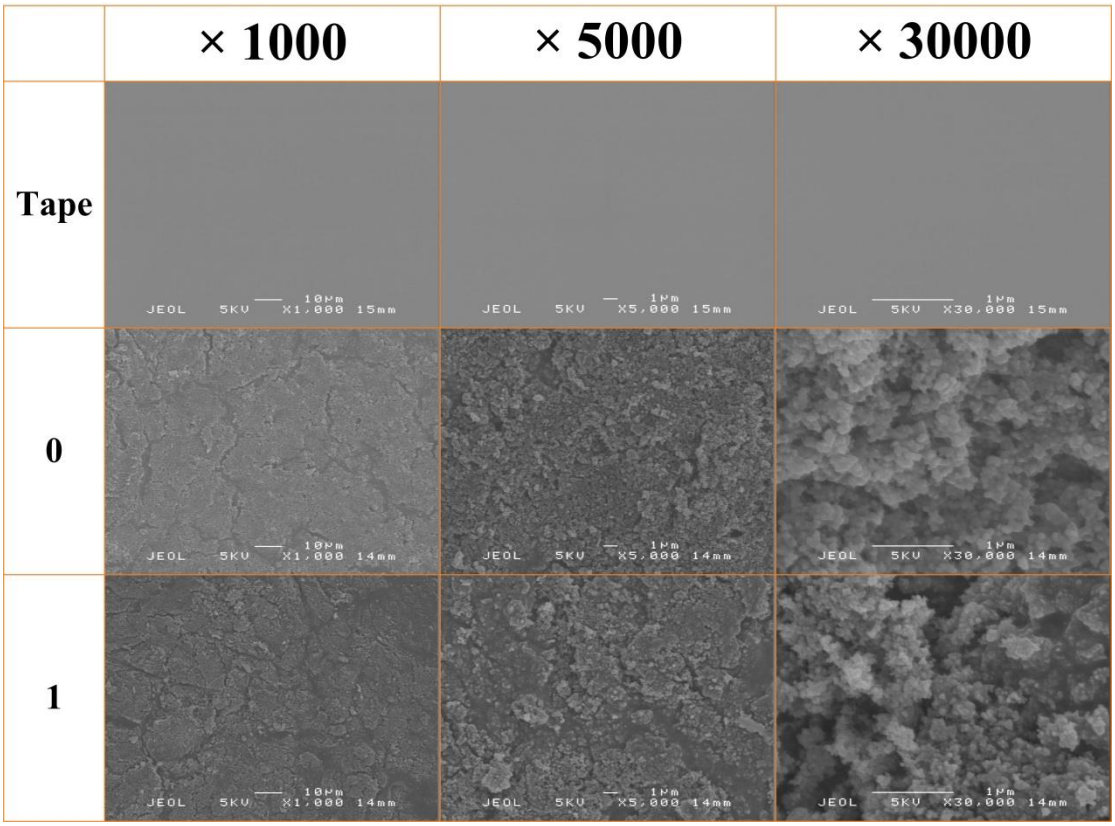

Fig. 3.24 SEM images that compare surface morphology between bare tape, painted tape and the painted tape after 1 cycle of abrasion (rows are magnifications and columns are cycles of abrasion).

There is not much difference between morphologies before and after 1 cycle of abrasion. As the number of cycles of abrasion increased, the difference could gradually be observed. Fig. 3.25 shows the SEM images of the painted tape surfaces after the 10^{th}, 20^{th}, 30^{th} and 40^{th} cycles of abrasion, respectively (rows are magnifications and columns are cycles of abrasion). Scratches were more obvious after the 10^{th} cycle than that after the 1^{st} cycle; however, in high magnification (x 30000), nanoparticles were embedded into the tape substrate. After the 20^{th}, 30^{th} and 40^{th} cycles of abrasion, even the tape substrate was slightly worn, the nanoparticles were still left in the tape, and surface roughness was kept even after the 40^{th} cycle of abrasion. This is the reason why the painted surface is very robust and retains superhydrophobicity after tens of cycles of sand paper abrasion.

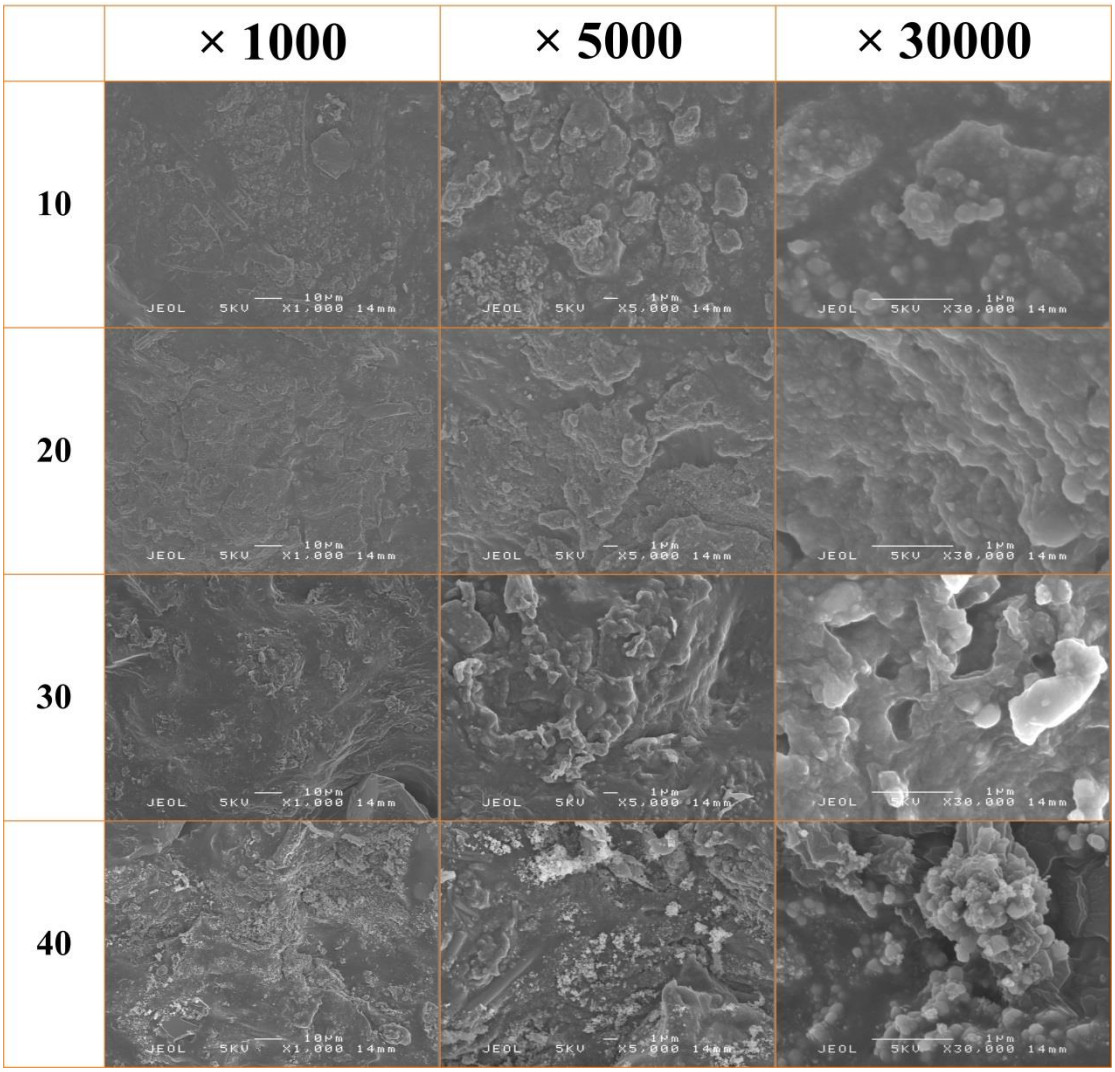

Fig. 3.25 SEM images that compare surface morphology between the painted tape surfaces after 10^{th}, 20^{th}, 30^{th} and 40^{th} cycles of abrasion (rows are magnifications and columns are cycles of abrasion).

3b. Sandpaper abrasion tests on superhydrophobic paint + spray adhesive + glass/steel/cotton wool/filter paper surfaces.

Spray adhesives were used to bond the superhydrophobic paint to the substrates (Fig. 3.26); one cycle of sandpaper abrasion was tested on these surfaces, and the surfaces remained superhydrophobic. In particular, the spray adhesive is also applicable for soft porous materials, for example, cotton wool. Although the superhydrophobic paint treated cotton wool is able to tolerate some robustness tests such as finger-print, the nanoparticles of the superhydrophobic paint could be easily abraded if they are not firmly attached to the body of

cotton wool (Fig. 3.27). However, the bonding between the superhydrophobic paint and the substrates could be greatly improved by adhesives.

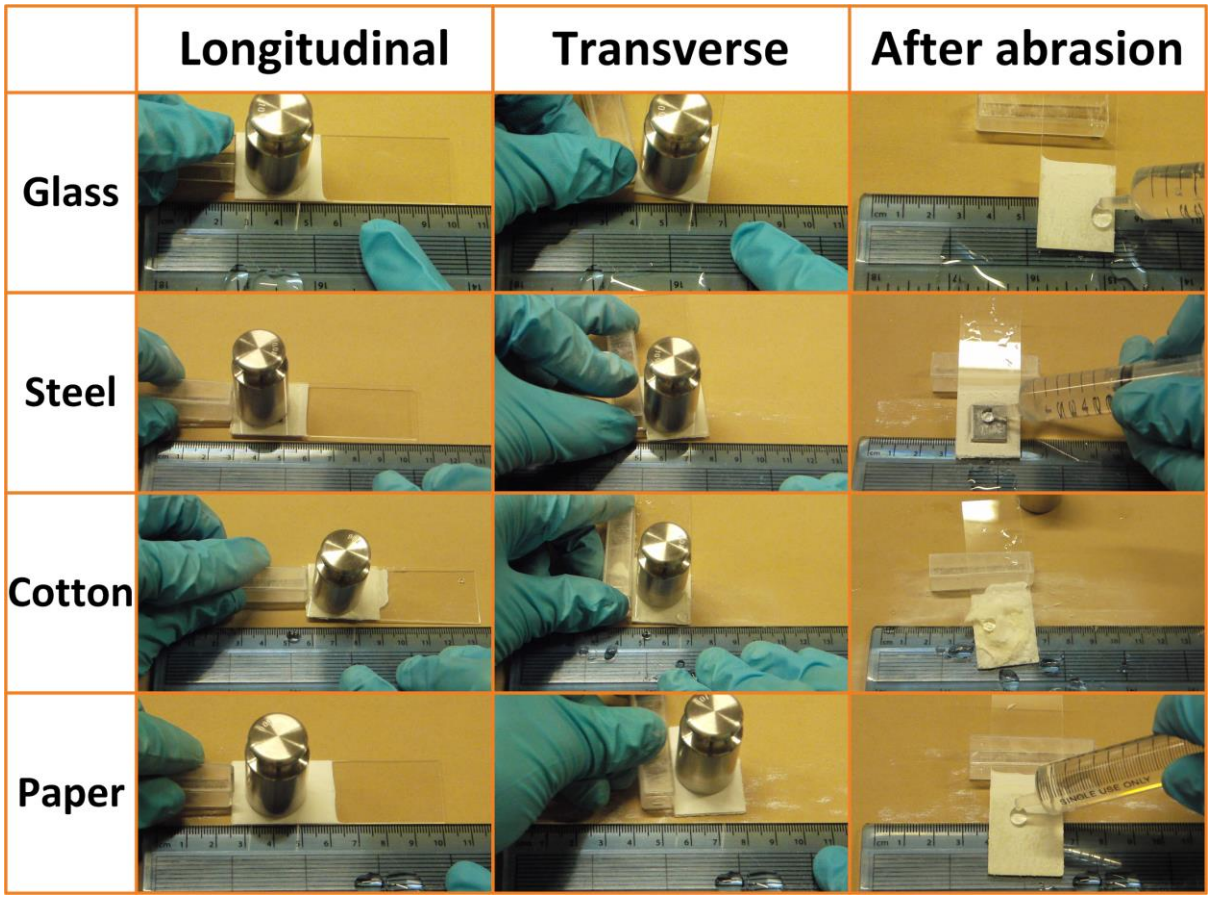

Fig. 3.26 Sandpaper abrasion test on superhydrophobic paint + spray adhesive + glass/steel/cotton wool/filter paper surfaces.

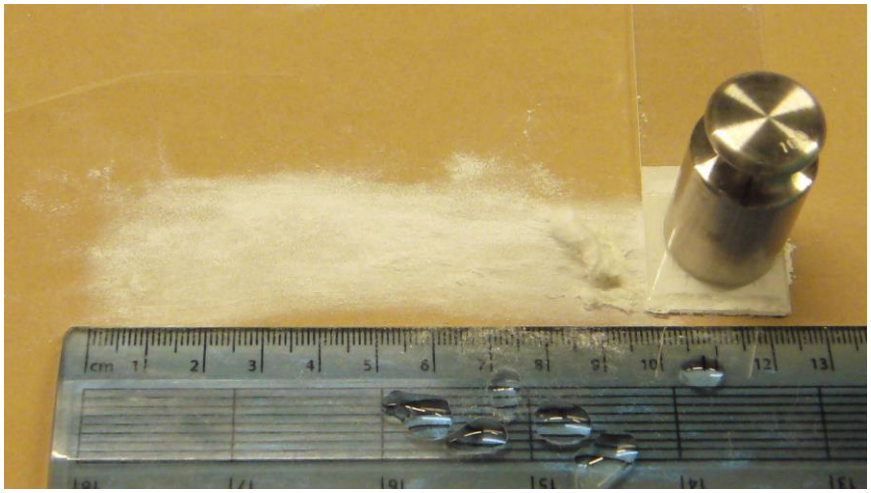

Fig. 3.27 In the sandpaper abrasion test, it is easy for the superhydrophobic paint to be abraded out if it was directly treated on soft substrates (cotton wool was used as an example).

3.4 Conclusions

In this chapter, a paint-like suspension was created to make superhydrophobic surfaces through mixing dual scaled TiO_2 nanoparticles and fluorosilane-solution. This paint could be easily treated onto both hard and soft substrates such as glass, steel, cotton wool and filter paper *via* dip-coating, spray-coating or simply with the extrusion of the paint from a syringe. The nanoparticles and fluorosilane were used to created surface roughness and lower the surface energy, respectively, to minimize the contact friction of water and the solid substrates.

The coated surfaces had remarkable self-cleaning properties. The surfaces remained dry and clean when they were contacted with methylene blue dyed water ("dirty" water); even the superhydrophobic paint treated cotton wool could retain its white colour when it was removed from "dirty" water. Dust powder could be easily removed from treated substrates when water was applied, the dirt-removal property also demonstrated the self-cleaning ability of the treated superhydrophobic substrates. In particular, the treated surfaces retained their "dirty" water repellence and dirt-removal properties when contaminated by oil and even immersed in oil. This is because a slippery state was formed when the air pockets were occupied by oil, and this state was still able to repel water and retain the self-cleaning properties.

The superhydrophobic paint is very compatible with commercial adhesives, which greatly improved the mechanical robustness of the superhydrophobic coatings on glass, steel, cotton wool and filter paper. The coating could be easily removed by a finger print without any adhesives especially on hard substrates. However, when the paint was bonded with adhesives, the treated surfaces remained superhydrophobic after finger-print, knife-scratch and even 40 cycles of sandpaper abrasions. The inorganic particles get pushed into the adhesive by friction and the adhesive flexibility stabilises the particles to abrasion. This idea is to apply more sophisticated and robust adhesive techniques to overcome the weak inherent mechanical robustness of superhydrophobic coatings. In industrial applications, adhesives can be selected based on the practical conditions, double sided tapes and spray adhesives were only shown here as two examples. In addition, particles could also be replaced by SiO_2, Fe_2O_3 etc. in consideration of cost, colour and/or some other aspects.

The coatings can be readily applied in harsh and oily circumstances when mechanical robustness is applied.

3.5 References

1. Lu, Y.; Sathasivam, S.; Song, J.; Chen, F.; Xu, W.; Carmalt, C. J.; Parkin, I. P. Creating superhydrophobic mild steel surfaces for water proofing and oil–water separation. *Journal of Materials Chemistry A* 2014, 2, 11628-11634.

2. Yin, B.; Fang, L.; Hu, J.; Tang, A.-Q.; Wei, W.-H.; He, J. Preparation and properties of super-hydrophobic coating on magnesium alloy. *Applied surface science* 2010, 257, 1666-1671.

3. Wang, Y.; Wang, W.; Zhong, L.; Wang, J.; Jiang, Q.; Guo, X. Super-hydrophobic surface on pure magnesium substrate by wet chemical method. *Applied Surface Science* 2010, 256, 3837-3840.

4. Xu, W.; Song, J.; Sun, J.; Lu, Y.; Yu, Z. Rapid fabrication of large-area, corrosion-resistant superhydrophobic Mg alloy surfaces. *ACS applied materials & interfaces* 2011, 3, 4404-4414.

5. Song, J.; Xu, W.; Lu, Y. One-step electrochemical machining of superhydrophobic surfaces on aluminum substrates. *Journal of Materials Science* 2012, 47, 162-168.

6. Crick, C. R.; Bear, J. C.; Kafizas, A.; Parkin, I. P. Superhydrophobic photocatalytic surfaces through direct incorporation of titania nanoparticles into a polymer matrix by aerosol assisted chemical vapor deposition. *Advanced Materials* 2012, 24, 3505-3508.

7. Crick, C. R.; Parkin, I. P. A single step route to superhydrophobic surfaces through aerosol assisted deposition of rough polymer surfaces: duplicating the lotus effect. *Journal of Materials Chemistry* 2009, 19, 1074-1076.

8. Crick, C. R.; Bear, J. C.; Southern, P.; Parkin, I. P. A general method for the incorporation of nanoparticles into superhydrophobic films by aerosol assisted chemical vapour deposition. *Journal of Materials Chemistry A* 2013, 1, 4336-4344.

9. Ma, M.; Hill, R. M. Superhydrophobic surfaces. *Current opinion in colloid & interface science* 2006, 11, 193-202.

10. Schellenberger, F.; Encinas, N.; Vollmer, D.; Butt, H.-J. How Water Advances on Superhydrophobic Surfaces. *Physical Review Letters* 2016, 116, 096101.

11. Xiu, Y.; Liu, Y.; Hess, D. W.; Wong, C. P. Mechanically robust superhydrophobicity on hierarchically structured Si surfaces. *Nanotechnology* 2010, 21, 155705.

12. Lu, Y.; Xu, W.; Song, J.; Liu, X.; Xing, Y.; Sun, J. Preparation of superhydrophobic titanium surfaces via electrochemical etching and fluorosilane modification. *Applied Surface Science* 2012, 263, 297-301.

13. Lu, Y.; Sathasivam, S.; Song, J.; Xu, W.; Carmalt, C. J.; Parkin, I. P. Water droplets bouncing on superhydrophobic soft porous materials. *Journal of Materials Chemistry A* 2014, 2, 12177-12184.

14. Chen, F.; Song, J.; Lu, Y.; Huang, S.; Liu, X.; Sun, J.; Carmalt, C. J.; Parkin, I. P.; Xu, W. Creating robust superamphiphobic coatings for both hard and soft materials. *Journal of Materials Chemistry A* 2015, 3, 20999-21008.

15. Chen, X.; Wu, Y.; Su, B.; Wang, J.; Song, Y.; Jiang, L. Terminating marine methane bubbles by superhydrophobic sponges. *Advanced Materials* 2012, 24, 5884-5889.

16. Zimmermann, J.; Reifler, F. A.; Fortunato, G.; Gerhardt, L. C.; Seeger, S. A Simple, One‐Step Approach to Durable and Robust Superhydrophobic Textiles. *Advanced Functional Materials* 2008, 18, 3662-3669.

17. Zhou, H.; Wang, H.; Niu, H.; Gestos, A.; Wang, X.; Lin, T. Fluoroalkyl silane modified silicone rubber/nanoparticle composite: a super durable, robust superhydrophobic fabric coating. *Advanced Materials* 2012, 24, 2409-2412.

18. Deng, B.; Cai, R.; Yu, Y.; Jiang, H.; Wang, C.; Li, J.; Li, L.; Yu, M.; Li, J.; Xie, L. Laundering durability of superhydrophobic cotton fabric. *Advanced Materials* 2010, 22, 5473-5477.

19. Lu, Y.; Song, J.; Liu, X.; Xu, W.; Xing, Y.; Wei, Z. Preparation of superoleophobic and superhydrophobic titanium surfaces via an environmentally friendly electrochemical etching method. *ACS Sustainable Chemistry & Engineering* 2012, 1, 102-109.

20. Deng, X.; Mammen, L.; Butt, H.-J.; Vollmer, D. Candle soot as a template for a transparent robust superamphiphobic coating. *Science* 2012, 335, 67-70.

21. He, Z.; Ma, M.; Lan, X.; Chen, F.; Wang, K.; Deng, H.; Zhang, Q.; Fu, Q. Fabrication of a transparent superamphiphobic coating with improved stability. *Soft Matter* 2011, 7, 6435-6443.

22. Barthlott, W.; Neinhuis, C. Purity of the sacred lotus, or escape from contamination in biological surfaces. *Planta* 1997, 202, 1-8.

23. Marmur, A. The lotus effect: superhydrophobicity and metastability. *Langmuir* 2004, 20, 3517-3519.

24. Gao, L.; McCarthy, T. J. The “lotus effect” explained: two reasons why two length scales of topography are important. *Langmuir* 2006, 22, 2966-2967.

25. Tuteja, A.; Choi, W.; Ma, M.; Mabry, J. M.; Mazzella, S. A.; Rutledge, G. C.; McKinley, G. H.; Cohen, R. E. Designing superoleophobic surfaces. *Science* 2007, 318, 1618-1622.

26. Wang, H.; Xue, Y.; Ding, J.; Feng, L.; Wang, X.; Lin, T. Durable, Self‐Healing Superhydrophobic and Superoleophobic Surfaces from Fluorinated‐Decyl Polyhedral Oligomeric Silsesquioxane and Hydrolyzed Fluorinated Alkyl Silane. *Angewandte Chemie International Edition* 2011, 50, 11433-11436.

27. Liu, T.; Kim, C. J. Turning a surface superrepellent even to completely wetting liquids. *Science* 2014, 346.

28. Horn, M.; Schwebdtfeger, C. F.; Meagher, E. P. Refinement of the structure of anatase at several temperatures. *Zeitschrift für Kristallographie-Crystalline Materials* 1972, 136, 273-281.

29. Castillo, R.; Koch, B.; Ruiz, P.; Delmon, B. Influence of the amount of titania on the texture and structure of titania supported on silica. *Journal of Catalysis* 1996, 161, 524-529.

30. Richard, D.; Clanet, C.; Quéré, D. Surface phenomena: Contact time of a bouncing drop. *Nature* 2002, 417, 811-811.

31. Bird, J. C.; Dhiman, R.; Kwon, H.-M.; Varanasi, K. K. Reducing the contact time of a bouncing drop. *Nature* 2013, 503, 385-388.

32. Grzybowski, B. A.; Bowden, N.; Arias, F.; Yang, H.; Whitesides, G. M. Modeling of menisci and capillary forces from the millimeter to the micrometer size range. *The Journal of Physical Chemistry B* 2001, 105, 404-412.

33. Breen, T. L.; Tien, J.; Scott, R. J.; Hadzic, T.; Whitesides, G. M. Design and self-assembly of open, regular, 3D mesostructures. *Science* 1999, 284, 948-951.

34. Bowden, N.; Terfort, A.; Carbeck, J.; Whitesides, G. M. Self-assembly of mesoscale objects into ordered two-dimensional arrays. *Science* 1997, 276, 233-235.

35. Wong, T.-S.; Kang, S. H.; Tang, S. K. Y.; Smythe, E. J.; Hatton, B. D.; Grinthal, A.; Aizenberg, J. Bioinspired self-repairing slippery surfaces with pressure-stable omniphobicity. *Nature* 2011, 477, 443-447.

36. Grinthal, A.; Aizenberg, J. Mobile interfaces: Liquids as a perfect structural material for multifunctional, antifouling surfaces. *Chemistry of Materials* 2013, 26, 698-708.

Chapter 4
Making slippery liquid infused porous surfaces (SLIPS)

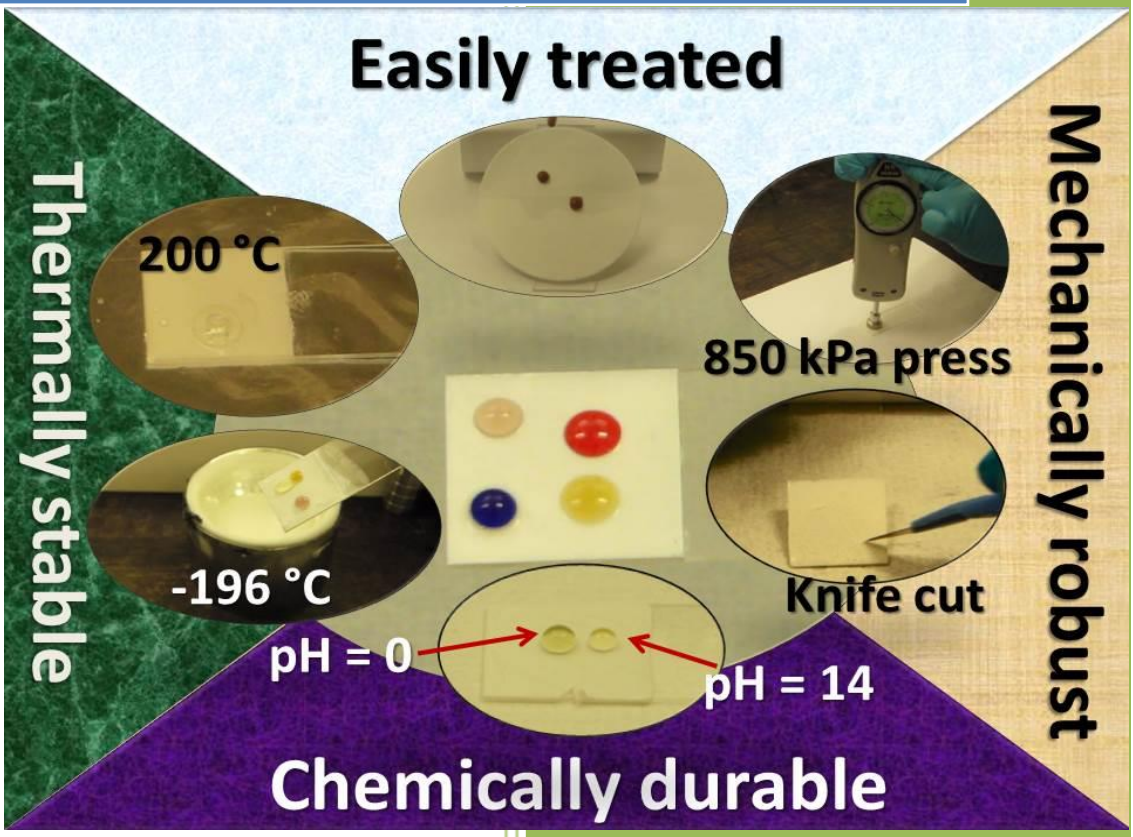

Yao Lu

UCL CHEM

About the cover image of Chapter 4

The SLIPS coating retained omniphobicity after thermal, mechanical and chemical tests.

This image is reproduced with permission from Ref.

"Y. Lu et al., *RSC Adv*., 2016, 6, 106491-106499"

About the figures in this chapter

All the figures except for Fig. 4.14 in Chapter 4 are reproduced with permission from Ref.

"Y. Lu et al., *RSC Adv*., 2016, 6, 106491-106499"

Chapter 4
Making slippery liquid infused porous surfaces (SLIPS)

4.1 Introduction

Slippery liquid infused porous surface (SLIPS) is also a self-cleaning surface that repels liquids and stops contamination from dirty water. However, SLIPS is conceptually different to Lotus Leaf inspired superhydrophobic surfaces. Instead of creating air pockets between surface roughness, SLIPS surfaces use surface micro/nano scaled structures to lock in a lubricating layer, to enable foreign liquids to slide/roll off the surfaces.[1] The design of SLIPS is inspired by the *Nepenthes* pitcher plants,[2] the peristome of which becomes slippery when it is wetted by rain, then the prey slides and is trapped by the "stomach" of the carnivorous plant. SLIPS surfaces repel water, oil, organic solvents and blood – namely omniphobic surfaces – with a superior anti-fouling property compared with superhydrophobic surfaces.[3-5] In addition, SLIPS surfaces have shown their great potential in anti-fouling,[3, 6, 7] corrosion-prevention,[8, 9] and anti-icing applications,[10, 11] and can be used in the conditions where lubricating and self-cleaning are both required (such as gears and bearings) as discussed in Chapter 3. However, there are some issues that must be addressed before practical applications including the ease of fabricating and applying the SLIPS coatings, and their durability such as thermal stability, mechanical robustness and chemical durability.

4.1.1 Fabrication and application of SLIPS surfaces

The fabrication of SLIPS surfaces is usually to lubricate a hydrophobic substrate, here three criteria must be addressed:[1] (1) the substrate must be wetted and stably adhered by the lubricating liquid; (2) the substrate must be preferentially wetted by the lubricant instead of the liquid that is to be repelled; (3) the lubricant and the testing liquid that is expected to be repelled must be immiscible.

In Chapter 3, the superhydrophobic coatings remained water repellent after being contaminated by oils; this phenomenon shows a slippery state and here the oil (either hexadecane or cooking oil) acted as the lubricating layer. In those experiments, the impinging test liquid is only water that is not miscible with oil. However, to make a SLIPS omniphobic surface that repels various liquids, hexadecane or cooking oil are not the ideal choice according to the 3rd criterion because they are easily dissolved in many oils and/or organic solvents. Therefore, Krytox perfluoro lubricating oils, silicone oils and ionic liquids etc. are usually selected as lubricants to make SLIPS surfaces.[5, 12-14]

Lynn et al.[4] fabricated SLIPS coatings by lubricating hydrophobic multilayers that were prepared through 35 repeated cycles of chemical bath treatments. Robust SLIPS coatings on

steel substrates were reported by Tesler et al.[15] *via* electrodeposition of nanoporous tungstite films followed by lubrication with Krytox 103. Whereas Wang et al.[16] used the method of anodization to make a textured surface morphology on aluminium substrates, which became hydrophobic after being fluorinated; the aluminium substrates were then transformed to SLIPS surfaces once lubricated. Zhang et al.[17] fabricated superhydrophobic surfaces *via* deposition of fluorinated silicone nanofilaments on glass substrates, and these surfaces became slippery through adding lubricants. The fabricated superhydrophobic and SLIPS surfaces could be reversibly interconverted *via* addition and evaporation of the lubricating layer.

Although SLIPS surfaces with certain functions were achieved, it is still challenging to use these methods for large scale production and applications due to limited size and the nature of the substrates, high cost, and complex fabrication etc. For instance, anodization is largely limited to coat metallic materials; chemical bath is more applied to coat smaller samples and so on. Therefore, a general and scalable method of coating SLIPS surfaces on different substrates is required.

4.1.2 Thermal stability

Thermal stability is a significant concern for the application of SLIPS surfaces. In contrast to superhydrophobic surfaces, SLIPS coatings require an additional lubricating layer that has an estimated useful range (a range of temperatures that are based on pour point and where evaporation is approximately 10%). Therefore, thermal stability should be taken into consideration while studying SLIPS surfaces.

Thermal stability of SLIPS coatings are usually tested at either high or low temperature. For the high temperature test, two methods are employed: the first method is to test the mobility of liquid droplets after cooling down from a high temperature;[18] here the mobility refers to whether the droplets stick on the surface or are repelled and easily slide off the surface. Sliding angle (SA) and/or contact angle hysteresis (CAH) are measured as a type of quantifiable data to describe this mobility. The second method is to test the omniphobicity of the SLIPS surfaces at elevated temperatures, that is, to test if the liquid droplets stick on the SLIPS surfaces at high temperatures (note: the environment can be approximately at room temperature, but the sample at a high temperature).[19] For low temperature research, anti-icing tests were carried out at -4 °C,[1] -10 °C,[20, 21] -15 °C,[22] -20 °C[10] etc. with a cooling rate of ~ 2 °C per second. Although these coatings retained slippery properties after defrosting, there

are few reports where the SLIPS surfaces could remain omniphobic after defrosting from a fast cooling down to an extremely low temperature (for instance, to put the SLIPS sample into liquid nitrogen).

In addition, most of the literature only focuses on only one aspect – either at high or low temperature. Therefore, a SLIPS surface that can survive in both high and low temperatures should be addressed for practical applications.

4.1.3 Mechanical robustness

Mechanical weakness of liquid repellent surfaces (superhydrophobic or SLIPS surfaces) normally hinders their practical applications because the micro/nano surface structures can be easily damaged by applied forces. A SLIPS surface is usually considered to be more mechanically robust than the respective superhydrophobic surface because the lubricating layer is basically a defect-free liquid that would cover and protect some of the damages on the solid hydrophobic substrates. Some tests on SLIPS surfaces were reported in previous literatures such as knife scratch,[1] repeated bending,[15] and particle abrasions.[15, 23] However, the mechanical durability of SLIPS surfaces was still difficult to quantify from these tests. In addition, damage from particle abrasion and knife scratch would be covered by the lubricating oil, and it is still not known if the SLIPS surfaces would retain self-cleaning properties when certain pressures were applied on a given area that is much larger than the scratches from a knife tip or particles.

4.1.4 Chemical durability

Chemical durability shows how stable a surface is when it contacts corrosive liquids, such as acids and bases.[14, 24] To make chemically durable SLIPS surfaces, neither the lubricants nor the hydrophobic substrate should react with or be dissolved in acids or bases. Making chemically durable SLIPS surfaces has great potential for applications of anti-corrosive coatings in aqueous environment such as tubes, drainage, and marine devices.

Even though there are many reported SLIPS surfaces showing that they could function at different temperatures, after mechanical impacts or contacting with corrosive chemicals, few reports have shown that their SLIPS surfaces could address thermal, mechanical and chemical durability under an even more rigorous condition, those that are applicable to real-world applications.

In this chapter, a SLIPS coating was fabricated through lubricating a superhydrophobic paint coated surface that was reported in the previous chapter.[25] The SLIPS coating could be easily

treated on both hard and soft substrates because these substrates can be simply transformed into superhydrophobic surfaces using the superhydrophobic paint. The prepared SLIPS coatings showed their omniphobicity by repelling water, coffee, red wine and cooking oil.

Thermal stability was studied at extremely high and low temperatures (-196 °C in liquid nitrogen and at 200 °C). To further understand the stability of the SLIPS at high temperatures, the relationship between heating time and the mobility of liquid droplets on SLIPS coatings was tested. Mechanical robustness was tested *via* knife scratch and quantified by measuring SA after applying different vertical pressures onto a given area on the SLIPS surfaces. Chemical durability was demonstrated by the repellence of water droplets with pH ranging from 0 to 14, and further acid-base neutralization (with pH of 0 and 14) was present on the SLIPS surfaces. Finally, a single SLIPS sample was used for all the extreme conditions of thermal, mechanical and chemical durability tests, and the sample retained omniphobicity even after all these tests.

In addition, the fabricated SLIPS surfaces were shown to function even when immersed into either water or oils. This opens up potential applications such as marine oil transportation, anti-fouling under water or oil, and making pipettes that are used in water and/or oil for air sensitive experiments.

4.2 Experimental

4.2.1 Materials

Substrates, including glass slides and filter paper were purchased from Fisher Scientific.

Superhydrophobic coatings were prepared using the method reported in Chapter 3, where two types of titanium dioxide nanoparticles were used. Titanium dioxide (anatase) nanoparticles (diameter, ~ 60 - 200 nm, which was estimated through scanning electron microscopy and transmission electron microscopy images) were purchased from Sigma-Aldrich; in the following texts, these TiO_2 nanoparticles will be called Sigma-TiO_2 to distinguish with the other type of titanium oxide. TiO_2 P25 (diameter, ~ 21 nm) was purchased from Degussa. 1H, 1H, 2H, 2H-perfluorooctyltriethoxysilane (also known as fluorosilane, or FAS, $C_8F_{13}H_4Si(OCH_2CH_3)_3$) was purchased from Sigma-Aldrich. All the laboratory solvents were purchased from Fisher Scientific and used as received.

Lubricating oils: Fluorinert FC-70 was purchased from Sigma-Aldrich. Krytox 100B and Krytox 104A were kindly donated by GBR Technology Limited, UK. The datasheet of these lubricating oils were as shown in Table 4.1.

Table 4.1 The table shows the viscosities (cST, at temperatures of 20, 40 and 100 °C, respectively), boiling points (1 atm) or estimated useful range (UR, based on pour point and where evaporation is approximately 10%), and the densities (that were calculated by weighing the mass of a 1 ml volume of the lubricants using an analytical balance Ohaus at room temperature, ~ 20 °C; δ = 0.01 mg) of three lubricating oils. According to the supplier's information, Krytox 100B and Krytox 104A are chemically the same, but with different values of "n" as shown in the row of "Chemical composition". However, the value "n" is not provided in the datasheet from the supplier.

Temperature (°C)	Fluorinert FC-70	Krytox 100B	Krytox 104A
20	~ 18	12.4	177
40	~ 5.6	5.5	60
100	~ 1.03	—	8.4
Boiling points/UR (°C)	215	-70 — 66	-51 — 179
Density at room temperature (g/cm^3)	2.01042	1.84292	1.85270
Chemical composition	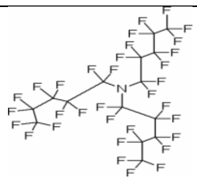	$F-(CF(CF_3)-CF_2-O)_n-CF_2CF_3$	$F-(CF(CF_3)-CF_2-O)_n-CF_2CF_3$

4.2.2 Preparation of SLIPS surfaces

The fabrication of the superhydrophobic paint is based on the method that was reported in Chapter 3. 1 g of FAS was dissolved into 99 g of ethanol solvent, and the resulting solution was mechanically stirred for 2 hours. 6 g of Sigma-TiO_2 and 6 g of TiO_2 P25 nanoparticles were then dispersed into the resulting FAS-ethanol solution to make a suspension. In this experiment, glass slides and filter paper were used as substrates, as representatives of hard and soft substrates, respectively.

Coating process of superhydrophobic paint:

On glass – a glass slide was fixed onto a dip-coater, and then it was partly inserted into the superhydrophobic paint; the sample was pulled out of the suspension by the dip-coater at a rate of 120 mm/min.

On paper – the superhydrophobic paint was extruded from a syringe onto the filter paper, until half of the filter paper was covered with the superhydrophobic coating.

After the paint was coated onto the substrates, the samples were dried in air at room temperature. It takes ~ 3-6 mins to dry on the glass substrates and ~ 10-15 mins on filter paper surfaces.

Lubrication process:

One of the lubricating oils (Fluorinert FC-70, Krytox 100B or Krytox 104A) was then dropped onto the superhydrophobic coating from a syringe to make a liquid infused layer. Note that lubricating oils could be dropped to the point of excess. Fluorinert FC-70 was used throughout this work unless otherwise specified. The thickness of the lubricating layer was calculated by measuring the weight and density of the lubricating layer at room temperature on a given area.

4.2.3 Characterization

The surface morphologies of the samples before lubricating were characterized by a scanning electron microscope (SEM, JEOL JSM-6700F), and after lubricating they were characterized by an environmental scanning electron microscope (ESEM, Philips XL30).

X-ray diffractometer (XRD, D4 ENDEAVOR, Cu-Ka radiation) was used to characterize the surface crystal structures of the samples before lubricating.

Attenuated total reflectance Fourier transform infrared spectroscopy (ATR-FTIR, BRUKER,

platinum-ATR) and Raman spectroscopy (633 nm laser wavelength) were used to characterize surface chemistry compositions before and after lubrication.

Contact angle (CA) was measured at ambient temperature *via* the sessile-drop method using an optical CA meter (FTA 1000). Contact angle hysteresis (CAH) was calculated as the value that advancing CA (θ_{adv}) minus receding CA (θ_{rec}). θ_{adv} and θ_{rec} were measured using two methods: tilting-plate goniometry (TPG) and captive-drop

goniometry (CDG).[26] Here, the CAH of SLIPS and superhydrophobic surfaces were measured using TPG and CDG methods, respectively, according to the feasibility of the experiments.

4.2.4 Liquid dropping tests

Four liquids, water, coffee, red wine and corn oil, were dropped onto the glass slide and filter paper surfaces that were partially coated with SLIPS (the top-half parts of these samples were coated with SLIPS surfaces while the bottom-half parts were left uncoated). The glass and paper samples were tilted at an angle of ~ 22°. In some of these tests, ketchup and hexadecane were also used.

Water: distilled, dyed with methylene blue to aid visibility and this does not change its behaviour.

Coffee: Nescafe instant; 11 g of coffee powder was mixed with 300 mL of water.

Red wine: 12.5% Vol.

Corn oil: Mazola pure corn oil, from Waitrose, London.

Hexadecane: purchased from Sigma-Aldrich.

Tomato ketchup: from McDonald, London.

4.2.5 Thermal stability tests

In the thermal stability tests, four experiments were performed, including recovery tests after exposure to an extremely cold environment, durability tests after exposure to an extremely hot environment, the relationship between heating time and surface slipperiness, and reversible transition between superhydrophobic and SLIPS states.

1. Recovery tests after exposure to liquid nitrogen (-196 °C). A glass slide was coated with superhydrophobic paint followed by FC-70 lubrication to make a SLIPS surface. The SLIPS surface was dipped into liquid nitrogen bath for ~3 s and was then removed. Coffee, red wine, corn oil, and water were dropped respectively onto the surface to test the slipperiness after the surface was defrosted.

2. Durability tests after exposure to an extremely hot environment. A glass slide was coated with superhydrophobic paint followed by Krytox 104A lubrication to make a SLIPS surface. This SLIPS surface was positioned onto a hot plate (200 °C) for over 1 min, and then water and cooking oil were dropped onto the heated SLIPS glass surface. After several seconds, the SLIPS surface was tilted to test its slipperiness to water and oil at high temperature.

3. The relationship between heating time and liquid mobility on SLIPS surfaces. Three glass slides were coated superhydrophobic paint followed by respective lubrication of FC-70, Krytox 100B and Krytox 104A. These samples were positioned onto a hot plate (98 ± 2 °C) and then the weight and CAH (of water, coffee, red wine, and corn oil) of three samples were measured for every 5 mins heating until they lose their slipperiness. Note that the weight and CAH were measured when the samples were cooled down to room temperature.

4. Reversible transition between superhydrophobic and SLIPS states. In this experiment, FC-70 was used as the lubricant. The sample was placed onto a hot plate (98 ± 2 °C) for 5 mins and then removed to measure the weight, CA and CAH of water to characterize the thickness of the lubricating layer and its repellence of water. Note that all the measurements were taken when the sample was cooled down to room temperature. After the measurements, the sample was lubricated again and then the same processes of measurements were repeated before lubricating. The aforementioned experiments are defined as one cycle of the transition test. In this thesis, the transition test was performed for 11 cycles. The reversible transition test also reflected the temperature durability of the superhydrophobic substrates.

4.2.6 Mechanical robustness tests

Mechanical robustness tests were carried out using knife cut and a Newton meter to press the samples. Here, all the SLIPS coatings were bonded onto the glass slides with double sided tapes as previously introduced in Chapter 3, to improve the robustness. The glass substrates were initially layered with double sided tapes, and then the superhydrophobic paint was applied on the upper surface of the double sided tape, followed by the lubricating process.

1. Knife scratch. FC-70, Krytox 100B and Krytox 104A lubricated samples were respectively scratched by a knife; the knife-scratch process was previously introduced in Chapter 3. Corn oil, red wine, coffee, and water were then dropped on respective samples.

2. Newton meter press. To quantify the slipperiness of the samples after mechanical impacts, the relationship between the pressures that were applied on the samples and sliding angles (SA) of the sample surfaces after pressure was studied. FC-70, Krytox 100B and Krytox 104A lubricated glass samples were vertically pressed by a Newton meter (note that the Newton meter was set in a "push" mode, with a circle bottom area, diameter, 16.2 mm). The initial applied forces were 2.6 N; this is the weight of the Newton meter, to give a brief understanding of how big these applied forces were. The following applied forces were 25 N, 50 N, 75 N, 100 N, 125 N, 150 N, and 175 N, respectively. In safety considerations, 175 N was used as the largest force in this experiment because a larger force might break the glass substrates. Pressures of each force could be calculated by being divided by the bottom area of the Newton meter (2.06×10^{-4} m^2). SAs of water and oil droplets were measured on the pressed area of the sample surfaces before and after each press, to quantify the mechanical durability of the SLIPS coatings.

4.2.7 Chemical durability tests

In chemical durability tests, water with different pH values (pH = 0, 2, 4, 6, 8, 10, 12, 14, verified by a pH meter - HANNA, HI9124) were prepared using acid (H_2SO_4 aqueous solutions, dyed with crystal violet) and base (NaOH aqueous solutions, dyed with acridine orange). In the sample preparation, glass slides and superhydrophobic paint were bonded with double sided tapes, followed by the lubrication of FC-70, Krytox 100B and Krytox 104A, respectively.

1. Acid and base dropping tests. FC-70, Krytox 100B and Krytox 104A lubricated samples were firstly scratched by a knife; this is to show the mechanical robustness of the samples and to increase the contacts between corrosive liquids and the sample surfaces. Liquids with pH

values of 0, 2, 4, 6, 8, 10, 12, 14 were then dropped onto these samples (positioned ~ 28° tilted).

2. Acid-base neutralization tests. Acid (pH = 0) and base (pH = 14) droplets were placed onto the FC-70, Krytox 100B and Krytox 104A lubricated samples, respectively. A knife was then used to guide the droplets to contact with each other and neutralize. After the neutralization, the merged droplet was allowed to travel on these SLIPS sample surfaces and eventually slid off.

4.2.8 Thermal, mechanical and chemical durability tests on one single sample

A single SLIPS glass slide was fabricated for thermal, mechanical and chemical durability tests. A glass slide and superhydrophobic paint was bonded using double sided tapes, Krytox 104A was then applied as lubricants to make a SLIPS surface.

1. Thermal test. The sample was positioned onto a hot plate (200 °C) for over 1 min.

2. Mechanical test. After the thermal test, the sample was cut using a knife followed by the Newton meter press at a force of 175 N.

3. Chemical test. After the mechanical test, acid (pH = 0) and base (pH = 14) droplets were positioned onto the sample, and then guided to neutralize.

4. Oil repellency test. After the chemical test, a droplet of corn oil was positioned onto the sample surface to test its slipperiness to oil.

4.2.9 Self-cleaning under water or oil

In these tests, SLIPS glass surfaces were lubricated with FC-70.

1. Underwater oil transportation and self-cleaning. Oil droplets (corn oil or hexadecane) were put onto the SLIPS surfaces that were immersed in water, a needle was used to guide the oil droplets travelling on the SLIPS surfaces in water. Then the SLIPS surfaces were taken out of water to test if there was any water or oil (corn oil or hexadecane) stain left.

2. Self-cleaning in oil phases. Water, coffee and red wine droplets were put onto the SLIPS surfaces that were immersed in corn oil, to test the liquid repellent properties. Then the SLIPS surfaces were taken out of corn oil to test if there was any stain left.

4.3 Results and discussion

In this section, the fabrication and characterization of the SLIPS surfaces are presented. In addition, the aforementioned liquid repellence, durability and self-cleaning under water/oil for the SLIPS surfaces are also presented.

4.3.1 Surface fabrication and characterization

There are two steps to make a SLIPS coating as shown in Fig. 4.1(a). In Step 1, the superhydrophobic paint was treated on the substrates (glass or filter paper) using the method that was introduced in Chapter 3,[25] the glass was dip coated and the filter paper was coated using a syringe with superhydrophobic paint. In Step 2, one of the lubricants (Fluorinert FC-70, Krytox 100B or Krytox 104A) was applied on the painted superhydrophobic surface to make a SLIPS coating. The droplets of the lubricants spontaneously spread across the superhydrophobic coatings and then formed a lubricating layer to make the surface slippery. Fig. 4.1(b) and (c) shows the SEM images and the XRD patterns of the superhydrophobic surface before lubrication that was fabricated as shown in Step 1. Here, glass slides were used as substrates. SEM images show the micro and nano morphologies of the superhydrophobic paint. XRD patterns of the surfaces were indexed to the standard phase of TiO_2 anatase (JCPDS No. 21-1272). Fig. 4.1(d) and (e) shows the FTIR and Raman spectra of the superhydrophobic samples before and after FC-70 lubricating, respectively. There are small differences in the FTIR spectroscopy for the surfaces before and after FC-70 lubrication from 920-1420 cm^{-1}. The peak at ~1240 cm^{-1} corresponded to the carbon sp^3 bound to nitrogen and the peaks at ~1308, ~1206 and ~1139 cm^{-1} referred to C-F stretching of FC-70.[27, 28] Raman spectra of the surfaces before and after FC-70 lubrication were similar with the same three main labelled peaks (at 396.4, 515.8 and 637.5 cm^{-1}), as shown in Fig. 4.1(e), which are assigned to Ti-O stretching vibrations.[29]

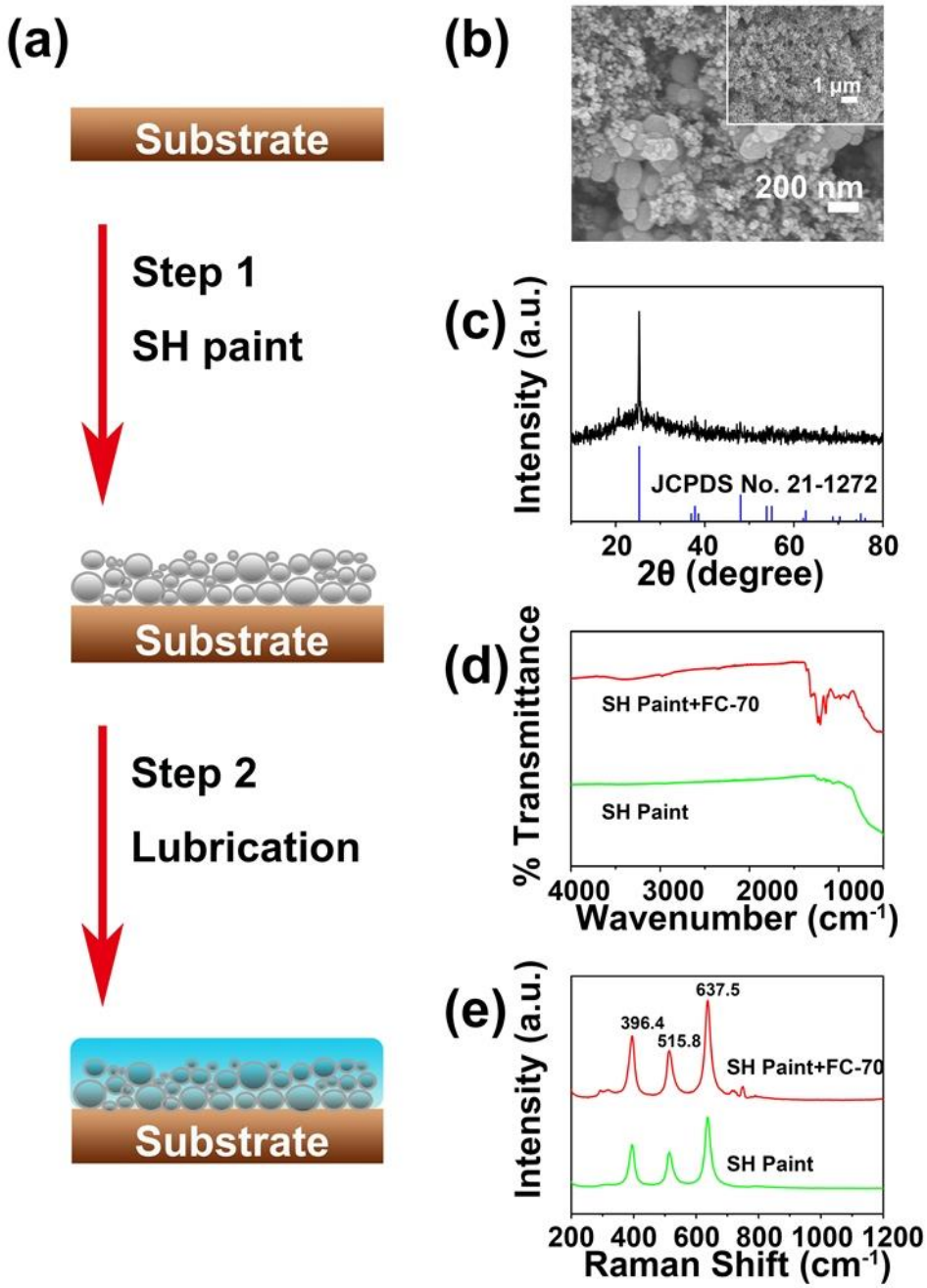

Fig. 4.1 (a) SLIPS surface fabrication was in two steps. Step 1: Superhydrophobic (SH) paint was coated on a substrate (glass); Step 2: Lubricant (FC-70) was dropped onto the superhydrophobic surface. (b) SEM images of the samples after Step 1. (c) XRD patterns of the sample after Step 1. (d) FTIR spectra of the samples before and after lubrication. (e) Raman spectra of the samples before and after lubrication.

4.3.2 Liquid repellence of SLIPS surfaces

The SLIPS coating can be simply treated on various substrates to make slippery omniphobic surfaces that repel water and oil. In this experiment, glass slides and filter papers were used as substrates.

Fig. 4.2 shows liquid dropping tests on the half-coated SLIPS glass slides and filter paper substrates with water (dyed blue), coffee, red wine and corn oil. These four liquids easily slid off the treated slippery parts (the upper half) and then stained the untreated parts (the other half), indicating that the treated surfaces were slippery and omniphobic. In the liquid dropping tests, individual liquid droplets were repelled by SLIPS surfaces. To further test the omniphobicity, the SLIPS coatings were given more contact time with different liquids, as shown in Fig. 4.3. Fig. 4.3 shows that hexadecane (dyed red), red wine (light red), coffee (yellow) and water (dyed blue) were dropped onto a SLIPS glass substrate. After travelling around on the SLIPS surface, these liquid droplets eventually slid off without any stains.

In practical conditions, common substrates can be stained by liquids in the kitchen, such as tomato ketchup, cooking oil and running water from taps. Fig. 4.4 shows that tomato ketchup, running corn oil and water from a tap were repelled by the SLIPS surfaces, indicating that the SLIPS surfaces have the potential to be used in practical conditions.

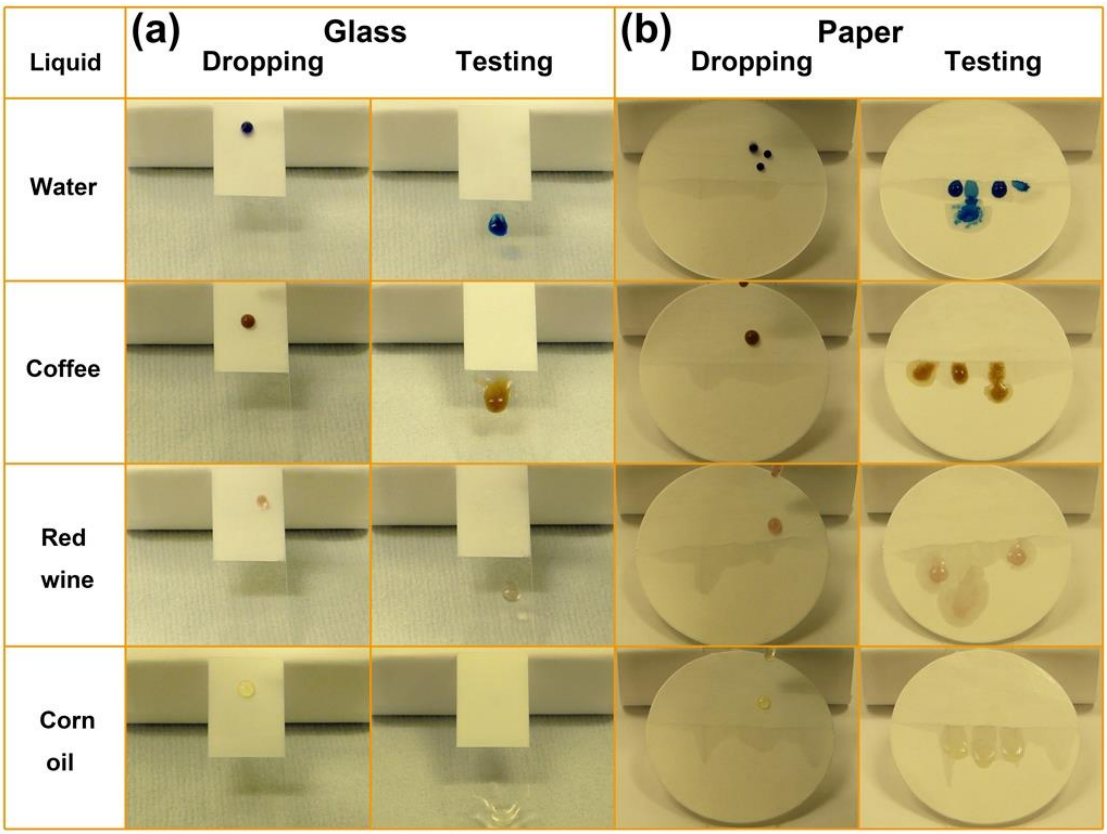

Fig. 4.2 Liquid dropping tests on (a) glass and (b) filter paper samples. The upper parts were coated SLIPS while the lower parts were original.

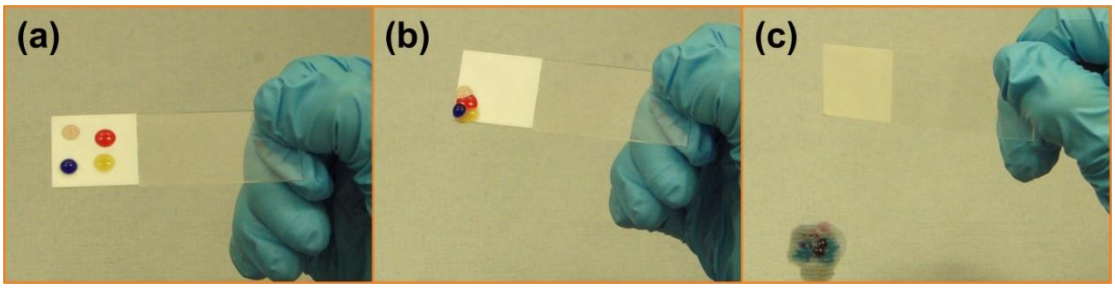

Fig. 4.3 Four liquids contaminating tests on a SLIPS glass surface, the liquids were hexadecane (red), red wine (light red), coffee (yellow) and water (blue), respectively. (a) Liquids were staying on the surface and moving slowly. (b) Liquids got together and tended to slide off. (c) Liquids slid off leaving the surface clean.

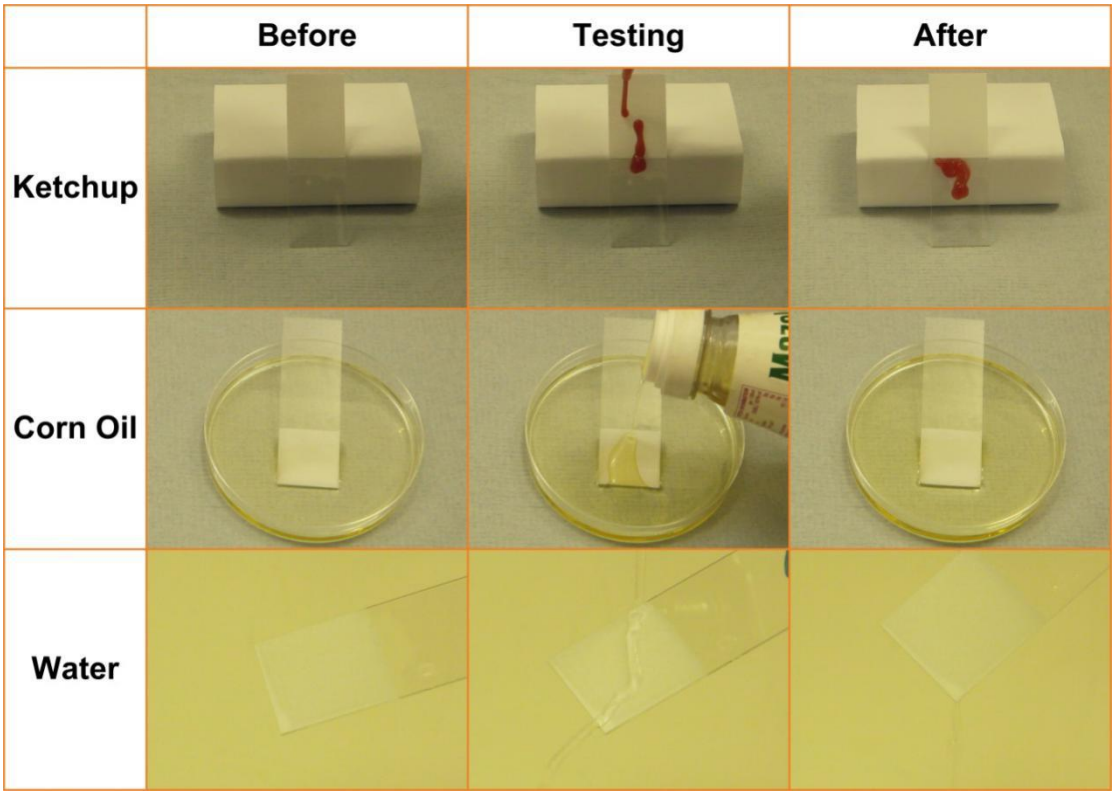

Fig. 4.4 Contamination-repellent tests on the SLIPS surfaces using ketchup, running corn oil and tapped water.

4.3.3 Thermal stability tests

Good durability is significant to maintain the omniphobic properties. In this section, thermal durability tests were carried out on SLIPS samples at both extremely low and high temperatures.

In the low-temperature test, a glass slide was coated with superhydrophobic paint followed by FC-70 lubrication. The sample was dipped into liquid nitrogen (-196 °C) for 3s and was then removed, as shown in Fig. 4.5(a). Coffee, red wine and corn oil were dropped onto the SLIPS sample and they were readily frozen in a few seconds; water was then added to aid melting. Finally, all the liquids slid off without staining the sample surface when the surface was defrosted.

In the high temperature test, a glass slide was coated with superhydrophobic paint followed by Krytox 104A lubrication. The sample was placed onto a hot plate that was at 200 °C as shown in Fig. 4.5(b). After 1 min, water and oil were dropped onto the surface and it can be seen that the oil-water mixture was "fried" to splash into smaller droplets. These droplets were finally repelled by the SLIPS surface at high temperature.

To understand the relationship between omniphobicity and heating time, sample weights and CAHs of water, coffee, red wine and corn oil on SLIPS samples were measured. In this test, three glass slides were coated with superhydrophobic paint and then were lubricated by FC-70, Krytox 100B and Krytox 104A, respectively. These samples were placed onto a hot plate at 100 °C and the sample weights and CAHs were measured for every 5 mins.

Fig. 4.5(c_i) shows the plot of CAHs and heating time on the SLIPS surfaces that were lubricated by FC-70 and Krytox 100B, respectively. At 0 min, the surfaces were not heated so that the four liquids could easily be repelled by either FC-70 or Krytox 100B lubricated SLIPS surfaces with small CAHs (below 5°). After heating the SLIPS samples for 5 mins, the lubricants evaporated. Water, red wine and coffee droplets still rolled off the surfaces easily with CAHs below 10°; and the droplet of corn oil was readily "pinned" onto the surfaces (the CAHs of corn oil on FC-70 and Krytox 100B lubricated surfaces were both above 30°). The samples after 5 mins heating only repelled water and water-based liquids such as red wine and coffee, but were easily stained by corn oil, indicating a typical superhydrophobic state. The thickness of the lubricating layer was calculated through measuring the weight difference of the samples before and after lubrication, and then the difference was divided by the surface area of the lubricating layer on the sample.

The transition between superhydrophobic and SLIPS states can be achieved through a process of "lubrication, evaporation, and re-lubrication",[17] however, to evaluate the thermal durability of a SLIPS/superhydrophobic surface, it is significant to test the transitions in multiple cycles. In this test, the SLIPS sample was fabricated through coating with the superhydrophobic paint followed FC-70 lubrication. As shown in Fig. 4.5(c_{ii}), the CA of water was measured before and after the evaporation of the FC-70 lubricant at 100 °C heating for 5 mins. The heated sample was then re-lubricated so that the surface retained its slipperiness. Table 4.2 shows the CA, sample weight and thickness of the lubricating layer in the tests of reversible transition. According to the CAs of water in this test, the sample was reversibly transferred between SLIPS and superhydrophobic states for over 10 cycles, and water was repelled by the sample in both states.

ESEM images were used to study the surface morphology of these samples in the thermal durability tests. The surface morphology of the samples that were lubricated by FC-70 and Krytox 100B and then heated at 100 °C for 5 mins, were as shown in Fig. 4.5(c_{iii}) and (c_{iv}). These samples that were dried for 5 mins showed a chapped surface structure without any lubricating layer *via* ESEM images compared with their respective SLIPS samples before heat tests, as shown in Fig. 4.6, indicating that the FC-70 and Krytox 100B lubricants were completely or almost removed from the superhydrophobic paint due to evaporation.

Fig. 4.5(d_i) shows the relationship between heating time and the CAH of water, red wine, coffee and corn oil on the SLIPS surface, which was fabricated through coating with superhydrophobic paint followed by Krytox 104A lubrication. The CAHs of water, red wine, coffee and corn oil were below 10° during the heating experiment from 0 to 35 mins, indicating that the Krytox 104A lubricated SLIPS coatings retained its omniphobicity. The Krytox 104A lubricated sample showed superior thermal durability compared with those of the FC-70 and Krytox 100B lubricated samples. Krytox 104A has a higher viscosity and useful range of temperature than those of FC-70 and Krytox 100B, therefore, Krytox 104A as well as the Krytox 104A lubricated samples has better thermal durability when it is under high temperature.

When the heating time reached 35 mins, the SLIPS sample was divided by two parts. One part appeared "dry" and the lubricant was hardly seen; on the other part, lubricant was still seen to cover the superhydrophobic paint and this part was considered to be the "wet" part. However, the CAHs of four liquids (between 2°-8°) did not significantly change from dry to

wet parts, indicating that there was still a very thin lubricating layer on the dry part, and even such a thin lubricating layer was able to achieve the surface slipperiness. In the thermal durability test, the mass of the SLIPS samples and the thickness of lubricating layers were as shown in Table 4.3. Fig. 4.5(d_{ii}) shows the ESEM image of the SLIPS sample that was fabricated through coating with superhydrophobic paint followed by Krytox 104A lubrication after heating for 5 min at 100 °C. The surface morphology of the Krytox 104A lubricated sample did not significantly change before (Fig. 4.6) and after 5 mins heating test – lubricating layers were seen on both samples, resulting in that the Krytox 104A lubricated sample retained its slipperiness and omniphobicity.

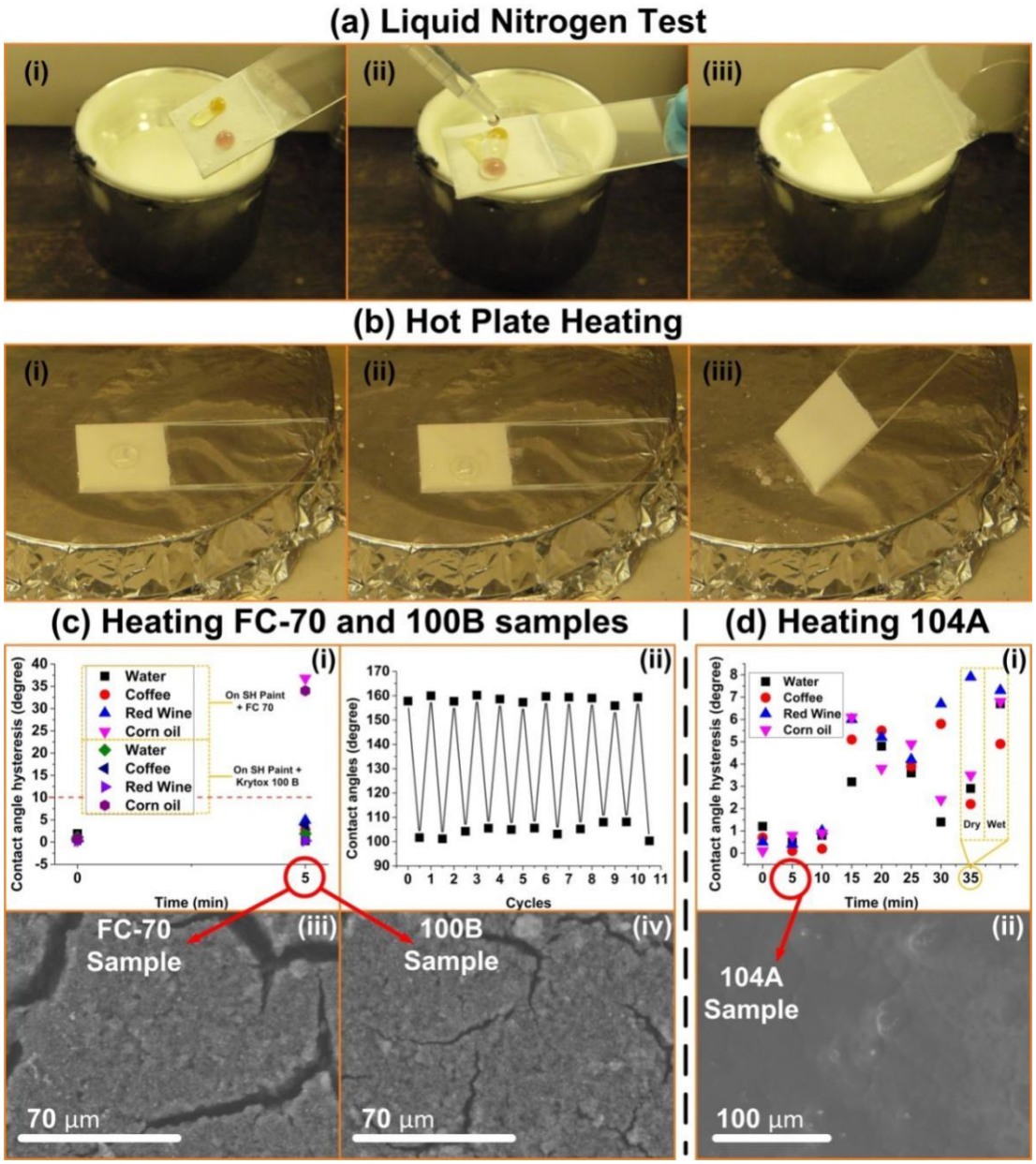

Fig. 4.5 (a) The FC-70 lubricated SLIPS sample was dipped into liquid nitrogen to test durability in extremely low temperature. Coffee (yellow), red wine (light red) and corn oil (light yellow) and water droplets were dropped onto the sample to test its slipperiness. (b) The Krytox 104A lubricated SLIPS glass surface was placed onto a hot plate (200 °C) for 1 min to test its slipperiness to water and oil at high temperature. (c) FC-70 and Krytox 100B lubricated samples were heated at 100 °C. (i) CAHs of four liquids on respective FC-70 and Krytox 100B lubricated samples before and after 5 mins of heating; (ii) transition tests of an FC-70 lubricated sample between superhydrophobic and SLIPS states for 10 cycles; ESEM images of (iii) FC-70 and (iv) Krytox 100B lubricated samples after heating for 5 mins at 100 °C. (d) Krytox 104A lubricated sample was heated at 100 °C. (i) Plot of CAHs of four liquids and heating time from 0 to 35 mins; (ii) ESEM images of Krytox 104A lubricated samples after heating for 5 mins at 100 °C.

Table 4.2 CA of water, weight of samples and the thickness of the FC-70 lubricating layer in the reversible transition tests for multiple cycles (the treated surface area was 25 mm x 28 mm). Note that the thickness was gained through calculation and its errors were subject to the measured weights.

Data / Cycles	CA ± 1 (°)	Weight ± 0.01 (g)	Thickness (µm)	Data / Cycles	CA ± 1 (°)	Weight ± 0.01 (g)	Thickness (µm)
0	157.8	4.7392	0	5.5	105.6	4.8622	88.8
0.5	101.7	4.8686	92. 0	6	159.7	4.7385	0
1	160.0	4.7386	0	6.5	103.1	4.8722	95.0
1.5	101.2	4.8789	99.7	7	159.4	4.7388	0
2	157.7	4.7387	0	7.5	105.2	4.8692	92.7
2.5	104.3	4.8526	80.9	8	159.0	4.7389	0
3	160.2	4.7390	0	8.5	108.0	4.8932	109.6
3.5	105.5	4.8357	68.7	9	155.9	4.7384	0
4	158.6	4.7383	0	9.5	108.1	4.8681	92.2
4.5	105.0	4.8593	86.0	10	159.4	4.7387	0
5	157.3	4.7372	0	10.5	100.3	4.8931	109.7

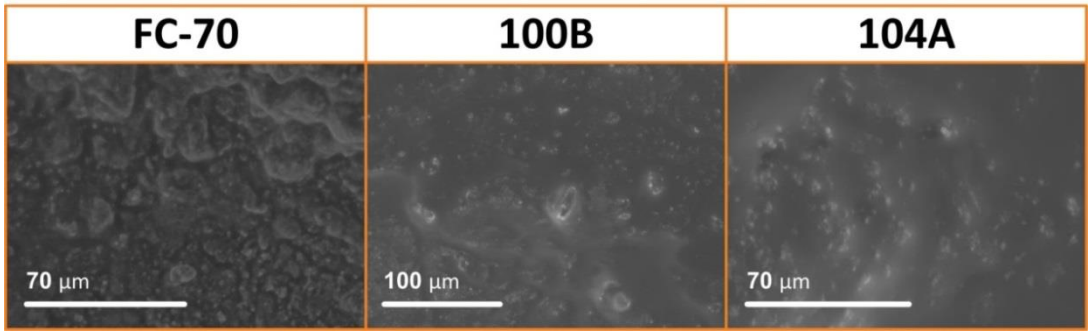

Fig. 4.6 ESEM images of FC-70, Krytox 100B and Krytox 104A lubricated SLIPS surfaces. It is shown that lubricants were embedded in the surface structures of the superhydrophobic coatings.

Table 4.3 Mass (g) of the FC-70, Krytox 100B and Krytox 104A lubricated samples and the corresponding average thickness (µm) of the lubricating layers as the increase of the heating time (the treated surface area was 25 mm x 25 mm). The errors of weight were ± 0.01 g, and the errors of the calculated thickness were subject to the measured weight.

Sample / Time	Fluorinert FC-70 Weight/Thickness	Krytox 100B Weight/Thickness	Krytox 104A Weight/Thickness
Before lubricants	4.5423/0	4.5575/0	4.5239/0
After lubricants	4.6522/87.5	4.6619/90.6	4.7543/199.0
After 5 min	4.5421/0	4.5571/0	4.6659/122.6
After 10 min	____	____	4.6314/92.8
After 15 min	____	____	4.5908/57.8
After 20 min	____	____	4.5862/53.8
After 25 min	____	____	4.5659/36.3
After 30 min	____	____	4.5590/30.3
After 35 min	____	____	4.5532/25.3

4.3.4 Mechanical robustness tests

In consideration of practical conditions, self-cleaning surfaces must be mechanically robust. Here, knife cut and Newton meter press were used to test the mechanical durability of these SLIPS samples.

Three glass slides were bonded with superhydrophobic paint using double sided tapes followed by FC-70, Krytox 100B and Krytox 104A lubrication, respectively. These samples were scratched by a knife, and were then tested with oil, red wine, coffee and water, as shown in Fig. 4.7. These samples remained clean after the liquid dropping tests, indicating that the surfaces retained omniphobicity after the knife cut tests.

Fig. 4.8 shows the ESEM images of knife samples. The traces of knife scratch were filled in by the lubricants, so that the SLIPS surfaces retained omniphobicity.

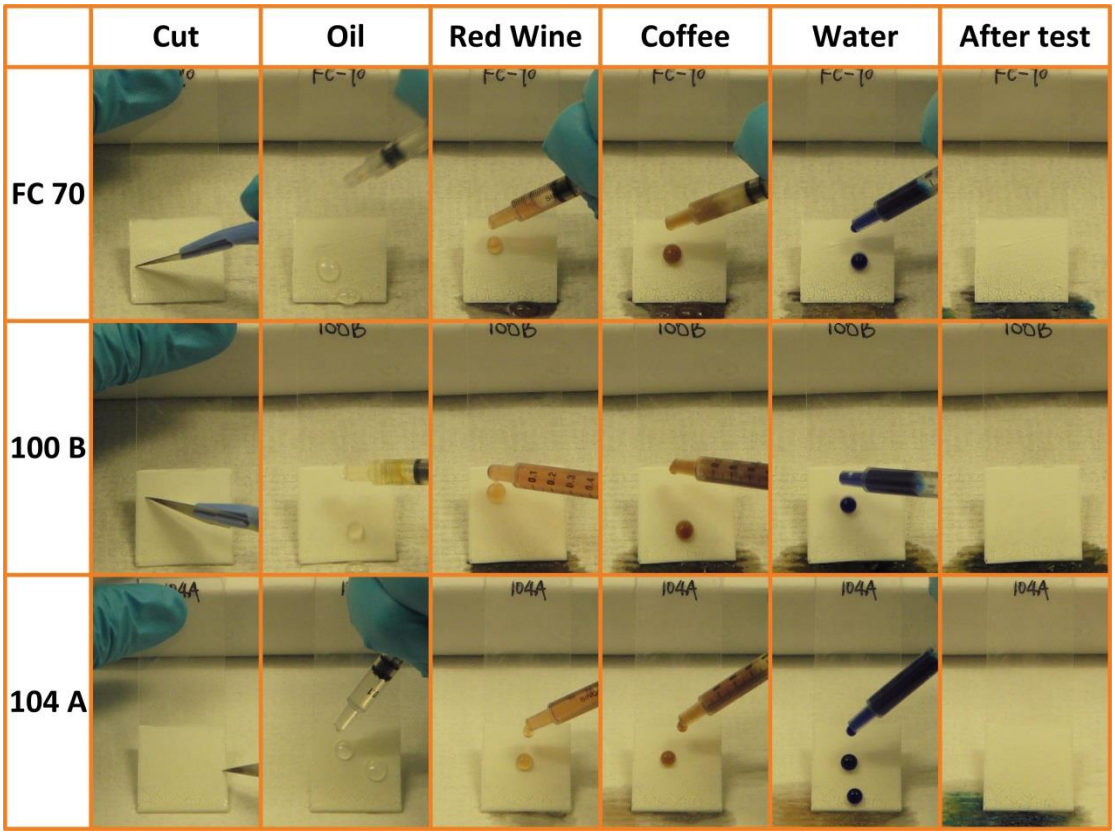

Fig. 4.7 FC 70, Krytox 100B and Krytox 104A lubricated samples were scratched by a knife, and then oil, red wine, coffee and water were dropped on those samples respectively to test their omniphobicity.

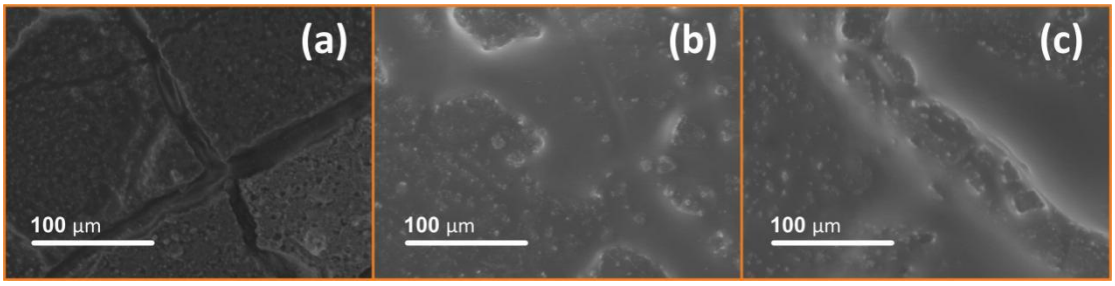

Fig. 4.8 ESEM images of knife scratched (a) FC-70, (b) Krytox 100B and (c) Krytox 104A lubricated samples.

To quantify the mechanical durability of the SLIPS coatings, a Newton meter was applied to press the SLIPS samples that were lubricated by FC-70, Krytox 100B and Krytox 104A, respectively. These samples were prepared *via* the same process of those in the knife cut tests. Fig. 4.9(a)-(c) shows that an FC-70 lubricated sample was vertically pressed by the Newton meter at 175 N. The sample retained the repellence to both water and oil after the press. Fig. 4.9(d)-(f) shows the plot of the pressure (kPa) and SAs of water and oil on FC-70, Krytox 100B and Krytox 104A lubricated samples, respectively. Here, 175 N (~ 850 kPa) was used as the largest force in consideration of safety. For the FC-70 and Krytox 100B lubricated samples, SAs increased as the increase of the applied pressure, but even the SAs under the highest pressure were still below 2.5°, indicating that the mechanical press did not significantly change the surface slipperiness. For the Krytox 104A lubricated sample, SA also increased as the increase of the applied pressure and the SA under the highest pressure was still below 10°, showing that the SLIPS coatings are able to retain the repellence to water and oil under the impact of these forces.

Fig. 4.10 shows the ESEM images of SLIPS surfaces after the Newton meter press tests. The FC-70, Krytox 100B and Krytox 104A lubricated samples were pressed to ~ 850 kPa. The trace of the press was seen on the FC-70 lubricated sample, and the lubricant partially filled in the cracks to retain the surface slipperiness. On the Krytox 100B and Krytox 104A samples, the surface structures were fully covered by the lubricants, so that the SLIPS coatings still repelled water and oil after the Newton meter press.

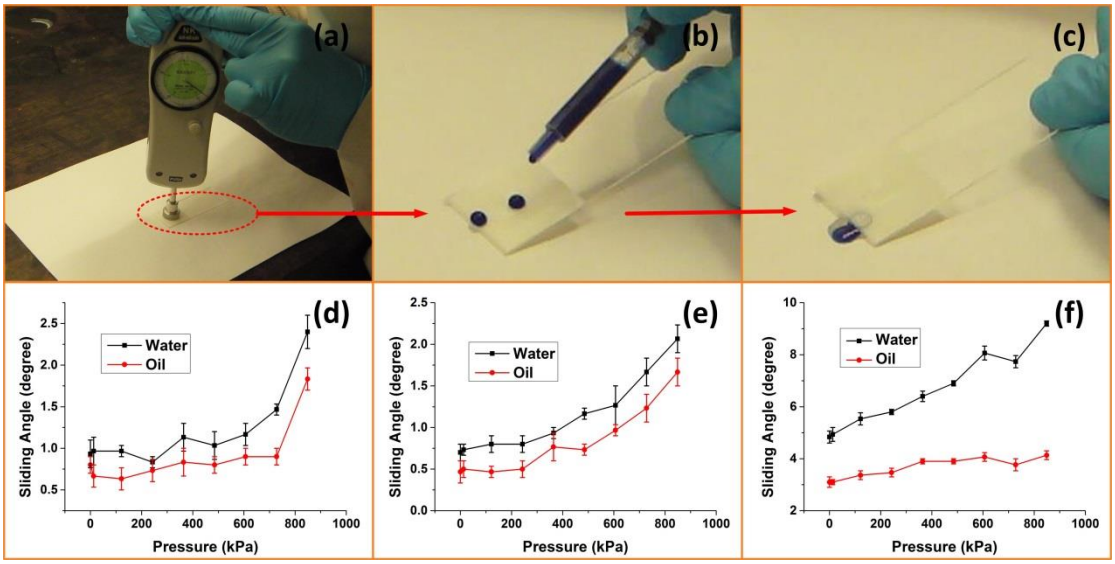

Fig. 4.9 (a) Newton meter was used to press an FC-70 lubricated sample at 175N (~850 kPa), (b) water and (c) oil were dropped onto the sample surface respectively to test its slipperiness. (d)-(f) Plot of SAs of water and oil and the pressure that was applied onto the (d) FC-70, (e) Krytox 100B and (f) Krytox 104A lubricated SLIPS surfaces.

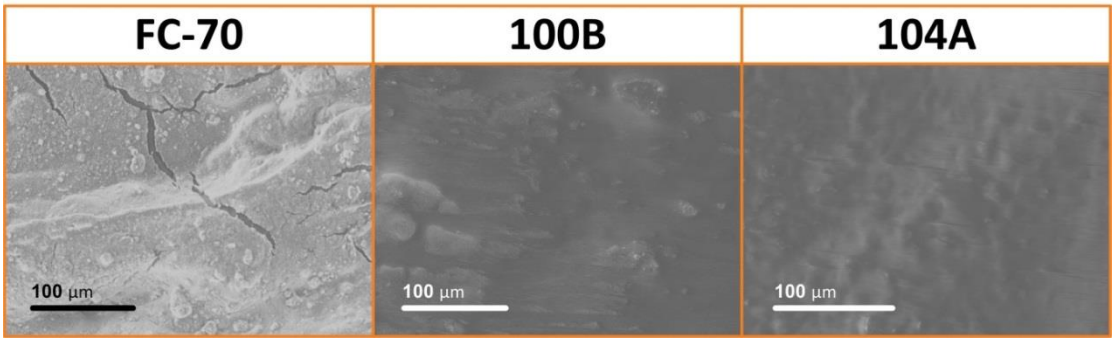

Fig. 4.10 ESEM images of FC-70, Krytox 100B and Krytox 104A lubricated samples that were pressed by ~850 kPa.

4.3.5 Chemical durability tests

Water droplets with pH of 0, 2, 4, 6, 8, 10, 12, and 14 were used to test the surface chemical durability of the SLIPS samples. In this test, three SLIPS samples was fabricated through bonding superhydrophobic paint and the glass slides using double sided tapes, followed by FC-70, Krytox 100B and Krytox 104A lubrication, respectively. These samples were initially cut by a knife followed by the acid/base liquids dropping tests as shown in Fig. 4.11(a). The samples were tilted at ~28°. After the test, all the samples were still clean, indicating that these SLIPS coatings were chemically durable.

To further test the chemical stability of the SLIPS samples, acid-base neutralization test was performed on the FC-70 lubricated SLIPS sample as shown in Fig. 4.11(b). The droplets of acid (pH = 0) and base (pH = 14) were placed onto the SLIPS sample, and then were guided to contact for neutralization as shown in Fig. 4.11(c). The combined droplet was allowed to travel around on the SLIPS sample and then slid off as shown in Fig. 4.11(d). The SLIPS surface remained clean after the acid-base neutralization test showing that the SLIPS coating is chemically durable.

The acid-base neutralization test was also performed on the Krytox 100B and Krytox 104A lubricated SLIPS samples, both samples retained their slipperiness after this test.

ESEM images shows the surface structures of the FC-70, Krytox 100B and Krytox 104A lubricated SLIPS samples that were tested through the acid-base neutralization as shown in Fig. 4.12. The surfaces were partially or fully covered by the lubricants and did not show much difference compared with untested SLIPS samples as shown in Fig. 4.6. All the chemical stability tests indicate that these SLIPS samples are robust to corrosive liquids such as strong acid and base. This is because both the lubricants and the superhydrophobic paint are stable upon the exposure to acid and base.

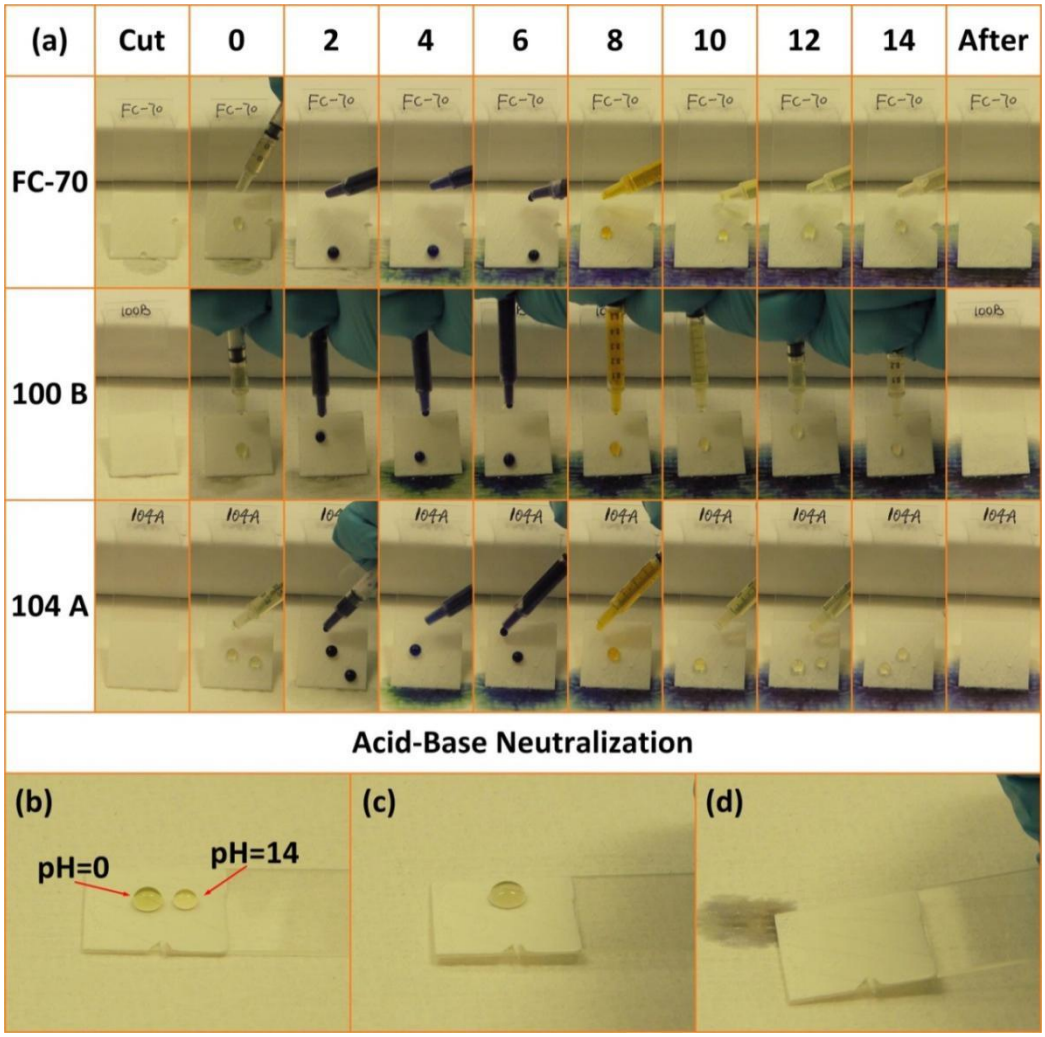

Fig. 4.11 (a) Acid and base dropping tests, the pH of these liquid droplets were from 0 to 14. (b)-(d) Neutralization of acid and base droplets on a scratched FC-70 lubricated SLIPS sample.

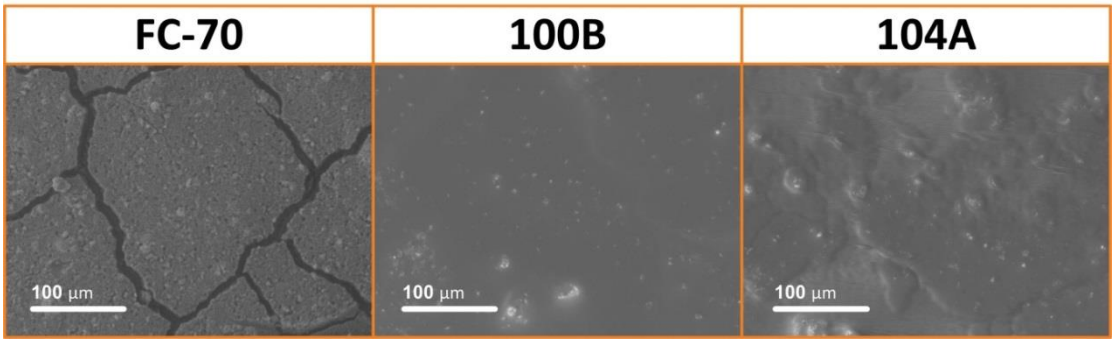

Fig. 4.12 ESEM images of SLIPS samples after the acid and base neutralization test.

4.3.6 Thermal, mechanical and chemical tests on one single SLIPS sample

In the above-mentioned experiments, SLIPS coatings were tested for their thermal, mechanical and chemical durability. However, in consideration of practical applications, a surface may be challenged by complex conditions. For example, the surface may suffer a high temperature, together with corrosive chemicals and severe mechanical impacts.

To meet the practical requirements, one individual sample was used to undergo thermal, mechanical and chemical tests. This sample was prepared through bonding a glass slide and superhydrophobic paint using double sided tapes, followed by the lubrication of Krytox 104A. Fig. 4.13 shows that the sample underwent 200 °C heating, knife cut, 175 N of Newton meter press and acid-base neutralization tests. After these tests, the corn oil droplet was still able to easily slide off the SLIPS sample, indicating that this sample retained omniphobicity after these durability tests. In the ESEM image, the sample surface was fully covered by the lubricant, and this is why the surface retained the slipperiness to water and oil.

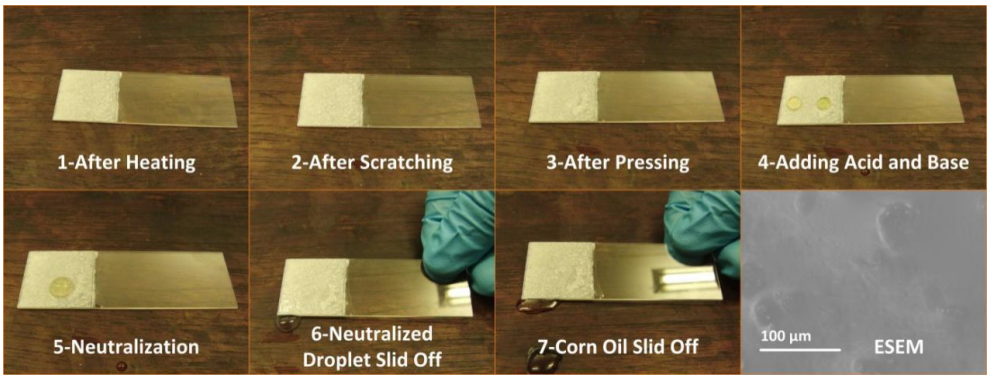

Fig. 4.13 Thermal, mechanical and chemical durability tests on one single sample. The sample was heated at 200 °C, scratched, pressed at 175 N, and then acid (the right droplet, pH = 0) and base (the left droplet, pH = 14) were positioned on the sample to neutralize. After these tests, a corn oil droplet was still able to slide off, indicating the surface retained slippery and omniphobic. ESEM image shows that the surface did not significantly change after these tests, indicating that the SLIPS surface is thermally, mechanically and chemically durable.

4.3.7 Self-cleaning underwater and under oil

The SLIPS surface can also be used under various media such as water and oil as well as in air. Fig. 4.14(a) shows oil droplets (corn oil and hexadecane) that were put on a SLIPS surface that was immersed in water. A needle could be used to guide the oil droplets attached to the SLIPS surface. The SLIPS surface remained clean without oil or water stains when they were taken out of the liquid. The behaviour of oils could be used for marine oil transportation, and it also shows that the SLIPS surface remained self-cleaning even in an oil-

water mixture. Fig. 4.14(b) shows water-based liquid droplets (water, coffee and red wine) that were put onto SLIPS surfaces that were immersed in corn oil. The SLIPS surfaces repelled these droplets just like a superhydrophobic surface in air repels water; and the surfaces remained self-cleaning once they were released from corn oil. These tests show that the SLIPS surfaces retain their pristine condition even if exposed to either water or oil.

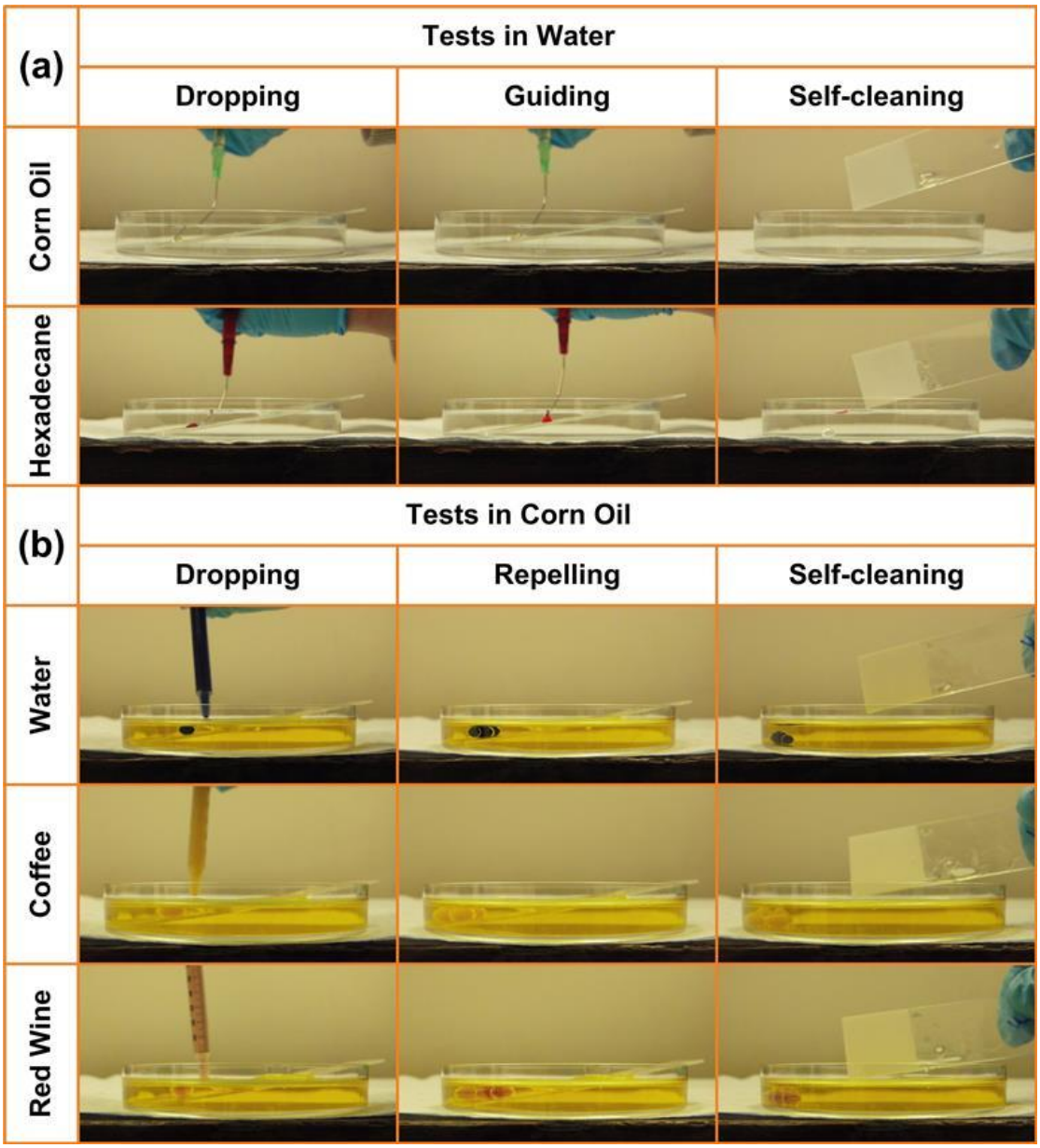

Fig. 4.14 (a) Corn oil and hexadecane droplets were put on the SLIPS surface that was immersed in water. (b) Water, coffee and red wine droplets were put on the SLIPS surface that was immersed in corn oil.

4.4 Conclusions

In this chapter, a durable omniphobic SLIPS coating was developed through lubricating a superhydrophobic paint-treated surface as introduced in Chapter 3. Compared with the superhydrophobic surfaces, the SLIPS coating can also be treated onto both hard and soft substrates such as glass and filter paper, but the SLIPS coating has a superior anti-fouling property – repelling water, corn oil, coffee, red wine and even ketchup.

Thermal, mechanical and chemical durability tests of the SLIPS surfaces were present to show the materials are practically applicable. Thermal stability tests were performed in extremely low (-196 °C in liquid nitrogen) and high temperatures (200 °C), which shows a larger range of temperature than that was previously reported. Through selecting the viscosity and estimated useful range of the lubricants, either a thermally durable SLIPS surface or a reversible transition between superhydrophobic and SLIPS states could be achieved. In particular, the transition between superhydrophobic and SLIPS surfaces were present for even more than ten cycles. In the tests of surface mechanical robustness, the scratch traces were partially or fully covered by the lubricants so that the surfaces retained their slippery character. The SLIPS samples were also pressed by a Newton meter at forces 2.6 N to 175 N (~850 kPa), the SAs of water and oil on the pressed samples did not significantly change. This method had effectively quantified the surface slipperiness and mechanical impacts using a plot of SAs and applied press, and further demonstrated that the SLIPS samples were mechanically robust. In the chemical stability tests, the SLIPS coatings retained omniphobicity after acid and base dropping and neutralization tests. Finally, one single sample was used for all the thermal (200 °C heating), mechanical (scratch and 850 kPa press) and chemical (acid and base dropping and neutralization) tests, and the surface retained repellence to acid, base and oil droplets. While very few reports of SLIPS coatings attempted to address thermal, mechanical and chemical issues in one goal.

The fabricated SLIPS surfaces can also be used for self-cleaning even after being immersed in either water or oil. Furthermore oil-droplets can be easily guided to travel along pre-scribed directions when put on SLIPS surfaces in water. This phenomenon could be used for marine oil transportation, anti-fouling under water or oil, and making pipettes that are used in water and/or oil for air sensitive experiments.

This coating could be treated on various substrates with extreme thermal, mechanical and chemical durability, and it is believed to be useful for self-cleaning, anti-fouling, and anti-

corrosion purposes in a range of large scale of industrial applications.

4.5 References

1. Wong, T.-S.; Kang, S. H.; Tang, S. K. Y.; Smythe, E. J.; Hatton, B. D.; Grinthal, A.; Aizenberg, J. Bioinspired self-repairing slippery surfaces with pressure-stable omniphobicity. *Nature* 2011, 477, 443-447.

2. Bohn, H. F.; Federle, W. Insect aquaplaning: Nepenthes pitcher plants capture prey with the peristome, a fully wettable water-lubricated anisotropic surface. *Proceedings of the National Academy of Sciences of the United States of America* 2004, 101, 14138-14143.

3. Leslie, D. C.; Waterhouse, A.; Berthet, J. B.; Valentin, T. M.; Watters, A. L.; Jain, A.; Kim, P.; Hatton, B. D.; Nedder, A.; Donovan, K. A bioinspired omniphobic surface coating on medical devices prevents thrombosis and biofouling. *Nature biotechnology* 2014, 32, 1134-1140.

4. Manna, U.; Lynn, D. M. Fabrication of Liquid‐Infused Surfaces Using Reactive Polymer Multilayers: Principles for Manipulating the Behaviors and Mobilities of Aqueous Fluids on Slippery Liquid Interfaces. *Advanced Materials* 2015, 27, 3007-3012.

5. Schellenberger, F.; Xie, J.; Encinas, N.; Hardy, A.; Klapper, M.; Papadopoulos, P.; Butt, H.-J.; Vollmer, D. Direct observation of drops on slippery lubricant-infused surfaces. *Soft matter* 2015, 11, 7617-7626.

6. Xiao, L.; Li, J.; Mieszkin, S.; Di Fino, A.; Clare, A. S.; Callow, M. E.; Callow, J. A.; Grunze, M.; Rosenhahn, A.; Levkin, P. A. Slippery liquid-infused porous surfaces showing marine antibiofouling properties. *ACS applied materials & interfaces* 2013, 5, 10074-10080.

7. Epstein, A. K.; Wong, T.-S.; Belisle, R. A.; Boggs, E. M.; Aizenberg, J. Liquid-infused structured surfaces with exceptional anti-biofouling performance. *Proceedings of the National Academy of Sciences* 2012, 109, 13182-13187.

8. Wang, P.; Lu, Z.; Zhang, D. Slippery liquid-infused porous surfaces fabricated on aluminum as a barrier to corrosion induced by sulfate reducing bacteria. *Corrosion Science* 2015, 93, 159-166.

9. Yang, S.; Qiu, R.; Song, H.; Wang, P.; Shi, Z.; Wang, Y. Slippery liquid-infused porous surface based on perfluorinated lubricant/iron tetradecanoate: Preparation and corrosion

protection application. *Applied Surface Science* 2015, 328, 491-500.

10. Liu, Q.; Yang, Y.; Huang, M.; Zhou, Y.; Liu, Y.; Liang, X. Durability of a lubricant-infused Electrospray Silicon Rubber surface as an anti-icing coating. *Applied Surface Science* 2015, 346, 68-76.

11. Chen, J.; Dou, R.; Cui, D.; Zhang, Q.; Zhang, Y.; Xu, F.; Zhou, X.; Wang, J.; Song, Y.; Jiang, L. Robust prototypical anti-icing coatings with a self-lubricating liquid water layer between ice and substrate. *ACS applied materials & interfaces* 2013, 5, 4026-4030.

12. Yao, X.; Hu, Y.; Grinthal, A.; Wong, T.-S.; Mahadevan, L.; Aizenberg, J. Adaptive fluid-infused porous films with tunable transparency and wettability. *Nature materials* 2013, 12, 529-534.

13. Howell, C.; Vu, T. L.; Lin, J. J.; Kolle, S.; Juthani, N.; Watson, E.; Weaver, J. C.; Alvarenga, J.; Aizenberg, J. Self-replenishing vascularized fouling-release surfaces. *ACS applied materials & interfaces* 2014, 6, 13299-13307.

14. Song, T.; Liu, Q.; Zhang, M.; Chen, R.; Takahashi, K.; Jing, X.; Liu, L.; Wang, J. Multiple sheet-layered super slippery surfaces based on anodic aluminium oxide and its anticorrosion property. *RSC Advances* 2015, 5, 70080-70085.

15. Tesler, A. B.; Kim, P.; Kolle, S.; Howell, C.; Ahanotu, O.; Aizenberg, J. Extremely durable biofouling-resistant metallic surfaces based on electrodeposited nanoporous tungstite films on steel. *Nature communications* 2015, 6.

16. Wang, P.; Zhang, D.; Lu, Z.; Sun, S. Fabrication of Slippery Lubricant-Infused Porous Surface for Inhibition of Microbially Influenced Corrosion. *ACS Applied Materials & Interfaces* 2016, 8, 1120-1127.

17. Zhang, J.; Wu, L.; Li, B.; Li, L.; Seeger, S.; Wang, A. Evaporation-induced transition from nepenthes pitcher-inspired slippery surfaces to lotus leaf-inspired superoleophobic surfaces. *Langmuir* 2014, 30, 14292-14299.

18. Miranda, D. F.; Urata, C.; Masheder, B.; Dunderdale, G. J.; Yagihashi, M.; Hozumi, A. Physically and chemically stable ionic liquid-infused textured surfaces showing excellent

dynamic omniphobicity. *APL Materials* 2014, 2, 056108.

19. Daniel, D.; Mankin, M. N.; Belisle, R. A.; Wong, T.-S.; Aizenberg, J. Lubricant-infused micro/nano-structured surfaces with tunable dynamic omniphobicity at high temperatures. *Applied Physics Letters* 2013, 102, 231603.

20. Kim, P.; Wong, T.-S.; Alvarenga, J.; Kreder, M. J.; Adorno-Martinez, W. E.; Aizenberg, J. Liquid-infused nanostructured surfaces with extreme anti-ice and anti-frost performance. *ACS nano* 2012, 6, 6569-6577.

21. Chen, X.; Ma, R.; Zhou, H.; Zhou, X.; Che, L.; Yao, S.; Wang, Z. Activating the microscale edge effect in a hierarchical surface for frosting suppression and defrosting promotion. *Scientific reports* 2013, 3.

22. Subramanyam, S. B.; Rykaczewski, K.; Varanasi, K. K. Ice adhesion on lubricant-impregnated textured surfaces. *Langmuir* 2013, 29, 13414-13418.

23. Yu, L.; Chen, G. Y.; Xu, H.; Liu, X. Substrate-Independent, Transparent Oil-Repellent Coatings with Self-Healing and Persistent Easy-Sliding Oil Repellency. *ACS Nano* 2016, 10, 1076-1085.

24. Ganesh, V. A.; Dinachali, S. S.; Jayaraman, S.; Sridhar, R.; Raut, H. K.; Góra, A.; Baji, A.; Nair, A. S.; Ramakrishna, S. One-step fabrication of robust and optically transparent slippery coatings. *RSC Advances* 2014, 4, 55263-55270.

25. Lu, Y.; Sathasivam, S.; Song, J.; Crick, C. R.; Carmalt, C. J.; Parkin, I. P. Robust self-cleaning surfaces that function when exposed to either air or oil. *Science* 2015, 347, 1132-1135.

26. Krishnan, A.; Liu, Y.-H.; Cha, P.; Woodward, R.; Allara, D.; Vogler, E. A. An evaluation of methods for contact angle measurement. *Colloids and Surfaces B: Biointerfaces* 2005, 43, 95-98.

27. Zheng, W. T.; Sjöström, H.; Ivanov, I.; Xing, K. Z.; Broitman, E.; Salaneck, W. R.; Greene, J. E.; Sundgren, J. E. Reactive magnetron sputter deposited CNx: effects of N2 pressure and growth temperature on film composition, bonding, and microstructure. *Journal*

of Vacuum Science & Technology A 1996, 14, 2696-2701.

28. Chaussé, A.; Chehimi, M. M.; Karsi, N.; Pinson, J.; Podvorica, F.; Vautrin-Ul, C. The electrochemical reduction of diazonium salts on iron electrodes. The formation of covalently bonded organic layers and their effect on corrosion. *Chemistry of Materials* 2002, 14, 392-400.

29. Ohsaka, T.; Izumi, F.; Fujiki, Y. Raman spectrum of anatase, TiO2. *Journal of Raman spectroscopy* 1978, 7, 321-324.

UCL CHEM

Chapter 5 Conclusions

Yao Lu

Chapter 5
Conclusions

Conclusions

Throughout the whole thesis, the most inventive step is to simply use an adhesive layer to achieve mechanically durable self-cleaning coatings (superhydrophobic or SLIPS coatings), which is the most significant concern in most cases for practical applications either in industry or in our daily life. The idea of improving the mechanical robustness is to "use the soft to beat the hard", which is also the spirit of the Chinese Tai Chi. When the micro-scaled posts were directly bonded with the substrate, they are easily broken by the applied forces as shown in Fig. 5.1. This is because the micron structures are comparably weak to the forces in the macroscopic world, for example forces from a finger print. However, when the micron structures were bonded by flexible adhesives as shown in Fig. 5.1, they are still attached with the substrate by adhesives after abrasion even if they partially fall, and it is very likely for these micron structures to recover with or without applied forces.

The principle of "use the soft to beat the hard" is also applicable to the particle-based coatings that were introduced in this thesis. Upon bonding with adhesives, the particles tend to be partially pushed into the adhesives or rotate on the adhesives under normal and shear stresses instead of being removed from the substrates, and this retains the functional properties (superhydrophobicity or slipperiness) of the particle-based self-cleaning coatings. The idea was further proved with mechanical tests through using a Newton meter to press a SLIPS coating (normal stress) and using sandpaper to abrade a superhydrophobic coating (shear stress); both coatings retained liquid repellence after mechanical tests.

By simply applying an adhesive layer between the substrate and the rough functional coatings, the self-cleaning (superhydrophobic/SLIPS) surface becomes very abrasive. A further aim was to transfer this technique to practical conditions; hopefully in the near future, there would be innovative products available in the market based on this technique.

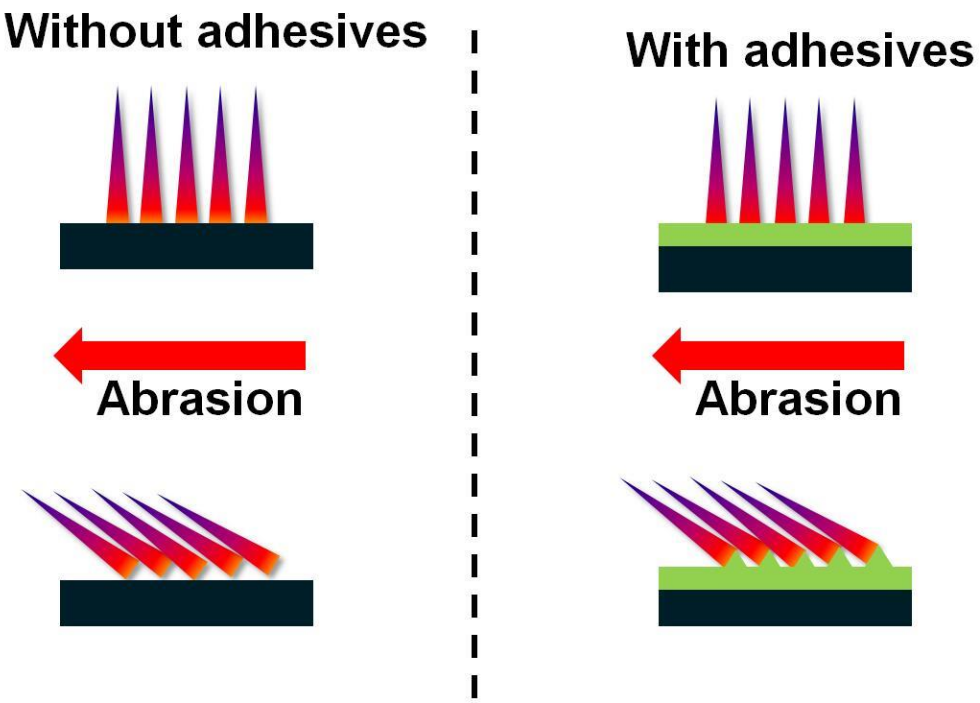

Fig. 5.1 Schemes that compare micro-scaled structures with and without adhesives after being exposed to applied forces.

Texts and schemes below show a small summary of the work in this thesis.

In Chapter 2 (Fig. 5.2), a chemical etching method was reported using $CuCl_2$ solution to roughen mild steel surfaces, the etched surfaces were made superhydrophobic after low surface energy modification. In order to reduce the pressure on the environment, the powder-like by-products from the reactions of Fe and $CuCl_2$ solution were deposited onto soft porous substrates such as cotton wool, filter paper and scouring pad. These soft materials became superhydrophobic after low surface energy modification. This chapter has shown that both hard and soft substrates could obtain superhydrophobicity through simple chemical reactions. However, the prepared superhydrophobic steel surface is mechanically weak, which is also a drawback of most superhydrophobic surfaces; the surface lost superhydrophobicity after six cycles of sandpaper abrasion. In addition, this technique does not apply to other substrates, such as copper and glass, which are not reactive to $CuCl_2$ solution. Therefore, two points needs to be addressed in the following work: 1) a general technique of making superhydrophobic surfaces that applies to a wide range of substrates, either hard or soft; 2) the prepared superhydrophobic surface needs to be mechanically durable.

To address the two aforementioned points, a paint-like suspension was developed in Chapter 3 (Fig. 5.3). The paint can be applied to almost all solid substrates, such as glass, metal, cotton and paper to make superhydrophobic surfaces. This paint is highly compatible with commercial adhesives; the strategy of "superhydrophobic paint + adhesives" greatly improved the surface robustness. The treated substrates (glass, steel, cotton and paper) retained superhydrophobicity after finger wipe, knife scratch and multiple cycles of sandpaper abrasion (even for 40 cycles). Moreover, the treated superhydrophobic surfaces retained self-cleaning (including water stain-resistance and dirt-removal) when they were contaminated by oils in air or even immersed into oil. However, these superhydrophobic surfaces still did not repel oil although they behaved in a self-cleaning manner after oil contamination.

In Chapter 4 (Fig. 5.4), the slippery liquid infused porous surfaces (SLIPS) were developed based on the superhydrophobic paint through adding a liquid lubricating layer onto the superhydrophobic surfaces. The SLIPS not only inherited most of the advantages from the superhydrophobic painted coatings (for example, it can be treated onto most solid substrates; it is mechanically robust etc.), but also repelled various liquids such as water, coffee, red wine, cooking oil and hexadecane. However, the liquid lubricating layer may be subjected to low/high temperatures or corrosive chemicals. To further test the thermal, mechanical and chemical durability, various experiments were performed on the SLIPS samples as shown in Fig. 5.4. The SLIPS samples retained omniphobicity after these tests, even when thermal, mechanical and chemical tests were performed on one single sample. The major idea of designing a robust self-cleaning coating is to use more sophisticated adhesive techniques to overcome the weakness of superhydrophobic/SLIPS coatings. The flexibility of adhesives stabilises the coatings to severe circumstances.

The final version is a SLIPS coating that can be applied to various substrates and repel a range of liquids. The reported SLIPS surfaces are expected to be practically applied due to their remarkable thermal, mechanical and chemical durability.

Chapter 2

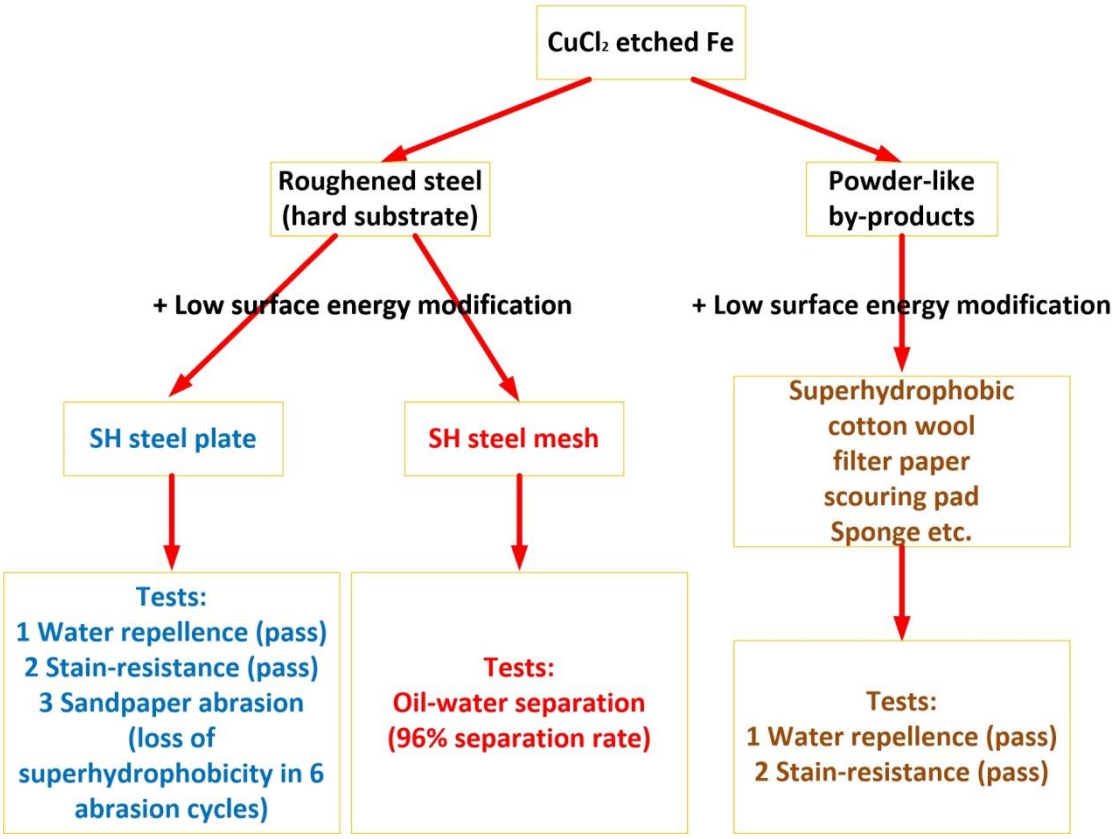

Fig. 5.2 Summary of Chapter 2.

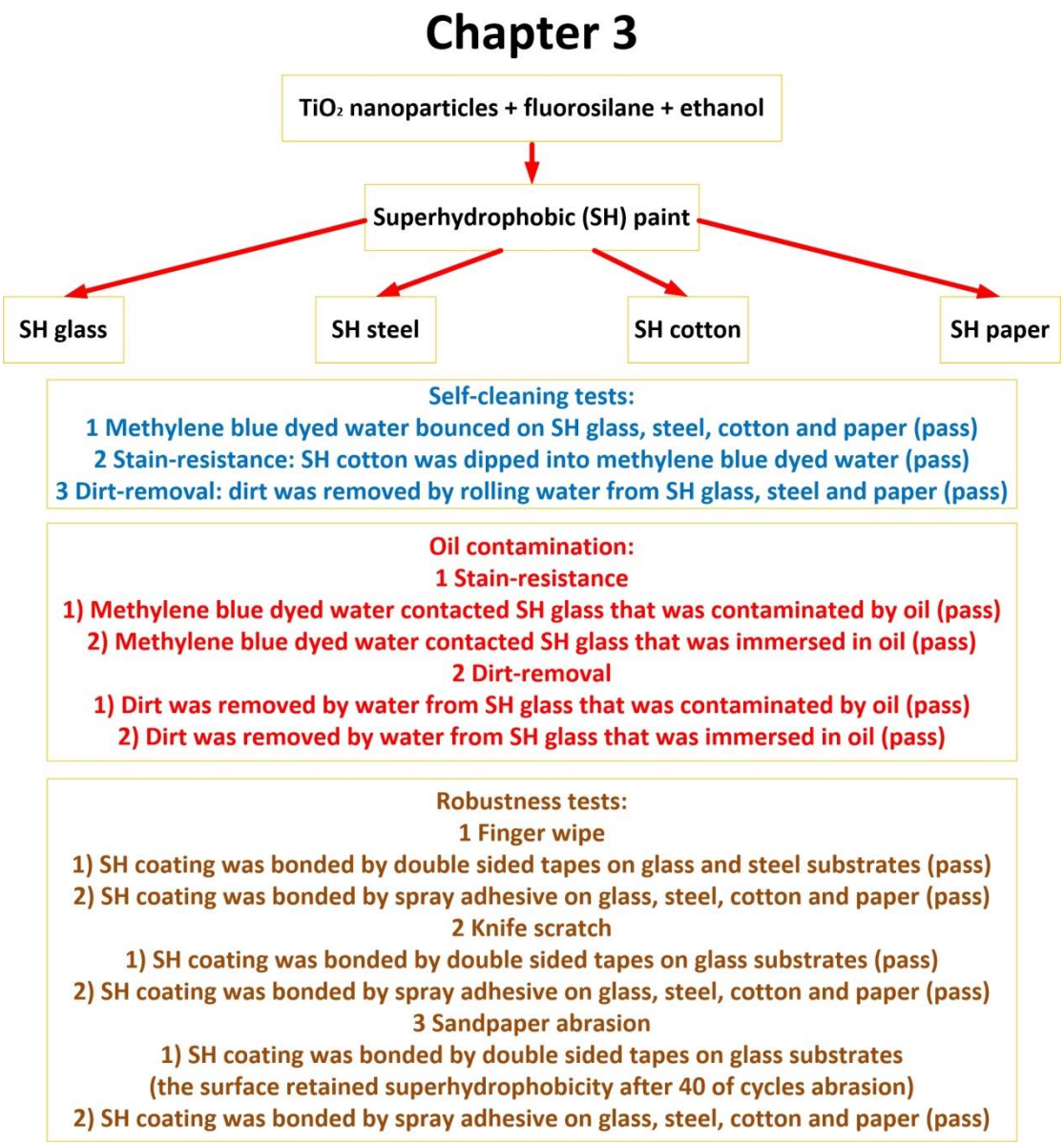

Fig. 5.3 Summary of Chapter 3.

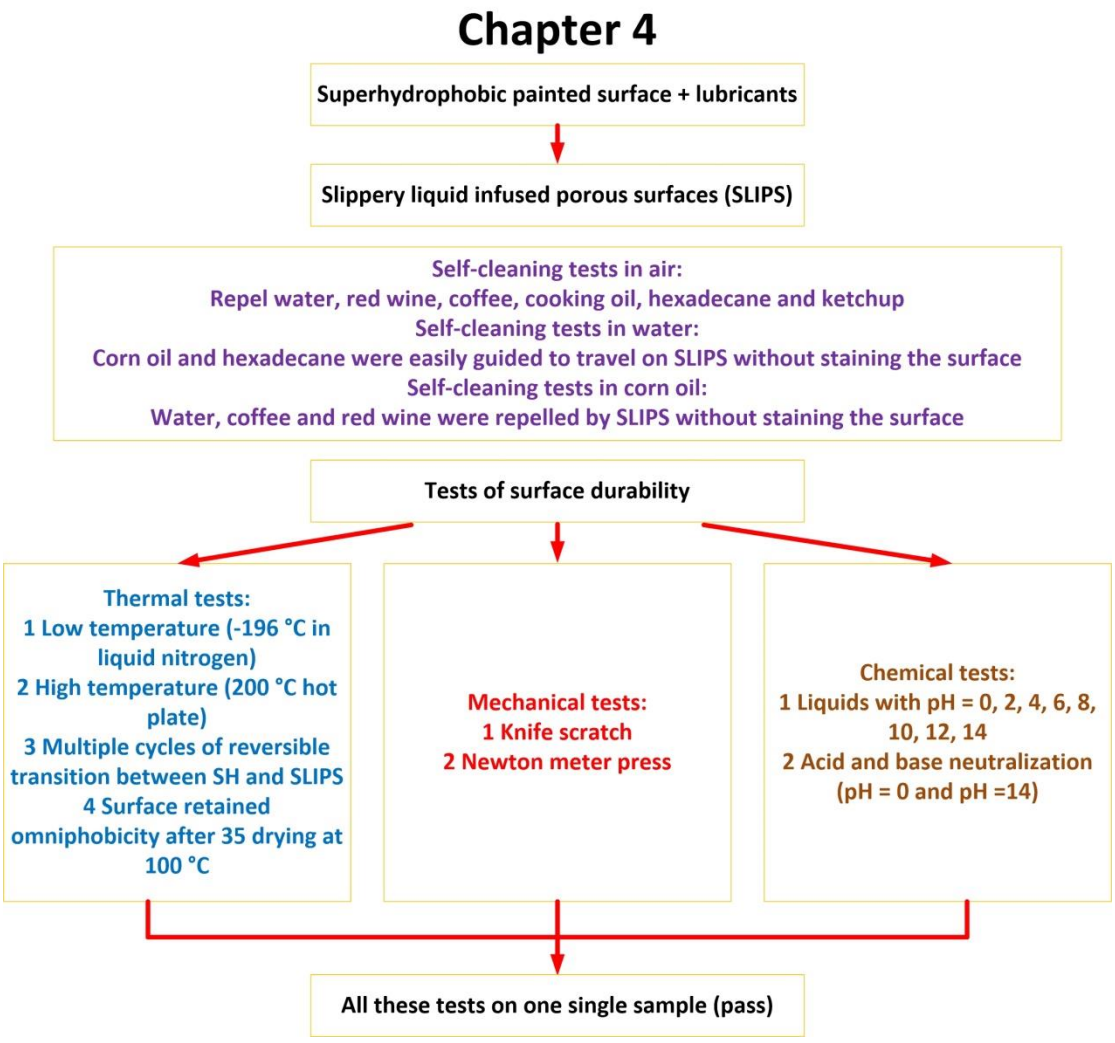

Fig. 5.4 Summary of Chapter 4.

Appendix

Peer-Reviewed Papers

1. **Y. Lu**, S. Sathasivam, J. Song, C. R. Crick, C. J. Carmalt, I. P. Parkin, Robust self-cleaning surfaces that function when exposed to either air or oil, ***Science*** 2015, 347, 1132–1135.
2. **Y. Lu**, S. Sathasivam, J. Song, W. Xu, C. J. Carmalt, I. P. Parkin, Water droplets bouncing on superhydrophobic soft porous materials, ***J. Mater. Chem. A*** 2014, 2, 12177–12184 (**Featured on issue back insert cover**).
3. **Y. Lu**, S. Sathasivam, J. Song, F. Chen, W. Xu, C. J. Carmalt, I. P. Parkin, Creating superhydrophobic mild steel surfaces for water proofing and oil-water separation, ***J. Mater. Chem. A*** 2014, 2, 11628–11634.
4. **Y. Lu**, G. He, C. J. Carmalt, I. P. Parkin, Synthesis and characterization of omniphobic surfaces with thermal, mechanical and chemical stability, ***RSC Adv***. 2016, 6, 106491-106499.
5. **Y. Lu**, J. Song, X. Liu, W. Xu, Y. Xing, Z. Wei, Preparation of superoleophobic and superhydrophobic titanium surfaces via an environmentally friendly electrochemical etching method, ***ACS Sustainable Chem. Eng.*** 2013, 1, 102−109.
6. **Y. Lu**, W. Xu, J. Song, X. Liu, Y. Xing, J. Sun, Preparation of superhydrophobic titanium surfaces via electrochemical etching and fluorosilane modification, ***Appl. Surf. Sci.*** 2012, 263, 297–301.
7. **Y. Lu**, J. Song, X. Liu, W. Xu, J. Sun, Y. Xing, Loading capacity of a self-assembled superhydrophobic boat array fabricated via electrochemical method, ***Micro Nano Lett.*** 2012, 7, 786–789.
8. J. Song, **Y. Lu**, J. Luo, S. Huang, L. Wang, W. Xu, I. P. Parkin, Barrel-shaped oil-skimmer designed for collection of oil from spills, ***Adv. Mater. Interfaces*** 2015, 2, 1500350 (**Featured on issue back cover**).
9. N. Wang, **Y. Lu**, D. Xiong, C. J. Carmalt, I. P. Parkin, Designing durable and flexible superhydrophobic coatings and its application in oil purification, ***J. Mater. Chem. A*** 2016, 4, 4107–4116.
10. J. Song, **Y. Lu**, S. Huang, X. Liu, W. Xu, Progress on research and application of extreme wettability surfaces, ***Science＆Technology Review*** 2015, 33, 92–100 (A review in Chinese).
11. J. Song, **Y. Lu**, S. Huang, X. Liu, L. Wu, W. Xu, A simple immersion approach for

fabricating superhydrophobic Mg alloy surfaces, ***Appl. Surf. Sci.*** 2013, 266, 445–450.

12. S. Huang, J. Song, **Y. Lu**, C. Lv, H. Zheng, X. Liu, Z. Jin, D. Zhao, C. J. Carmalt, I. P. Parkin, Power-free water pump based on a superhydrophobic surface: generation of a mushroom-like jet and anti-gravity long-distance transport, ***J. Mater. Chem. A*** 2016, 4, 13771-13777.
13. S. Huang, J. Song, **Y. Lu**, F. Chen, H. Zheng, X. Yang, X. Liu, J. Sun, C. J. Carmalt, I. P. Parkin, W. Xu, Underwater spontaneous pumpless transportation of nonpolar organic liquids on extreme wettability patterns, ***ACS Appl. Mater. Interfaces*** 2016, 8, 2942–2949.
14. F. Chen, J. Song, **Y. Lu**, S. Huang, X. Liu, J. Sun, C. J. Carmalt, I. P. Parkin, W. Xu, Creating robust superamphiphobic coatings for both hard and soft materials, ***J. Mater. Chem. A*** 2015, 3, 20999–21008.
15. J. Song, S. Huang, **Y. Lu**, X. Bu, J. E. Mates, A. Ghosh, R. Ganguly, C. J. Carmalt, I. P. Parkin, W. Xu, C. M. Megaridis, Self-driven one-step oil removal from oil spill on water via selective-wettability steel mesh, ***ACS Appl. Mater. Interfaces*** 2014, 6, 19858–19865.
16. J. Song, L. Huang, **Y. Lu**, X. Liu, X. Deng, X. Yang, S. Huang, J. Sun, Z. Jin, I. P. Parkin, Fabrication of long-term underwater superoleophobic Al surfaces and application on underwater lossless manipulation of non-polar organic liquids, ***Sci. Rep.*** 2016, 6, Article number: 31818.
17. X. Yang, X. Liu, **Y. Lu**, S. Zhou, M. Gao, J. Song, W. Xu, Controlling the adhesion of superhydrophobic surfaces using electrolyte jet machining techniques, ***Sci. Rep.*** 2016, 6, Article number: 23985.
18. X. Yang, X. Liu, **Y. Lu**, J. Song, S. Huang, S. Zhou, Z. Jin, W. Xu, Controllable water adhesion and anisotropic sliding on patterned superhydrophobic surface for droplet manipulation, ***J. Phys. Chem. C*** 2016, 120, 7233–7240.
19. N. Wang, D. Xiong, **Y. Lu**, S. Pan, K. Wang, Y. Deng, Y. Shi, Design and fabrication of the lyophobic slippery surface and its application in anti-icing, ***J. Phys. Chem. C*** 2016, 120, 11054–11059.
20. L. Huang, J. Song, **Y. Lu**, F. Chen, X. Liu, Z. Jin, D. Zhao, C. J. Carmalt, I. P. Parkin, Superoleophobic surfaces on stainless steel substrates obtained by chemical bath deposition, ***Micro Nano Lett.*** 2016 **(In press).**
21. S. Sathasivam, D. S. Bhachu, **Y. Lu**, N. Chadwick, S. A. Althabaiti, A. O. Alyoubi, S. N. Basahel, C. J. Carmalt, I. P. Parkin, Tungsten doped TiO_2 with enhanced photocatalytic and optoelectrical properties via aerosol assisted chemical vapor deposition, ***Sci. Rep.*** 2015, 5, Article number: 10952.

22. F. Chen, W. Xu, **Y. Lu**, J. Song, S. Huang, L. Wang, I. P. Parkin, X. Liu, Hydrophilic patterning of superhydrophobic surfaces by atmospheric pressure plasma jet, ***Micro Nano Lett.*** 2015, 10, 105–108. **(Win the IET Premium Awards 2016)**
23. S. Sathasivam, D. S. Bhachu, **Y. Lu**, S. M. Bawaked, A. Y. Obaid, S. Al-Thabaiti, S. N. Basahel, C. J. Carmalt, I. P. Parkin, Highly photocatalytically active iron(III) titanium oxide thin films via aerosol-assisted CVD, ***Chem. Vap. Deposition*** 2015, 21, 21–25. (**Featured on issue cover**)
24. J. Song, W. Xu, **Y. Lu**, L. Luo, X. Liu, Z. Wei, Fabrication technology of low–adhesive superhydrophobic and superamphiphobic surfaces based on electrochemical machining method, ***ASME Journal of Micro and Nano-Manufacturing*** 2013, 021003-1-7.
25. J. Song, W. Xu, **Y. Lu**, X. Liu, Z. Wei, J. Sun, Research on electrochemical and chemical machining technology of superamphiphobic surfaces on Al substrates (in Chinese), ***Chinese Journal of Mechanical Engineering*** 2013, 49, 182–190.
26. J. Song, W. Xu, **Y. Lu**, X. Liu, J. Sun, Fabrication of superhydrophobic surfaces on Mg alloy substrates via primary cell corrosion and fluoroalkylsilane modification, ***Mater. Corros.*** 2013, 64, 979–987.
27. J. Song, W. Xu, **Y. Lu**, X. Liu, Z. Wei, J. Sun, Fabrication of superhydrophobic surfaces with hierarchical rough structures on Mg alloy substrates via chemical corrosion method, ***Micro Nano Lett.*** 2012, 7, 204–207.
28. J. Song, W. Xu, **Y. Lu**, One-step electrochemical machining of superhydrophobic surfaces on aluminum substrates, ***J. Mater. Sci.*** 2012, 47, 162–168.
29. J. Song, X. Liu, **Y. Lu**, L. Wu, W. Xu, A rapid two-step electroless deposition process to fabricate superhydrophobic coatings on steel substrates, ***J. Coat. Technol. Res.*** 2012, 9, 643–650.
30. J. Song, W. Xu, **Y. Lu**, X. Fan, Rapid fabrication of superhydrophobic surfaces on copper substrates by electrochemical machining, ***Appl. Surf. Sci.*** 2011, 257, 10910–10916.
31. W. Xu, J. Song, **Y. Lu**, X. Liu, Q. Dou, Preparation of large–area superhydrophilic/superhydrophobic aluminum plate by moving–typed cathode (in Chinese), ***Materials for Mechanical Engineering*** 2012, 36, 37–45.
32. S. Sathasivam, R. R. Arnepalli, D. S. Bhachu, **Y. Lu**, J. Buckeridge, D. O. Scanlon, B. Kumar, K. K. Singh, R. J. Visser, C. S. Blackman, C. J. Carmalt, Single step solution processed GaAs thin films from $GaMe_3$ and $^tBuAsH_2$ under ambient pressure, ***J. Phys. Chem. C*** 2016, 120, 7013–7019.
33. G. He, M. Qiao, W. Li, **Y. Lu**, T. Zhao, R. Zou, B. Li, J. A. Darr, J. Hu, M. M. Titirici, I.

P. Parkin, S, N-co-doped graphene-nickel cobalt sulfide aerogel: improved energy storage and electrocatalytic performance, ***Adv. Sci.*** 2016, 1600214.

34. J. Song, S. Huang, K. Hu, **Y. Lu**, X. Liu, W. Xu, Fabrication of superoleophobic surfaces on Al substrates, ***J. Mater. Chem. A*** 2013, 1, 14783-14789.
35. S. Dixon, N. Noor, S. Sathasivam, **Y. Lu**, I. P. Parkin, Synthesis of superhydrophobic polymer/tungsten (VI) oxide nanocomposite thin films, ***Eur. J. Chem.*** 2016, 7, 139–145.
36. J. Song, W. Xu, X. Liu, **Y. Lu**, J. Sun, Electrochemical machining of super-hydrophobic Al surfaces and effect of processing parameters on wettability, ***Appl. Phys. A*** 2012, 108, 559–568.
37. W. Xu, J. Song, J. Sun, **Y. Lu**, Z. Yu, Rapid fabrication of large-area, corrosion-resistant superhydrophobic Mg alloy surfaces, ***ACS Appl. Mater. Interfaces*** 2011, 3, 4404–4414.
38. J. Song, W. Xu, X. Liu, **Y. Lu**, Z. Wei, L. Wu, Ultrafast fabrication of rough structures required by superhydrophobic surfaces on Al substrates using an immersion method, ***Chem. Eng. J.*** 2012, 211–212, 143–152.
39. W. Xu, J. Song, J. Sun, **Y. Lu**, Rapid fabrication of hard superhydrophobic surfaces with low roughness on aluminum substrates via anodization, ***J. Chin. Ceramic Soc.*** 2011, 39, 145-149.
40. X. Liu, F. Chen, S. Huang, X. Yang, **Y. Lu**, W. Zhou, W. Xu, Characteristic and application study of cold atmospheric-pressure nitrogen plasma Jet, ***IEEE Trans. Plasma Sci.*** 2015, 43, 1959–1968.
41. J. Song, W. Xu, Z. Feng, X. Liu, **Y. Lu**, J. Sun, Fabrication of low-adhesive superhydrophobic Al surfaces via self-assembled primary cell assisted etching, ***J. Disper. Sci. Technol.*** 2013, 34, 908–913.
42. X. Yang, J. Song, W. Xu, X. Liu, **Y. Lu**, Y. Wang, Anisotropic sliding of multiple-level biomimetic rice-leaf surfaces on aluminium substrates, ***Micro Nano Lett.*** 2013, 8, 801-804.
43. J. Song, W. Xu, X. Liu, Z. Wei, **Y. Lu**, Fabrication of superhydrophobic Cu surfaces on Al substrates via a facile chemical deposition process, ***Mater. Lett.*** 2012, 87, 43–46.
44. W. Xu, J. Song, X. Liu, J. Sun, **Y. Lu**, Electrochemical machining of large-area superhydrophobic Al surfaces (in Chinese), ***Mater. Sci. Technol.*** 2012, 20, No. 2, 52–60.
45. X. Liu, J. Song, L. Wu, W. Xu, **Y. Lu**, J. Sun, Fabrication of superhydrophobic surfaces with high adhesive forces towards water on steel substrates, ***Micro Nano Lett.*** 2012, 7, 456–459.
46. Z. Wei, W. Xu, B. Tao, J. Song, L. Wei, **Y. Lu**, Crown shaping technique of bearing

raceway by electrochemical mechanical machining, ***Int. J. Electrochem. Sci.*** 2013, 8, 2238–2253.

47. S. Noimark, K. Page, J. C. Bear, C. Sotelo-Vazquez, R. Quesada-Cabrera, **Y. Lu**, E. Allan, J. A. Darr, I. P. Parkin, FD175: Functionalised gold and titania nanoparticles and surfaces for use as antimicrobial coatings, ***Faraday Discuss.*** 2014, 175, 273–287.
48. J. Sun, F. Zhang, J. Song, L. Wang, Q. Qu, **Y. Lu**, I. P. Parkin, Electrochemical fabrication of superhydrophobic Zn surfaces, ***Appl. Surf. Sci.*** 2014, 315, 346–352.
49. G. He, X. Han, R. Zou, T. Zhao, Z. Weng, S. Ho-Kimura, **Y. Lu**, H. Wang, Z. Guo, I. P. Parkin, A targeted functional design for highly efficient and stable cathodes for rechargeable Li-ion batteries, ***Adv. Funct. Mater***. 2016 **(In press).**

Conference Publications

50. **Y. Lu**, C. J. Carmalt, I. P. Parkin, E5.12 Designing robust self-cleaning surfaces (abstract), Symposium E: Engineering and Application of Bioinspired Materials, 2015 MRS Fall Meeting & Exhibit in Boston, Massachusetts, USA, 30th, November 2015.
51. **Y. Lu**, J. Song, W. Xu, I. P. Parkin, Preparation of superamphiphobic surfaces on titanium substrates (abstract), Photocatalytic and superhydrophilic surfaces workshop, PSS2013, Manchester, 12th/13th December 2013.
52. F. Chen, J. Song, **Y. Lu**, S. Huang, X. Liu, W. Xu, E13.02 Fabrication of robust superamphiphobic coatings on stretchable substrate (abstract), Symposium E: Engineering and Application of Bioinspired Materials, 2015 MRS Fall Meeting & Exhibit in Boston, Massachusetts, USA, 2nd, December 2015.
53. J. Song, X. Liu, **Y. Lu**, L. Wu, W. Xu, Fabrication of superhydrophobic surfaces on aluminum substrates via electrochemical etching and re-deposition, ***Appl. Mech. Mater.*** 2012, 197, 351–355. International Conference on Mechanical Science and Engineering (ICMSE 2012) in Beijing, China, 20th – 22th July, 2012.
54. S. Huang, J. Song, H. Zheng, **Y. Lu**, X. Liu, J. Sun, W. Xu, E7.05 Underwater antigravity pumpless fluid transport on extreme wettability patterns (abstract), Symposium E: Engineering and Application of Bioinspired Materials, 2015 MRS Fall Meeting & Exhibit in Boston, Massachusetts, USA, 1st, December 2015.

Patents

55. **Y. Lu**, I. P. Parkin, C. J. Carmalt, Composite particles, coatings and coated articles, New British Patent Application (Number 1518826.1).
56. W. Xu, **Y. Lu**, J. Song, X. Liu, J. Sun, Method for preparing titanium or titanium alloy super-hydrophobic surface. Granted. CN102618913B.
57. W. Xu, **Y. Lu**, J. Song, X. Liu, Y. Xing, J. Sun, Method for preparing titanium or titanium alloy superoleophobic surface. Granted. CN102677141B.
58. W. Xu, J. Song, S. Huang, **Y. Lu**, X. Liu, An oil slick of collecting device. Granted. CN103774629B.